Aus der Klinik für Dermatologie, Venerologie und Allergologie
Universitätsklinikum Mannheim der Medizinischen Fakultät Mannheim
der Ruprecht-Karls-Universität Heidelberg
(Direktor: Prof. Dr. med. S. Goerdt)

Expression and Processing of Lyve-1 in Macrophages

INAUGURALDISSERTATION

zur Erlangung der Doktorwürde der
Naturwissenschaftlich-Mathematischen Gesamtfakultät
der Ruprecht-Karls-Universität Heidelberg

VORGELEGT VON

Claudia Dollt, M.Sc. Biotechnologie

Aus der Klinik für Dermatologie, Venerologie und Allergologie
Universitätsklinikum Mannheim der Medizinischen Fakultät Mannheim
der Ruprecht-Karls-Universität Heidelberg
(Direktor: Prof. Dr. med. S. Goerdt)

Expression and Processing of Lyve-1 in Macrophages

INAUGURALDISSERTATION

zur Erlangung der Doktorwürde der
Naturwissenschaftlich-Mathematischen Gesamtfakultät
der Ruprecht-Karls-Universität Heidelberg

VORGELEGT VON

Claudia Dollt, M.Sc. Biotechnologie

DISSERTATION

submitted to the combined Faculties
for the Natural Sciences and for Mathematics

of the Ruperto-Carola University
of Heidelberg, Germany

for the degree of
Doctor of Natural Science

Presented by
Claudia Dollt, M.Sc. Biotechnology
Born in: Landau in der Pfalz

Oral Examination: December 12th 2016

Expression and Processing of Lyve-1 in Macrophages

REFEREES:

Prof. Dr. rer. nat. Viktor Umansky

PD Dr. med. Astrid Schmieder

CONTENTS

TABLES

FIGURES

ABSTRACT

Besides malignant cells, tumours are composed of vascular, hematopoietic and mesenchymal cells, amongst which in particular macrophages can be found numerously within the tumour infiltrate. So called tumour-associated macrophages (TAM) exert important tumour-supportive roles and are involved in tumour initiation, progression and metastasis as providers of angiogenic, anti-inflammatory and matrix remodelling factors. In numerous different cancers, high TAM density correlates with poor patient prognosis. The plasticity of gene regulation allows macrophages to adapt their phenotype to local requirements. Therefore TAM populations are highly heterogeneous and adapt to the corresponding microenvironment of the particular tumour region. The identification of further TAM macrophage markers is indispensable regarding the necessity of functional characterization of distinct TAM subsets.

In the past years, our group has identified Ms4a8a, Stabilin-1 and Lyve-1 as novel markers of murine TAM. *In vitro*, Lyve-1 expression could be induced in murine bone marrow derived macrophages by the stimulation with tumour conditioned medium, dexamethasone and IL-4. In this thesis the main aim was to comprehensively characterize expression and processing of Lyve-1 in macrophages *in vitro* and *in vivo*. The type I transmembrane glycoprotein Lyve-1 is part of the link domain superfamily with 43% sequence homology to the hyaluronan receptor CD44. Lyve-1 has first been identified as a lymphatic endothelial cell specific HA receptor which also binds different growth factors like FGF-2 and VEGF. Lyve-1 is involved in lymphangiogenesis in endothelial cells.

By immunohistological analyses we could demonstrate the presence of Lyve-1$^+$ macrophages in human melanoma specimen and in murine B16 transplant tumours. In human peripheral blood mononuclear cells (PBMC), which were isolated from buffy coats, seven days of stimulation with M-CSF/dexa/IL-4 (MDI) led to the induction of Lyve-1 in 25% of the stimulated cells. Expression analysis of combinations of macrophage marker revealed that Lyve-1$^+$ PBMC were more oriented towards a M2-like phenotype. In addition, we found that the induction of Lyve-1 *in vitro* is crucially dependent on the activation of the glucocorticoid receptor (GR) and can be impaired by inhibition of the p38 MAPK signalling cascade. *In vivo*, the activation of GR seems to play a secondary role for Lyve-1 induction, as Lyve-1$^+$ macrophages were detected in murine B16F10 tumours derived from mice with a myeloid specific deletion of the GR.

Functional analyses were accomplished using genetically engineered Lyve-1 overexpressing cell lines. In the human macrophage like cell line U937 Lyve-1

was expressed in a highly glycosylated state. Even though binding to HA could be demonstrated, ligand binding did not induce proliferation as it has been reported for Lyve-1^{+} endothelial cells. In an adhesion assay we identified fibronectin as a further binding partner of Lyve-1.

In analogy to CD44, which is shedded from the cell surface by proteolytic cleavage, we supply evidence for the existence of a soluble form of Lyve-1 in the cell culture supernatant of transgenic U937. Soluble Lyve-1 (sLyve-1) is produced by a metalloproteinase mediated shedding process in macrophages and endothelial cells in a comparable fashion. To address our hypothesis that sLyve-1 might function as a decoy receptor, we incubated melanoma cell lines with macrophage derived and synthetic sLyve-1 and observed reduced tumour cell proliferation. Physiological relevance of Lyve-1 shedding was demonstrated by the quantification of sLyve-1 in human plasma. The concentration of sLyve-1 was significantly increased in plasma samples derived from psoriasis patients.

To examine the relevance of Lyve-1^{+} macrophages for tumour growth we injected B16 melanoma tumour cells subcutaneously into the flank of Lyve-1$^{-/-}$ mice. After ten days enhanced tumour growth due to increased tumour cell proliferation was observed in the knockout mice in comparison to wild type controls. The exact contribution of Lyve-1^{+} macrophages to this effect still needs further clarification.

Therefore, we could demonstrate that Lyve-1 is a marker of a M2-like macrophage subpopulation in human and murine melanoma. By proteolytic cleavage of the ectodomain the function of Lyve-1 is modulated and thus plays also an important role for tumour growth and progression.

ZUSAMMENFASSUNG

Tumore sind komplexe organ-ähnliche Strukturen, die neben malignen Zellen von vaskulären, hämatopoetischen und mesenchymalen Zellen gebildet werden, wobei insbesondere Makrophagen zahlreich im Tumorinfiltrat zu finden sind. So genannte Tumor-assoziierte Makrophagen (TAM) führen wichtige tumor-unterstützende Funktionen aus. Als Quelle von angiogenen, anti-inflammatorischen und Matrix-umbauenden Faktoren beeinflussen TAM maßgeblich die Tumorinitiierung, die Progression und auch die Metastasierung. In diversen Krebserkrankungen korreliert eine hohe TAM Dichte im Tumor mit einer schlechten Prognose für die Patienten. Aufgrund der Plastizität der Gen-Regulation können Makrophagen sich funktionell auf lokale Bedingungen einstellen. Daher bilden auch TAM eine stark heterogene Zellpopulation, da sie ihren Phänotyp an das sie umgebende Mikromillieu der jeweiligen Tumorregion anpassen. Zur funktionellen Charakterisierung von TAM Subpopulationen ist die Identifizierung weiterer TAM Marker somit unabdingbar.

In den letzten Jahren hat unsere Gruppe Ms4a8a, Stablilin-1 und Lyve-1 als neue Marker für murine TAM identifiziert. Die Expression von Lyve-1 konnte *in vitro* in Knochenmarkmakrophagen durch die Stimulation mit Tumor-konditioniertem Medium, Dexamethason und IL-4 induziert werden. Das Hauptziel der vorliegenden Arbeit war es die Expression und die Prozessierung von Lyve-1 in Makrophagen *in vitro* und *in vivo* umfassend zu charakterisieren. Das Typ I transmembrane Glykoprotein Lyve-1 gehört zu der Link-Domäne Superfamilie und teilt 43 % Sequenzhomologie mit dem Hyaluronsäure (HS) Rezeptor CD44. Zunächst wurde Lyve-1 als spezifischer HS Rezeptor des lymphatischen Endotheliums identifiziert. Zusätzlich wurden Interaktionen zwischen Lyve-1 und Wachstumsfaktoren wie FGF-2 und VEGF nachgewiesen. Im lymphatischen Endothelium ist Lyve-1 in der Regulation der Lymphangiogenese involviert.

Mittels immunohistochemischer Analysen konnten wir die Existenz von Lyve-1$^+$ Makrophagen in humanen Melanomen und in murinen B16 Tumoren nachweisen. Im Menschen führt eine sieben tägige Stimulation mit M-CSF, Dexamethason und IL-4 (MDI) von peripheren Blutmonozyten (PBMZ) aus Buffy Coats zu einer Lyve-1 Induktion in 25 % der Zellen. Expressionsanalysen einer Kombination von verschiedenen Makrophagenmarkern zeigten, dass Lyve-1$^+$ PBMZ mehr in Richtung M2 differenziert sind. Außerdem hat sich herausgestellt, dass die Lyve-1 Induktion *in vitro* maßgeblich von der Aktivierung des Glukokortikoidrezeptors (GR) abhängt und durch Inhibition des p38 MAPK Signalwegs beeinträchtig werden kann. *In vivo* scheint die GR Aktivierung eine untergeordnete Rolle zu spielen, da Lyve-1$^+$

Makrophagen in murinen B16F10 Tumoren, welche von Mäusen mit einer myeloid-spezifischen Deletion des GR stammten, nachgewiesen werden konnten.

Funktionelle Analysen wurden mit transgen modifizierten Lyve-1 überexprimierenden Zelllinien durchgeführt. In der humanen Makrophagen-ähnlichen Zelllinie U937 wird Lyve-1 in einer stark glykosylierten Form exprimiert. Obwohl die Bindung an HS nachgewiesen werden konnte, hatte die Interaktion mit Liganden keinen Einfluss auf die Proliferationsrate der U937-Zellen. Mit Hilfe eines Adhäsionsassays konnten wir Fibronektin als weiteren Bindungspartner von Lyve-1 identifizieren.

In Analogie zu CD44, dessen Ectodomäne proteolytisch abgespalten wird, konnten wir eine lösliche Form von Lyve-1 (sLyve-1) im Zellkulturüberstand von transgenen U937 Zellen nachweisen. sLyve-1 wird in Makrophagen und Endothelzellen in ähnlicher Weise durch Metalloproteinase vermitteltes Shedding produziert. Unsere Hypothese, dass sLyve-1 als Decoy-Rezeptor fungiert, überprüften wir durch Inkubation von Melanomzellen mit synthetisiertem sLyve-1 und sLyve-1, welches von Makrophagen stammte, und stellten eine verminderte Proliferationsrate der Krebszellen fest. Die physiologische Relevanz des Lyve-1 Sheddings belegten wir mit der Quantifizierung von Lyve-1 in humanem Plasma. Die Konzentration von löslichem Lyve-1 war hierbei im Plasma von Psoriasis Patienten signifikant erhöht.

Um die Bedeutung von Lyve-1$^+$ Makrophagen für das Tumorwachstum zu klären, injizierten wir B16 Melanomzellen subkutan in die Flanke von Lyve-1 Knockout Mäusen. Nach zehn Tagen Tumorwachstum konnten wir im Vergleich zu den Wildtyp Mäusen in den Knockout Tieren ein verstärktes Tumorwachstum feststellen, welches durch eine erhöhte Tumorzellproliferation bedingt wurde. Der genaue Beitrag von Lyve-1$^+$ Makrophagen zu diesem Effekt muss im Detail noch weiter untersucht werden.

Wir konnten somit zeigen, dass Lyve-1 ein Marker von einer M2-ähnlichen Makrophagen Subpopulation im humanen und murinen Melanom ist. Durch proteolytische Abspaltung der Ectodomaine wird die Funktion von Lyve-1 maßgeblich beeinflusst und spielt daher auch für das Tumorwachstum eine wichtige Rolle.

1. INTRODUCTION

1.1 Macrophages

Macrophages are innate immune cells of myeloid hematopoietic origin, which can be found in all body tissues, where they exert important homeostatic, tissue-specific functions and provide a first line defence against health threatening pathogens. Macrophages were first described by the comparative zoologist Elie Metchnikoff. His studies on larvae of starfish (Hydra) in 1883 allowed him to observe phagocytosis of foreign material by specific migratory cells of mesodermal origin, at which he noted distinct similarities to vertebrate blood cells. Further experiments lead Elie Metchnikoff to the discovery of the mechanism of cellular innate immune response for which he was awarded with the Nobel Prize in 1908 together with Paul Ehrlich for his findings in humoral immunity [1].

The identification of further phagocytic active cells and the efficient clearance function of tissue-specific macrophages (histiocytes) led to the introduction of the concept of the reticulo-endothelial system by Aschoff in 1924. He grouped cells of different origins and ranked them in ascending order according to their phagocytic capacity which was evaluated by experiments with vital dyes [2]. This concept was challenged by van der Furth and his colleagues in the 1970s, when they presented the mononuclear phagocyte system (MPS), which comprises monocytes and macrophages as well as their bone-marrow derived progenitor cells. MPS included cells were related in morphology, function and origin. However, van der Furth et al. assumed that tissue-macrophages are non-proliferative terminally differentiated cells, which are steadily replenished by circulating monocytes which originate from the bone marrow [2, 3].

Even though the definition of the MPS holds true for dermal and gut macrophages, which are constantly replaced by monocytes, fate mapping experiments demonstrated that early embryonic haematopoiesis contributes to the pool of tissue-resident macrophages. Thus, most of the macrophages are established prenatally and persist through adulthood by local proliferation independently from monocytic input. During embryogenesis first hematopoietic cells can be detected in blood islands of the extraembryonic yolk-sac (YS). These cells are progenitors of erythrocytes and so-called primitive macrophages, which develop without a

monocytic intermediate. During a second wave of haematopoiesis, erythromyeloid (EMP) and lymphoid-myeloid progenitors emerge in the YS. After the establishment of blood circulation, EMP seed the fetal liver and further tissues. Subsequently, the haematogenic endothelium of the aorto-gonadal-mesonephros vessels give rise to hematopoietic stem cells (HSC), which translocate to the fetal liver to establish definitive haematopoiesis [4, 5].

In vivo lineage tracing experiments provided first hints of the embryonic origin of microglia, which are specific macrophages of the central nervous system. The direct origin of microglia from YS derived progenitors could be demonstrated, whereas postnatal monocytes are not involved significantly in the maintenance of the adult microglia population [6]. In contrast to microglia, Langerhans cells of the epidermis where found to derive mainly from fetal liver monocytes that replace YS-derived Langerhans cells during embryogenesis [7]. The contribution of YS macrophages to adult tissue resident macrophages was further substantiated by a study with $Myb^{-/-}$ mice. The transcription factor Myb is required for the development of HSC in the fetal liver, but primitive macrophages can develop in the YS independently from Myb activity and give later rise to $F4/80^{bright}$ $CD11b^{low}$ macrophages. Lineage tracing of these macrophages demonstrated that YS-derived progenitors give rise to microglia, liver Kupffer cells and epidermal Langerhans cells, whereas a part of the $F4/80^{bright}$ $CD11b^{low}$ macrophages in lung and kidney and the majority of these macrophages in pancreas and spleen were replaced in the adult organism by bone marrow derived progenitors [8].

1.1.1 Tissue-specific functions of macrophages in homeostasis

Macrophages constitute a highly heterogeneous population of cells with a wide range of various functions. They do not only play a major role in host defence, but are also involved in developmental processes, systemic metabolism, clearance of apoptotic cells, extracellular matrix (ECM) remodelling and homeostasis. Tissue specialization enables resident macrophages to adapt to their local environment and to exert particular functions. The Immunological Genome Project was able to demonstrate the transcriptomal diversity of different tissue-resident macrophage subsets as only few transcripts are in fact shared amongst different macrophage populations [9]. The distinct macrophage phenotype is formed by a combination of differentiation and polarization signals, which regulate epigenetic modifications and the accessibility of gene expression regulatory elements. In this connection, the hierarchically organized control of gene expression by transcriptional regulators leads to the shaping of tissue-specific macrophage characteristics [10]. First of all, lineage determining transcription factors enable the expression of common macrophage associated genes. The ETS family member PU.1 acts as such a so-called pioneer transcription factor in early myeloid differentiation by opening long segments of chromatin around enhancer and promoter regions, thus controlling a

wide range of macrophage-specific regulatory regions, which are then amenable for interactions with further transcription factors. PU.1 regulatory elements can be found in nearly all expression regulatory elements of myeloid specific genes. Myeloid lineage differentiation is further influenced by CCAAT/enhancer-binding protein (CEBP) controlling the development of granulocyte/monocyte progenitor cells and MAF/MAFB, which is involved in terminal differentiation of macrophages [4, 11]. On the next level of transcriptional control, tissue-specific transcription factors like e.g. peroxisome proliferator-activated receptor γ (PPARγ) in alveolar macrophages or GATA6 in peritoneal cavity macrophages, further remodel chromatin structures such that local differentiation of tissue resident macrophages is achieved. The corresponding local microenvironment made up of cytokines, chemokines and metabolites leads to further specialization and maintenance of macrophages [4].

Under homeostatic conditions the different macrophage subpopulations vary greatly in their functions depending on their anatomical location; examples are described in the following. Bone marrow osteoclasts are multinucleated macrophage-derived cells which are involved in bone remodelling processes [12]. So called alveolar macrophages are located in the lungs where they are exposed to the alveolar lumen. Besides phagocytosis and clearance of inhaled particles, these macrophages also recycle surfactant molecules of epithelial cells [13]. The sinusoidal vessels of the liver are lined by Kupffer cells. The stellate-shaped phagocytes are mainly involved in local immune response to blood-borne antigens [14]. Microglia on the other hand carry out tissue remodelling functions by synaptic pruning and are important sources of neurotrophic factors, additionally they are key components of the immune response in the central nervous system [15]. In other organs like the gut, diverse macrophage subpopulations exist that cooperate to ensure tolerance to gut flora and food [16]. In second lymphoid tissues too, heterogeneous populations of macrophage subsets can be found, like lymph node subcapsular sinus (SCS) macrophages. By presenting lymph derived antigens to B cells the SCS macrophages promote the induction of antiviral humoral responses [17]. Many further subpopulations of macrophages with particular functions exist, which contribute to maintenance of tissue homeostasis.

1.1.2 Macrophages in the inflammatory response

When microorganisms succeed in overcoming the physical barriers of our body, macrophages build the first cellular defence against the invading pathogens. Their abundant occurrence in the connective tissue facilitates the immediate combat of microorganisms, at which macrophages play also an important role in the recruitment of further inflammatory cells to the site of infection and the induction of an inflammatory response. The distinct functions of macrophages during challenge with pathogens are described in the following in more detail.

PATHOGEN RECOGNITION Macrophages express numerous invariable pattern-recognition-receptors (PRR) on their surface, which allow them to detect pathogens by recognition of pathogen associated molecular patterns (PAMP), such as bacterial and fungi cell wall components and viral nucleic acids. PRR are able to discriminate between self and non-self, as PAMP are not present in higher eukaryotes and thus are unique to disease causing pathogens. PRR can serve as phagocytic receptors, membrane-bound signalling receptors or cytosolic signalling receptors [18]. The recognition of cytosolic pathogens is mediated by intracellular PRR, like NOD (nucleotide-binding oligomerization domain) and NRL (leucine-riche repeat-containing receptors) that act as sensors for viral nucleotides and nucleic acids and operate in all cells. Exogenous pathogenic stimuli on the other hand are sensed by PRR in the plasma membrane of macrophages and dendritic cells (DC) [19]. PRR expressed on macrophages are for example members of the C-type lectin-like family like Dectin-1 and mannose receptor (MR). One important family of signal transducing PRR in macrophages are the Toll-like receptors (TLR) which comprise at least 11 members in mammals, amongst which some are expressed on the cellular surface and others are located intracellular in endosomal membranes. TLR signalling activates transcription factors like nuclear factor κ-light-chain-enhancer of activated B cells (NFκB) and AP-1 which in turn induce the expression of pro-inflammatory genes orchestrating both innate and adaptive immune response [20].

PHAGOCYTOSIS AND RESPIRATORY BURST Phagocytosis is defined as the process of uptake of large particles (> 0.5µm). Macrophages are so-called professional phagocytes which are characterized by a high phagocytic capacity and efficiency due to expression of numerous phagocytic receptors. By phagocytosis, macrophages mediate clearance from pathogens, microorganisms and apoptotic cells. Phagocytic receptors can be PRR, like e.g. MR. Hence binding of macrophage to a pathogen via its phagocytic receptors triggers the polymerization of actin. This facilitates the formation of membrane extensions leading to the engulfment of the bound particle. The ingested particle is enclosed in a membranous vesicle called phagosome. After its formation the phagosome experiences a step-wise maturation. In the course of the endocytic pathway the phagosome is subsequently fused with early and late endosomes. The maturation process is terminated by a final fusion with preformed lysosomes which contain large amounts of hydrolytic enzymes and defensins in an acidic milieu. The formation of the so-called phagolysosome results in the destruction of the pathogen and its digestion for antigen presentation [21-23]. Phagocytosis can also be initiated and enhanced by interaction with opsonized particles, which means loading of pathogens with complement components (opsonins) or antibodies. In the latter case for example, an antibody binds in a highly specific manner to its corresponding antigen on the pathogen surface,

subsequently the constant region of the antibody is bound to Fc receptor (FcR) expressed by phagocytes and again phagocytosis is induced [24]. Microbial contact also has an influence on the plastic phenotype of macrophages and induces an activated status of the cells. Interestingly, phagocytosis induced by FcR interactions leads to a pro-inflammatory phenotype, whereas complement-receptor mediated phagocytosis is rather non-inflammatory [25]. Phagocytosis is a fundamental mechanism of the microbicidal activity of macrophages.

Pathogen-receptor interactions further increase the defensive properties of macrophages by stimulating the production of microbicidal agents like reactive nitrogen species (NOS) and reactive oxygen species (ROS). NOS production is mediated by inducible nitric oxide synthase (iNOS) by conversion of arginine and oxygen. Moreover, PRR signalling activates protein kinase C (PKC) which in turn phosphorylates cytosolic subunits of NADPH oxidase which translocates to the phagolysosomal plasma membrane and assembles with its corresponding subunits to form the active multiunit complex NADPH oxidase. The enzyme uses oxygen to convert cytosolic NADPH to superoxide anion. The superoxide anion either converts spontaneously to hydrogen peroxide or is converted by peroxide dismutase. The production of ROS, like peroxide and superoxide, and NOS increases the microbicidal activity of macrophages. Besides this induction of an additional potent killing mechanism, hydrogen peroxide can also act as a second messenger by inducing pro-inflammatory signalling pathways via the activation of NFκB and AP-1 transcription factors [26].

CHEMOTAXIS Macrophages play an essential role in host defence as mediators of innate immunity. However, in many infections the number of tissue-resident macrophages is insufficient to overcome the pathogenic burden. Activated tissue-resident macrophages produce chemoattractant cytokines in order to recruit blood stream circulating monocytes to the site of infection or inflammation, where they differentiate into distinct subsets of dendritic cell and macrophages. Monocytes are divided into two subsets according to their expression of surface receptors. Classical human monocytes are characterized by the expression of $CD14^{++}CD16^{-}$ (mice: lymphocyte antigen 6 complex; $Ly6C^{high}$ monocytes) and are rapidly recruited to the inflammatory site by chemotaxis [27]. A key regulator of monocyte recruitment produced by macrophages is monocyte chemoattracting protein-1 (MCP-1, also known as CCL2). Interactions with the corresponding G-protein coupled receptor CCR2, expressed on classical monocytes, promotes the migration of monocytes along the chemokine gradient to the inflamed foci [28].

Recruitment of phagocytes from the blood stream requires transendothelial migration, a process also known as leukocyte extravasation. Pro-inflammatory cytokines activate the endothelium to express selectins on the luminal surface which allows the binding to their carbohydrate ligands on leukocytes. Due to

weak interactions the binding to the endothelium is only transient and the monocytes roll along the blood vessel wall as a result of the shearing force of the blood flow. However, stronger linking to the endothelial cells is induced upon binding of chemokine receptors to their corresponding ligands that are present on the endothelial surface. Activation of the chemokine receptor leads to conformational changes of integrins on monocytes, thus leading to enhanced adhesion via the interaction with endothelial intercellular adhesion molecule (ICAM). The mononuclear phagocyte is now able to pass between endothelial cells to enter the subendothelial tissue along the chemokine gradient and begins to differentiate according to the stimuli of the local microenvironment [18].

The second subset of human monocytes is marked by the expression of $CD14^{low}$ $CD16^{+}$ (mice: $Ly6C^{low}$) [27]. These cells do not respond to chemotaxis and thus are not recruited during an inflammatory response. Their primary function seems to be patrolling, as microscopic studies in mice demonstrated that these cells continuously migrate along the luminal surface of endothelial cells [29].

In general, activation of macrophages induces the production and secretion of a broad array of different substances including chemokines, cytokines, growth factors, matrix remodelling proteases, protease inhibitors and further mediators of inflammation [30].

THE INTERFACE BETWEEN INNATE AND ADAPTIVE IMMUNITY Macrophages and dendritic cells are phagocytic antigen presenting cells (APC) which are crucial for the activation of the adaptive immune response. In order to activate naïve T cells APC must generate pathogen derived antigenic peptides and associate them with specialized surface glycoproteins called major histocompability complex (MHC) class I and class II. Priming of T cells with their corresponding antigen presented via MHC occurs in a highly specific manner and results in the clonal expansion of T cells and their subsequent differentiation into particular T cell effector subsets [18]. Intracellular antigens of e. g. viral origin are assembled with MHC class I, which is expressed on all nucleated cells, to induce activation of $CD8^{+}$ cytotoxic T cells. In contrast, extracellular antigens are presented via MHC class II expressed only on APC. The phagocytes internalize extracellular pathogens, like bacteria, fungi or parasites and present phagosomal derived antigens to activate $CD4^{+}$ T helper cells. A particular property of APC is cross presentation which implies presentation of exogenous antigens via MHC class I and cytosolic antigens via MHC class II, respectively [31]. The former occurs in a time-dependent manner. After phagocytosis of the extracellular pathogen the production of antigen peptides occurs during the maturation of the phagolysosome. The activation of NADPH oxidase and the successive ROS production create an alkylating milieu which impedes the activation of lysosomal proteases. Consequently, antigenic peptides remain available for assembly with MHC class I molecules. The time-dependent decrease of

ROS production leads to an acidification of the phagolysosme. Proteolysis is initiated and antigens that are derived from the late lysosome are presented via MHC class II molecules. Cross presentation of soluble antigens is localization-dependent, at which the route of internalization determines association with MHC class I or MHC class II [32].

1.1.3 Macrophage polarization and activation

As described above macrophages constitute a highly heterogenic population. Macrophages are distributed throughout the body and can be found in nearly all tissues, where they are exposed to distinct microenvironments. Due to their plasticity of gene expression, macrophages are capable of functional adaption during steady state and disease.

In 1964, Mackaness and colleagues performed studies on macrophage activation by infecting mice with the intracellular pathogens mycobacterium bovis bacillus Calmette-Guerin (BCG) or *Listeria monocytogenes*. They were able to observe diverse morphological and functional changes regarding the microbicidal activity of macrophages. Enhanced anti-microbial functions of the macrophages occurred in a non-specific although antigen dependent manner [33]. The following findings that lymphocytes are the key antigen specific cells wich are involved in macrophage activation paved the way for the identification of the pro-inflammatory cytokine interferon-γ (IFN-γ), which is produced by $CD4^+$ T helper 1 (Th1) cells, $CD8^+$ cytotoxic T cells and natural killer (NK) cells, as an inducer of oxidative metabolism and microbicidal activity of macrophages [34]. Thus, IFN-γ was the first identified stimulus of macrophage activation which was therefore designated as classical activation. In contrast to that, T helper 2 (Th2) cell derived cytokines interleukine-4 (IL-4) and IL-13 were described to induce alternative activation of macrophages which was marked by enhanced expression of the scavenger receptor MR, increased expression of MHC class II proteins and decreased expression of pro-inflammatory cytokines [35, 36]. Continuative research in the field of macrophage activation manifested the plasticity of these cells, whereupon several models of macrophage classification were developed in order to comprehensively illustrate macrophage diversity.

S. Gordon and colleagues proposed the first model of macrophage classification. Mirroring the Th1/Th2 dichotomy, macrophages are divided into pro-inflammatory M1 macrophages or classically activated macrophages and anti-inflammatory M2 macrophages or alternatively activated macrophages. The classical activation profile is induced by pro-inflammatory cytokines like mediators of Th1 response, e.g. IFN-γ and tumour necrosis factor-α (TNF-α), granulocyte macrophage-colony stimulating factor (GM-CSF) and microbial antigens like lipopolysaccharide (LPS). The main functions of M1 polarized macrophages are the combat of intracellular bacteria and virus infections, immune stimulation and tumour resistance. Char-

acteristically, M1 macrophages are potent APC with abundant expression of MHC molecules and promote immune response by the secretion of inflammatory mediators such as IL-12, IL-23 and TNF-α. In the murine system expression of iNOS and the concomitant production of NOS is a further hallmark of classically activated M1 macrophages. In contrast to that, Th2 cytokines IL-4 and IL-13 and further anti-inflammatory agents like glucocorticoids (GC) and IL-10 induce alternative activation of macrophages. M2 macrophages are primarily involved in homeostatic processes such as angiogenesis, tissue-remodelling, wound healing as well as regulation of immune suppression and killing of parasites. M2 macrophages are poor antigen presenters due to reduced expression of MHC class II proteins. Alternatively activated macrophages secrete low amounts of IL-12 and high amounts of anti-inflammatory cytokines and chemokines like IL-10, transforming growth factor-β (TGF-β) and CCL18. In murine M2 macrophages the arginine metabolism is shifted towards the arginase mediated conversion to ornithine and urea, thus lower levels of NOS are produced. Markers of M2 macrophages are diverse scavenger receptors like CD163, Stabilin-1 and MR (also known as CD206) [37-39]. However, it is important to note that M1-M2 polarization is an oversimplification of the *in vivo* situation and only represents two extremes of a wide spectrum of intermediate macrophage activation stages.

In order to differentiate the broad range of alternatively activated macrophages in more detail, Mantovani et al. suggested in 2002 the subdivision of M2 into M2a, M2b and M2c. At which M2a polarization is induced by IL-4 and IL-13, and M2b by immune complexes or agonists of TLR and IL-1R. These two subclasses execute immune-regulatory functions and drive type II responses. The M2c subset on the other site is induced in response to IL-10 and glucocorticoids and is overridingly involved in immunosuppression and tissue remodelling [40].

To paint a more realistic picture of the *in vivo* situation Moser and Edwards developed a further model of classification which groups macrophages according to their three primary functions: host defence, wound healing and immune regulation. The functional groups are associated with the three primary colours that were arranged in the colour wheel of macrophage activation. The different hues blending the primary colours represent the various macrophage subsets with mixed phenotypes [41].

However, macrophages are highly dynamic cells, which easily adapt to different signals from their environment and thus are subjected to constant changes in their phenotype indicating that all classification models are still insufficient to reflect the enormous plasticity and diversity of macrophage phenotypes. The limitation of classification models led Murray and further leading researchers in the field of macrophage activation to recommend guidelines concerning the description of properties of the specific macrophage population under investigation. Most importantly, they recommend the exact definition of the stimulus such as M(IL-4) or

M(IL-10) of macrophage activation to avoid unprecise term of M1 or M2 activation, whose definition might be dissimilar in between different labs. Moreover, the activation profile of macrophages should be examined by expression analysis of combinations of macrophage markers to define specific macrophage subsets [42].

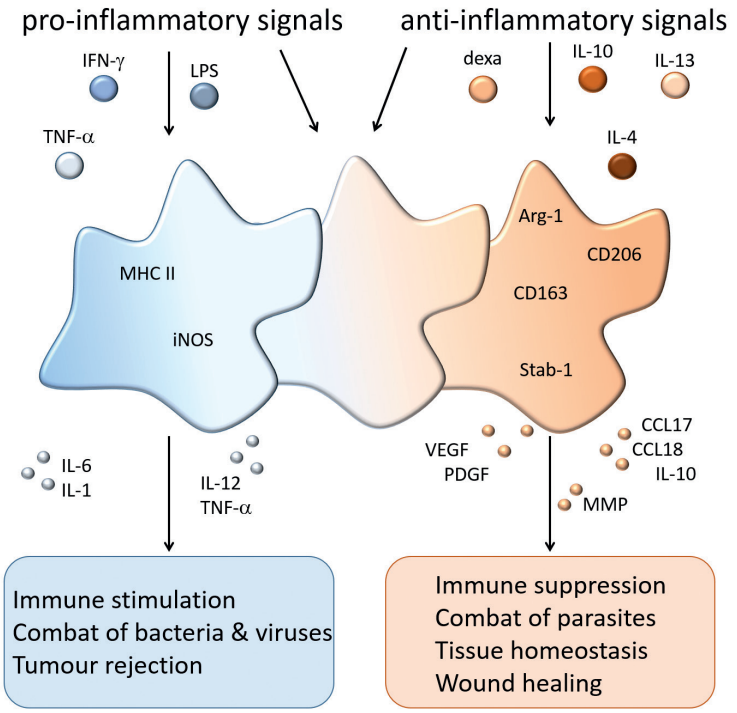

FIGURE 1: The microenvironment determines the functional phenotype of macrophages. *Inflammatory conditions (e.g. IFN-γ) induce the formation of an inflammation promoting M1-like phenotype, whereas anti-inflammatory mediators (e.g. dexa, IL-4) shape an immunosuppressive, trophic M2 like phenotype. Depending on the composition of the micromilieu, macrophages with a mixed phenotype develop.*

1.2 Tumour immunology

The growth of a tumour is a multistep process in which normal cells evolve progressively to become malignant. The transformation is caused by genetic instability, by which genetic heterogeneity of neoplastic cells is formed. Hanahan and Weinberg conceptualized common traits of neoplastic cells as the six hallmarks of cancer in 2000, and based on prevailing research subjoined two further hallmarks in 2013, namely:

1) Sustained proliferative signalling
2) Evasion of growth suppression
3) Resistance to cell death
4) Replicative immortality
5) Invasion and formation of metastasis
6) Induction of angiogenesis

Newly added hallmarks:

7) Reprogramming of energy metabolism
8) Tumour promoting inflammation

The acquirement of these characteristics of self-sufficiency enables transformed cancer cells to form tumours. Tumours are complex tissues which are composed of several cell types – besides neoplastic cells and non-malignant stromal cells, infiltrating leukocytes represent a further important integrant, which can be found during all tumour stages [43]. First links between cancer and inflammation were already made in the late 19th century, when Rudolph Virchow discovered that chronic inflammations may promote tumour growth already pointing towards macrophages as key players of cancer-related inflammation [44]. Accumulating evidence by continuative studies of the past years revealed the close relationship between local inflammation and tumour growth. Epidemiological studies revealed that the regular use of non-steroidal anti-inflammatory drugs (NSAID) such as aspirin reduces the risk of developing colorectal cancer and adenoma by inhibiting cyclooxygenase (COX), which is overexpressed in numerous cancers [45]. In 2008 approximately 16 % of malignancies worldwide were attributable to infectious agents [46]. Designative features of cancer-related inflammation are the presence of inflammatory cells and mediators, also in tumours arising without inflammatory predisposition, as well as tissue remodelling and induction of angiogenesis.

The promoting effects of inflammation to tumour development can be subdivided into intrinsic and extrinsic pathway. The intrinsic pathway requires the occurrence of a genetic event. Mutations in oncogenes or tumour suppressor genes in neoplastic cells establish the activation of signalling pathways that create an inflammatory tumour promoting microenvironment [47]. One of the most common cancer related mutations affects the proto-oncogenes RAS. Aberrant regulated activation of GTPases of the RAS family facilitates increased proliferative

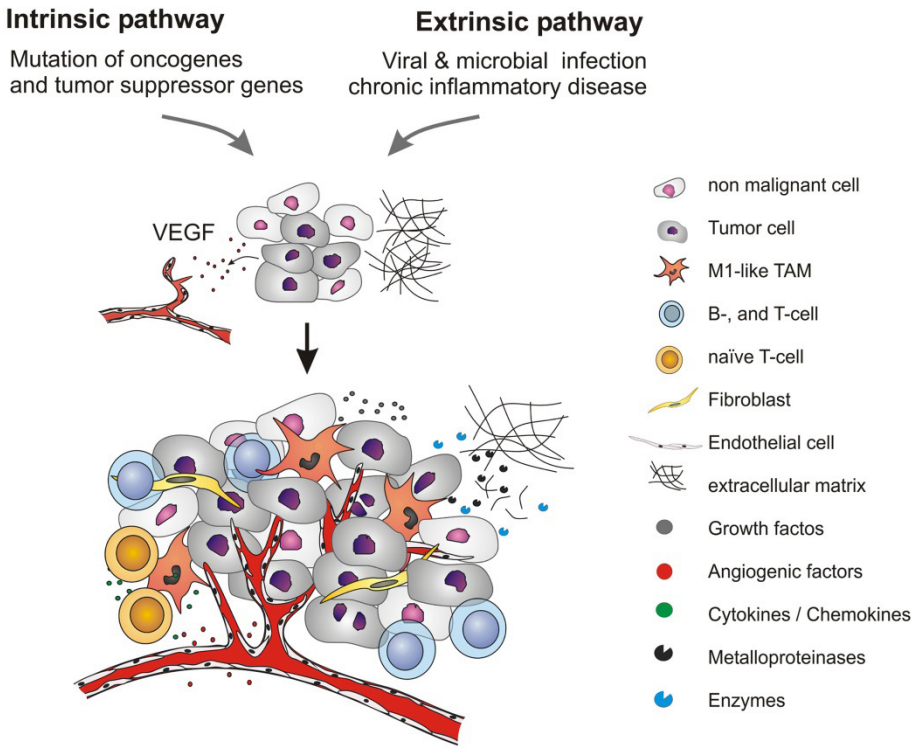

FIGURE 2: Inflammation related tumourigenesis. *Cancer promoting effects of inflammation can be conceptualized by the concurrence of an intrinsic and an extrinsic pathway. The intrinsic pathway comprises mutations in oncogenes and tumour suppressor genes which create an inflammatory tumour promoting environment. The extrinsic pathway promotes tumourigenesis via the presence of a smouldering inflammation due to an infection or chronic inflammation. Both pathways converge to promote tumour initiation [55].*

potential and reduced susceptibility to apoptosis of neoplastic cells through activation of mitogen activated protein kinase (MAPK) downstream signalling [48]. In approximately 50 % of melanoma a mutation in the BRAF gene, a downstream target of RAS belonging to the RAF family, leads to its continuative activation independent from extracellular stimuli [49]. BRAF mutated melanoma cells create and anti-inflammatory and pro-angiogenic microenvironment due to increased secretion of IL-6, IL-10 and vascular endothelial growth factor (VEGF) facilitating the immune evasion of the neoplastic cells [50].

On the other hand infections, autoimmune disease and further inflammatory conditions, which can occur before or during carcinogenesis, contribute to tumour development via the extrinsic pathway [47]. Excessive production of ROS and NOS by inflammatory cells, especially macrophages in the course of the respiratory burst (described in 1.1.2) may result in the formation of mutagenic peroxynitrite. Hence, activated inflammatory cells facilitate genomic alterations by interactions with the DNA in the proliferating epithelium during tissue regeneration [51, 52]. Chronic inflammations like Crohn's disease and inflammatory bowel disease pre-

dispose to development of colon carcinoma. Virus infections like Hepatitis B/C are associated with liver carcinoma and infection with the gram negative bacterium *Helicobacter pylori* is a major cause of gastric cancer, to give just a few examples that link inflammatory conditions to cancer [51, 53]. The extrinsic and intrinsic pathways contribute simultaneously to the formation of a so called smouldering inflammation, which is described as a subclinical inflammation where the resolution reaction of inflammation failed and thus creates a mutagenic environment that promotes cancer initiation [54]. Numerous inflammatory cytokines and chemokines recruit and activate immune cells, such as T cells and macrophages to the site of the smouldering inflammation which in turn promote immune evasion, tumour cell proliferation and angiogenesis.

1.3 Tumour associated macrophages

Tumours constitute complex organ like structures which are composed of proliferating malignant cells, mesenchymal cells and cells of hematopoietic origin like endothelial cells and leukocytes, amongst which in particular macrophages can be found numerously within the tumour infiltrate. The macrophages are shaped by the tumour microenvironment resulting in a phenotype which promotes tumour growth. So called tumour associated macrophages (TAM) can be found during all stages of tumour development. In general, TAM are involved in tumour initiation, progression and metastasis as providers of angiogenic, anti-inflammatory and matrix remodelling factors [56]. The important tumour supportive functions of macrophages are reflected by the findings that in many different cancers high TAM density correlates with poor patient prognosis [57, 58]. In melanoma for example significantly increased numbers of TAM have been found in thick melanomas which correlated with increased invasiveness and the formation of metastasis [59]. Further evidence for the tumour promoting effect of macrophages was provided by a murine model of breast cancer; monocyte recruitment was genetically prevented, resulting in delayed tumour development and decreased formation of metastasis [60].

TAM originate from recruited Ly6C^{high} monocytes which are derived from the bone marrow where their release is augmented during tumour growth [61]. The recruitment of the monocytes is mediated by various chemokines, cytokines and growth factor. One major chemoattractant is the C-C chemokine CCL2, also known as MCP-1. Already in 1992 researchers demonstrated that CCL2 overexpression in murine melanoma promoted monocyte infiltration [62]. Furthermore, the relevance of CCL2 has been substantiated by the finding that non-tumourigenic melanoma cells which were genetically engineered to express CCL2 give rise to tumours due to modest monocyte/macrophage infiltration [63]. Further chemo-

kines involved in monocytes recruitment are CCL5, CCL7, CXCL8 as well as CXCL12 [64]. Besides chemokines, different cytokines and most importantly CSF-1 are involved in the tumour mediated recruitment of monocytes. Similar to the previously described CCL2 tumour model, Dorsch et al. generated a CSF-1 transgenic plasmacytoma cell line and observed augmented monocyte infitration in a transplant tumour model using BALB/C mice [65]. In addition, VEGF has been shown to be implicated in the recruitment of TAM into beast carcinoma [66, 67].

A hallmark of macrophages is their plastic gene expression profile. While in early stages of tumour development M1-like macrophages prevail, M2-like TAM are predominantly found in fully developed solid tumours [68]. As already described above, a pro-inflammatory milieu fostered by M1-like macrophages and further immune cells promotes tumour development. Suppression of anti-inflammatory functions of macrophages by ablation of IL-10 or its downstream target signal transducer and activator of transcription 3 (STAT3) supports the generation of a smouldering inflammation which in turn is associated with tumourigenesis in the colon [69, 70]. Besides STAT3, NFκB constitutes an important transcriptional regulator of innate immune response by acting downstream of TLR to regulate the expression of pro-inflammatory cytokines such as IL-1 and TNF-α [71]. Targeted deletion of inhibitor of NFκB kinase subunit β (IKKβ) and thus impaired NFκB signalling in $LysM^{+}$ myeloid cells in a murine mouse model of colitis-associated cancer led to significant reduction of tumour size [72]. In the course of immunoediting, tumour cells create an anti-inflammatory environment by secretion of anti-inflammatory cytokines like IL-4 and TGF-β that promotes M1/M2 transition thus in developed solid tumours macrophages are trophic M2-like.

In tumours discrete TAM subpopulations with site specific functions exist. In hypoxic regions TAM characteristically express MHC II^{low} and exhibit a pro-angiogenic M2-like phenotype, while in well oxygenated tumour regions TAM are MHC II^{high} [73, 74]. In these hypoxic areas TAM secrete growth factors like VEGF and platelet derived growth factor (PDGF) to induce angiogenic sprouting of blood and lymph vessels, which in turn facilitates tumour cell intravasation and the development of metastasis. In perivascular areas, TAM are sources of growth factors like epidermal growth factor (EGF) and hepatocyte growth factor (HGF) which induce tumour cell proliferation. By secretion of metalloproteinases (MMPs) TAM mediate matrix remodelling which is important both for angiogenesis and tumour tissue invasion. In addition, TAM inhibit an efficient anti-tumour immune response by producing anti-inflammatory mediators like IL-10, TGF-β and prostaglandin E2, while expression of IL-12 is down-regulated [37, 75].

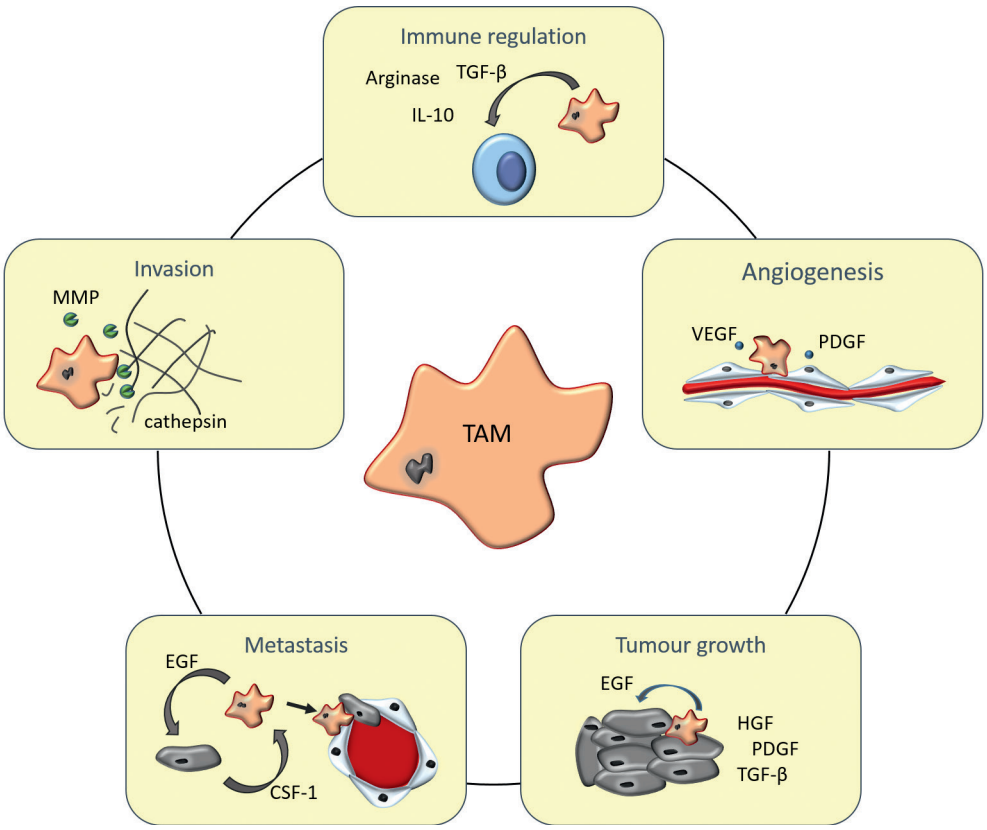

FIGURE 3: Tumour associated macrophages promote tumour progression. TAM *are key players in the tumour stroma as sources of tumour growth supporting chemokines, cytokines, growth factors and matrix remodelling enzymes. Thus* TAM *mediate immunoediting and regulate the angiogenic switch to induce tumourangiogenesis. Furthermore,* TAM *promote tumour cell proliferation and direct tumour cell migration towards blood vessels to facilitate intravasation of tumour cells and the formation of metastasis. By secretion of matrix remodelling enzymes* TAM *support tumour cell invasion.*

1.3.1 Tumour progression and angiogenesis

An essential event during the conversion from benign to malignant in the course of tumour progression is the development of a tumour vasculature. Tumour growth beyond a critical mass requires the establishment of a vascular network to warrant sufficient supply with nutrients, oxygen and growth factors. In addition, the tumour vessel system is required to deposit tumour cell metabolism derived waste products. The induction of tumour mediated angiogenesis is called 'angiogenic switch', which is characterized by tilting of the balance between pro- and anti-angiogenic signals in favour of the angiogenesis promoting mediators. Under physiological conditions, angiogenesis is a tightly regulated process whereas the development of tumour vessels occurs in a rather deregulated manner hence resulting in malformed leaky vessels [76, 77]. Different cell types are involved in controlling tumour angiogenesis amongst which macrophages play a central role.

Lin and colleagues demonstrated that shortly before the formation of a tumour vessel network in a model of breast cancer, the pre-malignant lesion is infiltrated by macrophages. Recruitment of monocytes to the tumour was found to be impaired in CSF-1 null mutant mice, which in turn inhibited the formation of tumour vessel system and tumour growth, respectively [78]. In a similar fashion various studies based on TAM depletion strategies demonstrated inhibition of angiogenesis resulting in reduced tumour growth [79, 80]. A specific subpopulation of TAM marked by the expression of CD11b and the angiopoietin receptor TIE2 has been identified as angiogenic macrophages [81]. By interaction with the TIE2 ligand angiopoietin-2 (ANG-2) on the endothelial surface these macrophages have been found to be aligned to the abluminal surface of blood vessels. The majority of TIE2 expressing macrophages (TEM) reside in viable, highly vascularized areas of the tumour and at the tumour periphery [82]. TIE2 expressing monocytes, the progenitors of TEM, have been detected in peripheral blood both from healthy donors and cancer patients, whereas $TIE2^+$ macrophages have solely been found in tumours and not in adjacent healthy tissues. Furthermore, co-injection of isolated human $CD14^+/TIE2^+$ monocytes and a glioblastoma cell line resulted in enhanced tumour vascularization and accordingly increased tumour growth [81]. Both depletion of the TEM subset and disruption of TIE2-ANG-2 based interactions between endothelial cells and TAM have been shown to inhibit angiogenesis and tumour progression [83, 84]. Consequently, recruited macrophages promote the development of a new high-density capillary network by induction of sprouting of tumour adjacent blood vessels which facilitates the immense expansion of proliferative malignant cells and further promote the progression of metastasis by establishing the routes for tumour cell intravasation.

1.3.2 TAM promote tumour growth

As already described above, the majority of tumours benefits from macrophage infiltration as TAM support tumour growth, angiogenesis and the formation of metastasis. TAM secrete a broad array of different mediators which create a tumour promoting microenvironment, like e.g. IL-10 and TGF-β. TAM derived IL-10 prevents the production of pro-inflammatory cytokines in an autocrine manner fostering an immunosuppressive microenvironment and promotes an alternative activation profile in TAM. In addition, IL-10 is involved in the differentiation of monocytes to macrophages, simultaneously preventing the maturation of dendritic cells [85]. Autocrine IL-10 stimulation leads to the up-regulation of programmed death-ligand 1 (PD-L1) expression in TAM which facilitates efficient blockade of anti-tumour response mediated by cytotoxic T cells [86]. TGF-β on the other hand induces differentiation of regulatory T cells (Treg) which are potent immunosuppressive cells [87]. Chemokines secreted from TAM like CCL13, CCL18 and CCL22 are further involved in the recruitment of Treg cells to the tumour to

suppress cytotoxic T cell responses [40]. While CCL2 plays a crucial role in macrophage recruitment, the chemokine also promotes Th2-responses which in turn induce M2-like polarization of TAM [88]. TAM are also an important source of the growth factors PDGF and VEGF, which promote tumour growth by inducing tumour cell proliferation and angiogenesis [78, 89]. Matrix remodelling is required for both tumour angiogenesis and invasive tumour growth. TAM contribute to matrix degradation by the secretion of various MMPs. Especially expression of MMP-9 has been linked to increased angiogenesis and tumour growth, which could be inhibited in a MMP-9 knock out model [90]. The TAM characteristic up-regulation of arginase-1 in response to IL-4 and IL-13 has been associated with impaired T cell function due to downregulation of CD3 ζ expression as a result of arginine depletion [91]. Moreover, TAM have been identified as sources of cysteine cathepsins. This family of proteases is implicated in terminal protein degradation, as well as activation of growth factors and transcription factors. With the aid of the RIP1-TAG2 (RT2) mouse model of pancreatic islet cell cancer, Gocheva et al. demonstrated that IL-4 induced macrophage derived cathepsins substantially enhance tumour growth, invasiveness and angiogenesis *in vivo* [92]. Diverse cathepsins are up-regulated in different cancer types, which is associated with increased tumour growth, invasion, angiogenesis and metastasis [93].

1.3.3 TAM promote metastasis

Monocytes and macrophages were found to direct tumour cell migration, intra- and extravasation, as well as homing to metastatic sites. By their matrix remodelling functions, e.g. by secretion of metalloproteinases like MMP-9, TAM have been found to localize at the invasive front of aggressively growing tumours. A meta-analysis revealed that high expression of MMP-9 correlated with poor patient prognosis [94]. In a model of murine breast cancer, Wyckoff and colleagues combined a chemotaxis-based *in vitro* invasion assay with multiphoton-based intra-vital imaging which allowed them to observe that macrophages and tumour cells migrate side by side in response to chemotactic factors. Tumour cells produce CSF-1 which attracts TAM and in turn stimulates the myeloid cells to produce EGF inducing tumour cell migration. Hence a paracrine-loop is established causing tumour cells and macrophages to co-migrate along collagen fibres in a lock-step fashion [95]. Macrophages direct tumour cells towards blood vessels leading to the formation of so a called tumour microenvironment for metastasis (TMEM), which serves as a prognostic factor for the formation of metastasis in breast cancer [96]. In addition, the number of perivascular macrophages correlates with the number of circulating tumour cells pointing towards the pivotal role of macrophages for tumour cell migration and intravasation [97].

Distinct TAM subsets are further involved in the formation of the pre-metastatic niche. Already in 1889, Steve Paget formulated the hypothesis of 'seed and

soil' in which he proposed that a pro-tumoural microenvironment is requisite at the site of metastasis. The primary tumour releases soluble factors to induce the formation of the pre-metastatic niche at distant sites. Myeloid VEGFR$^+$, CD11b$^+$ cells are recruited to these sites before circulating tumour cells arrive and create a receptive environment to promote tumour cell engraftment [98]. Upon arrival at the pre-metastatic niche, circulating tumour cells aggregate with platelets to form microclots which adhere to the blood vessel adjacent to the target tissue. The arrested tumour cells recruit monocytes via the assembly of a CCL2 chemoattractant gradient. The monocytes in turn express VEGF which permeablises the blood vessels facilitating tumour cell extravasation [56].

1.3.4 TAM as targets in cancer immunotherapy

Recent research and substantiated knowledge of tumour immunology have highlighted the significant contribution of smouldering inflammation and immune cells, especially of TAM to tumour initiation, progression and metastasis, thus TAM have evolved to interesting new targets in adjuvant cancer therapies. TAM directed anti-cancer therapies rely principally on TAM depletion, blocking of monocyte recruitment and strategies to re-educate TAM towards a tumouricidal, pro-inflammatory phenotype.

A promising strategy to target specific cell populations is the immunotoxin therapy of cancer. The directed depletion of TAM is achieved by coupling of toxins to monoclonal antibodies which bind to macrophage specific surface receptors and thus are able to induce apoptosis and to reduce the number of TAM. In human glioblastomas, folate receptor β has been identified to be expressed by TAM which could be targeted by a monoclonal antibody coupled to Pseudomonas exotoxin A. In a murine *in vivo* model, glioma tumour growth could be reduced by treatment with the immunotoxin due to successful depletion of TAM [99]. Another approach uses bisphosphonates such as clodronate or zoledronic acid (ZA) to achieve TAM depletion. Non-resorptive ZA is actively taken up by phagocytes by fluid-phase endocytosis eliciting reduced migration and proliferation, whereas the apoptosis rate is increased. Interestingly, ZA treatment also impairs MMP-9 secretion by TAM thus inhibiting angiogenesis and promoting re-education of TAM towards a tumouricidal M1-like phenotype [100]. Blocking of the pro-survival signal M-CSF via the administration of a monoclonal antibody (RG7155) which binds to the corresponding receptor CSF-1R, results in depletion of TAM due to induced cell death. Moreover, treatment of cancer patients with RG7155 resulted in declined infiltration of CSF-1R$^+$CD163$^+$ macrophages in tumour tissues [101].

To circumvent monocyte recruitment to the tumour, blocking of CCL2 signalling showed encouraging results in cancer therapy, as administration of neutralizing CCL2 antibodies in mice reduced tumour growth in different cancer models [102]. A humanized monoclonoal antibody (MLN1202) that binds to CCR2 thereby

inhibiting binding of CCL2 recently went through a phase II clinical trial including patients suffering from bone metastasis at which antibody administration elicited a positive effect (NCT01015560). Similarly, CCL5 is involved in chemoattraction of monocytes, as well as Treg's and myeloid derived suppressor cells (MDSC). The interaction with its respective receptors CCR1 and CCR5 represents a potential new target in adjuvant therapy of breast cancer. CCR5 antagonist are already used for the treatment of HIV patients, as blocking of the receptor prevents virus intrusion into the host cell [103]. Treatment of mice bearing subcutaneous tumours with the chemokine antagonist resulted in reduction of total tumour weight and volume accompanied by reduced numbers of infiltrating macrophages [104].

Induction of a tumouricidal macrophage phenotype has been achieved by activation of co-stimulatory CD40 with monoclonal antibodies (MAB). In a murine model of pancreatic cancer treatment with the CD40 directed MAB resulted in enhanced expression of MHC class II in macrophages and serum levels of pro-inflammatory cytokines IL-12, TNF-α and IFN-γ were increased, subverting the immunosuppressive tumour microenvironment. Furthermore, therapeutic efficacy could be demonstrated in patients suffering from pancreatic ductal adenocarcinoma when the antibody was administrated in combination with gemcitabine increasing the time period of progression free survival and overall survival rates [105]. NFκB activation in macrophages induces a pro-inflammatory gene expression profile. Several strategies aim at TLR mediated activation of NFκB in order to re-program TAM towards a M1-like phenotype. In macrophages, treatment with the TLR7 agonist Imiquimod stimulates the production of pro-inflammatory cytokines like IFN-α, TNF-α, IL-6, IL-8 and IL-12 and is used for the treatment of non-melanoma skin cancers such as basal cell carcinoma [106]. Further TLR agonists are under current evaluation. Administration of TLR9 agonist CpG-b also induces reprogramming of macrophages and thus increased innate immune response against tumours [107]. Intratumoural injection of the novel TLR7/8 agonist (3M-052) has been shown to raise a systemic anti-tumour response to the primary tumour as well as growth suppression at distant sites due to reprogramming of TAM towards tumouricidal phenotype in a model of murine melanoma [108]. Due to these promising effects several TLR agonists are currently in Phase I and Phase II clinical trials. The multikinase inhibitor Sorafenib, which is an approved drug for renal cell carcinoma and hepatocellular carcinoma, acts on the RAF/MEK/ERK signalling pathway. *In vivo* studies revealed that the inhibition of this pathway leads to downregulation of IL-10 expression in murine macrophages and simultaneous restoration of pro-inflammatory IL-12 reverting the TAM phenotype towards tumouricidal [109]. Similar results were obtained when IL-10 was targeted with CpG oligonucleotides which were administrated intravenously to tumour bearing mice resulting in suppression of the tumour promoting functions of TAM [110].

In summary, lots of strategies to prevent tumour supporting functions and to eliminate TAM have been successfully developed. The relevance of these adjuvant therapies is illustrated by the findings that TAM can influence the response to chemotherapeutics by counteracting chemotherapy induced tumour damage through misdirected tissue repair mechanisms thus supporting tumour growth during treatments [111]. Hence, targeting TAM might positively influence the responsiveness to classical anti-cancer therapies.

1.4 Lymphatic vessel endothelial hyaluronan receptor (Lyve-1)

1.4.1 Structure and Expression of Lyve-1

Lyve-1, also known as cell surface retention sequence binding protein 1 (CRSBP-1), has been first identified as a lymphatic vessel specific hyaluronic acid (HA) receptor in the course of a search for homologs of CD44, which aimed at the identification of further receptors for HA. Lyve-1 consists of 322 amino acids, containing a short hydrophobic leader sequence, followed by a serine and threonine rich hydrophilic region (212 amino acids), a single transmembrane domain and a short C-terminal intracellular cytoplasmic tail build by 70 amino acids. The greatest sequence similarities between Lyve-1 and CD44 were attributed to a single link domain which is located in the N-terminal extracellular portion of the receptors. The consensus sequence of the link domain can be found in the majority of HA-binding proteins. The hydrophobic pocket, which is responsible for interactions with HA, is formed by two β-sheets and two short α helices stabilized by two disulphide bridges between four cysteine residues. Both in CD44 as well as in Lyve-1 the link domain is extended by two further cysteine residues forming a third disulphide bridge, resulting in the formation of four additional β-sheets thus enlarging the pocket for HA-binding. A further unpaired cysteine residue is located in the transmembrane domain facilitating the formation of homodimers by disulphide linkage. In the region of the link-motif of Lyve-1, two sites for N-linked glycosylation have been identified while O-linked glycosylation sites were found in the transmembrane proximal region [112-114]. Northern blot analysis and immunohistological staining revealed abundant Lyve-1 expression in spleen, lymph nodes, heart, lung and fetal liver, as well as moderate expression levels in appendix, bone marrow, placenta, muscle and adult liver. Initially, Lyve-1 surface expression was assumed to be exclusive to lymphatic endothelial cells, equally distributed on the luminal and the basolateral surface of the vessels with the exception of expression in sinusoidal endothelial cells in the kidney and syncytiotrophoblasts, while being absent from blood vessels [112]. However, by immunohistological means Lyve-1 expression could also be demonstrated in liver sinusoidal endothelial cells and

Kupffer cells, which were CD68$^+$/Lyve-1$^+$ double positive [115]. In 2006, Schledzewski et al. provided further evidence for extra-lymphatic expression of Lyve-1. In murine tumour and wound healing models a subpopulation of F4/80$^+$, CD11b$^+$ macrophages had been discovered to express Lyve-1. In vitro, Lyve-1 expression was induced in murine bone-marrow derived macrophages (BMDM) by the combined stimulation with B16F1 tumour condition medium, IL-4 and glucocorticoids in approximately 25-40 % of the cells [116].

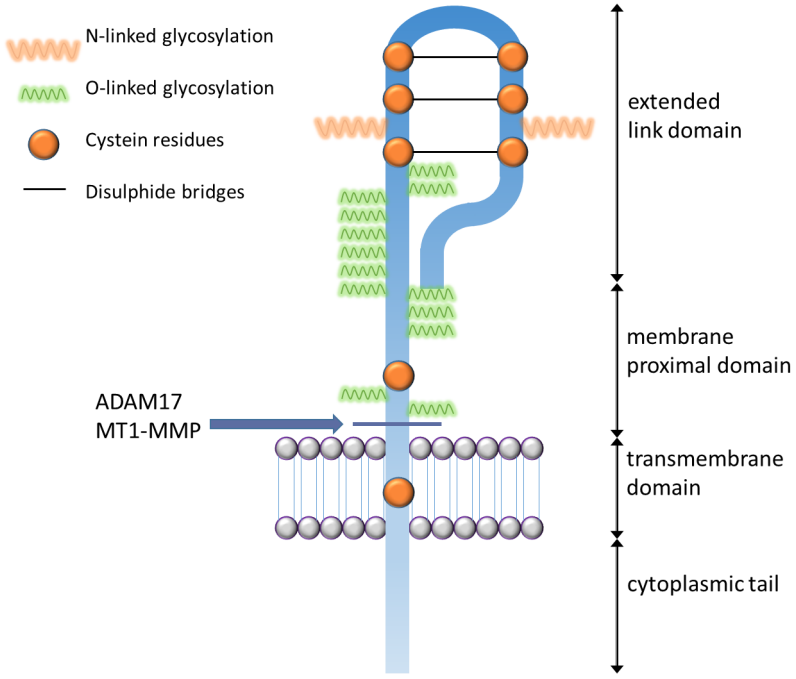

FIGURE 4: Structure of Lyve-1. *Lyve-1 is type I transmembrane glycoprotein. The N-terminal ectodomain contains an extended link domain which is stabilized by three disulphide bridges. In the region of the link domain two sites for N-linked glycosylation have been identified, while the membrane proximal domain is heavily O-glycosylated. In the transmembrane region an unpaired cysteine residue facilitates dimerization. ADAM17 and MT1-MMP mediate shedding of the Lyve-1 ectodomain (adapted from Jackson et al. [117]).*

1.4.2 Binding properties of Lyve-1

The functionality of the link domain of Lyve-1 was examined by binding assays using a recombinant fusion protein composed of the extracellular soluble domain of Lyve-1 (1-232) fused to human F_c. Highly specific interactions of Lyve-1 F_c with both soluble and immobilized HA were shown [112]. In addition, up-take of HA by fibroblasts which were genetically engineered to express murine Lyve-1 was demonstrated, pointing towards a possible role of Lyve-1 as a lymphatic specific endocytosis receptor for HA [118]. Further biochemical analyses examining the nature

of Lyve-1/HA binding revealed that the binding is mediated mainly by electrostatic interactions. Moreover, it was shown that the monomeric complete ectodomain (amino acids 1-232) efficiently bound HA, whereas the isolated Lyve-1 link domain (amino acids 1-169) was not competent of HA-binding indicating that elements from the membrane proximal stalk region are required for successful interactions [119]. Yet, binding of hyaluronic acid to endogenously expressed Lyve-1 in lymphatic vessels and cultured lymphatic endothelial cells could not be proofed. In a cell specific-manner Lyve-1 encounters glycosylation dependent masking of the HA-binding site. Enzymatic treatment with neuroaminidase of Lyve-1 in primary lymphatic endothelial cells resulted in the removal of sialylation sites and thus reconstitution of the HA-binding capacity of the receptor. Physiological mechanisms leading to the activation of Lyve-1 remained elusive [120]. Only recently, the importance of Lyve-1 density on the cell surface of lymphatic endothelial cells for HA-binding has been recognized. A critical threshold of Lyve-1 molecules on the cell surface is needed to enable HA binding, which could be achieved in human dermal lymphatic endothelial cells by lentiviral overexpression of Lyve-1. Artificial clustering of the receptor by cross-linkage with antibodies or complexation of HA also facilitated ligand interactions with the endogenous receptor in primary lymphatic endothelial cells [121]. Contemporaneously, CRSBP-1/Lyve-1 was recognized to be involved in cell surface retention of growth factors and cytokines, thus identifying cell surface retention sequence (CRS) motif carrying proteins PDGF-β, VEGF-α and insulin like growth factor-binding protein-3 (IGFBP-3) as further ligands of Lyve-1. The binding site for the growth factors does not coincide with the link domain, as HA-binding did not prevent interaction with CRS containing proteins [122-124]. At last, high affinity interactions between FGF-2 and Lyve-1 have been demonstrated in solution and on the cell surface of lymphatic endothelial cells. The glycosylation status of Lyve-1 played a critical role in growth factor binding, as deglycosylation of Lyve-1 resulted in decreased interactions. Furthermore, FGF-2 stimulation induced LYVE-1 expression *in vitro* and *in vivo* [125].

1.4.3 Processing of Lyve-1

In an attempt to determine possible Lyve-1 activation stimuli researchers found that the surface expression of the receptor is impaired in response to the pro-inflammatory stimuli TNF-α and TNF-β in primary lymphatic endothelial cells as well as in TNF-treated mouse ear dermal explants. Under inflammatory conditions the receptor is internalized and finally degraded in phagolysosomes, accompanied by reversible discontinuance of LYVE-1 gene expression [126]. In analogy to CD44, which undergoes proteolytic cleavage, two recent studies supplied evidence for ectodomain shedding of Lyve-1. Two cleavage sites for MT1-MMP (membrane-type metalloproteinase, also known as MMP-14) were identified in the ectodomain of Lyve-1, namely G^{64}-L in the link domain and A^{235}-L in the stalk region. MMP-14

mediated shedding of Lyve-1 negatively regulates Lyve-1 mediated signalling and lymphangiogenesis [127]. Almost simultaneously another group showed VEGF-A dependent ectodomain shedding of Lyve-1. The shedding process is dependent on VEGFR2 mediated phosphorylation of extracellular signal regulated kinase 1/2 (ERK1/2) and the subsequent activation of a disintegrin and metalloproteinase 17 (ADAM17) which cleaves Lyve-1 between the amino acid sequence 226–229 [128].

1.4.4 Lyve-1 signalling and functional implications

To characterize the function of Lyve-1, murine knockout models have been generated. Lyve-1$^{-/-}$ mice display a normal phenotype. The mice develop a functional lymphoid system and development and trafficking of the lymphocyte subset is unperturbed as well. Both metabolism and levels of HA in blood and tissue are not affected by the ablation of Lyve-1 from the organism. Furthermore, resolution of inflammation is comparable to wild type mice and no differences regarding growth of B16 and Lewis lung carcinoma (LLC) tumours have been noticed [129]. However, in a second study morphological changes of lymphatic vessels in the liver and intestine of Lyve-1$^{-/-}$ mice were observed. Enlargement of the vessels accelerated removal of intradermal injected macromolecular dextran pointing toward an increased interstitial lymphatic flow [130]. A possible explanation for this observation came from a study which demonstrated that Lyve-1 receptor engagement disassembles a complex formed by Lyve-1, PDGF-βR, β-catenin and VE-cadherin resulting in the internalization of VE-cadherin and thus leading to the opening of lymphatic endothelial cells (LEC) intercellular junctions and increased vascular permeability [131]. While no distinct function of Lyve-1 on HA metabolism has been noticed, stimulation with low molecular weight HA (LMW-HA) promotes Lyve-1 dependent lymphangiogenesis though the underlying mechanism is not fully understood yet. In the lymphatic endothelial cell line SVEC4-10, stimulation with LMW-HA induced Lyve-1 dependent proliferation, migration and tube formation by intracellular activation of PKC and ERK1/2 [132]. A second study demonstrated that LMW-HA stimulation induced co-localization of Lyve-1 with sphingosine 1 phosphate 3 receptor (S1P3) and the subsequent phosphorylation of the downstream targets Src and ERK1/2 in SVEC4-10 cells. Silencing either S1P3 or Lyve-1 expression attenuated intracellular downstream signalling [133]. FGF-2 constitutes an additional binding partner of Lyve-1 known to induce lymphangiogenesis. *In vitro*, the addition of the soluble Lyve-1 ectodomain inhibited migration, invasion and proliferation of FGF-2 stimulated lymphatic endothelial cells, while knockdown of Lyve-1 expression of LEC also reduced FGF-2 induced cell proliferation and tubulogenesis. Micropockets containing FGF-2 alone or in combination with Lyve-1, which were implanted in the cornea of mice, substantiated the modulating effect of Lyve-1 on FGF-2 mediated lymphangiogenesis [125]. Lyve-1 has further been identified to be involved in cell surface retention of growth factors,

which express a CRS motif like PDGF, VEGF and IGF-β. In cells, which expressing the *v-sis* gene product, overexpression of Lyve-1 was associated with increased cell proliferation and enhanced tumourigenicity *in vivo* via activation of PDGF β-type receptor. Hence, Lyve-1 is involved in autocrine growth regulation mediated by growth factors carrying the CRS motif [124].

1.4.5 Lyve-1 expression in TAM

In the past years, research in the field of tumour associated macrophages has revealed their tumour promoting effects making them interesting new targets in adjuvant cancer therapy. Though it became apparent that TAM constitute a highly heterogenic population within the tumour stroma, as different subpopulations executing different functions have been recognized. Consequently, a need for further TAM-specific marker exists to identify subpopulations and analyze their features in more detail. Our group concentrated on the identification and characterization of such macrophage markers. In murine models Ms4a8a, Stabilin-1 and also Lyve-1 have been discovered by our group to be expressed by TAM in different tumour models. *In vitro* these markers can be induced in BMDM by stimulation with a combination of tumour-conditioned medium, glucocorticoids and IL-4 [116, 134, 135]. In 2015, Dr. Kathrin Schönhaar published her doctoral thesis with the title 'Expression analysis of murine and human tumour associated macrophages'. The aim of her thesis was to compare similarities and differences concerning the expression of the three mentioned macrophages markers between human and murine TAM. In addition, she conducted continuative experiments to examine the nature of the Lyve-1 expression in human TAM. Her observations are the basis of this work and the results concerning Lyve-1 will be presented in the following.

Histopathological analyses of different human tumour entities revealed the presence of Lyve-1$^+$ macrophages in colon carcinoma, ovarian carcinoma and primary melanoma. *In vitro*, LYVE-1 was induced in PBMC after 7 days of stimulation with M-CSF, dexamethasone and IL-4. The addition of the glucocorticoid receptor (GR) antagonist mifepristone to the stimulation cocktail suppressed induction of LYVE-1 expression. In PBMC, co-cultivation with the human melanoma cell line WM115, which was derived from a primary melanoma, was able to induce LYVE-1 expression too, whereas co-incubation with the metastatic cell line WM266 was not. By immunoblotting and ELISA, a soluble form of Lyve-1 was detected in the cell culture supernatants of Lyve-1$^+$ PBMC, which were derived either from M-CSF/dexa/IL-4 (MDI) cytokine stimulation or by co-cultivation with WM115. The murine macrophage cell line RAW 264.7 and a human analogous cell line U937 were genetically engineered to express Lyve-1 to analyze protein processing of Lyve-1 in more detail. By immunoblot analysis a shorter version of Lyve-1 was detected with a molecular weight of approximately 55 kDa in the culture supernatant of the transgenic cells, while full length Lyve-1 was routinely detected at

around 70 kDa in the cell lysates. Stimulation of the transgenic cell lines with the shedding inducer APMA led to accumulation of the 55 kDa Lyve-1 form in the cell culture supernatant, while in the cell lysates the amount of full length Lyve-1 was reduced. The opposite was true, when the cells were treated with different sheddase inhibitors. Hence, the macrophage cell lines secreted soluble Lyve-1 by metalloproteinase mediated shedding.

In summary, Schönhaar outlined the existence of human Lyve-1$^+$ TAM and the dexamethasone dependent gene induction in PBMC. In addition, metalloproteinase mediated ectodomain shedding has been observed [136].

1.5 Aims of the study

We and others were able to demonstrate that Lyve-1 expression is in fact not restricted to the lymphatic endothelium. Schönhaar provided evidence for the existence of Lyve-1$^+$ tumour infiltrating macrophages which define a distinct subpopulation of TAM. In order to develop novel cancer treatment strategies involving TAM, it is essential to determine the net effect of distinct macrophage subpopulations. Thus this study focuses on the following:

VALIDATION OF LYVE-1 AS A MARKER OF MACROPHAGES PRESENT IN HUMAN MELANOMA

For this purpose, serial sections of human melanoma samples will be prepared for immunohistological analyses of Lyve-1 and macrophage differentiation markers. The newly established method of sequential staining will be applied on human melanoma sections for the successive staining of Lyve-1 in combination with macrophage markers for the explicit detection of Lyve-1$^+$ macrophages.

CHARACTERIZATION OF PBMC AS AN IN VITRO MODEL FOR LYVE-1$^+$ TAM

After prolonged stimulation of PBMC with MDI Lyve-1$^+$ cells were detected *in vitro*. Further analyses of this primary cell model regarding time course and activated signalling pathways will define the basal requirements for Lyve-1 expression *in vitro*. The type of macrophage differentiation resulting from stimulation of PBMC with MDI will be characterized by macrophage associated markers such as CD163 and CD206:

DETERMINATION OF THE BIOLOGICAL RELEVANCE OF LYVE-1$^+$ IN TRANSGENIC CELLS

For functional analyses of Lyve-1, transgenic human and murine cell models will be established. These will be used to get first hints for a possible role of Lyve-1 in macrophages in basal cell tests like proliferation and migration assays.

Shedding of Lyve-1 will be examined in analogy to its homolog CD44, which is processed by metalloproteinases.

EFFECTS OF LYVE-1 AND GR SIGNALLING ON TUMOUR GROWTH IN ANIMAL MODELS

Tumour progression will be monitored in Lyve-1$^{-/-}$ mice to identify the net effect of Lyve-1$^+$ cells on tumour growth. The model of LysMcre;GRflox mice that impairs GR signalling in myeloid cells will be used to define the contribution of GR signalling to LYVE-1 induction in TAM *in vivo* and for the analysis of TAM differentiation in general.

2. METHODS

2.1 Biochemical Methods

2.1.1 RNA Isolation and cDNA Synthesis

After cultivation, eukaryotic cells were harvested and washed once in phosphate buffered saline (PBS), the cell suspension was spun down and the supernatant was discarded. The cell pellets were used for RNA isolation by spin column based purification with either the RNeasy Kit (Qiagen) or the innuPREP RNA Mini Kit (Jena Analytik) according to the manufacturer's protocol. In both cases RNA was eluted in a volume of 40 µL RNase free water. After isolation of total RNA with the RNeasy kit, removal of contaminating genomic DNA was achieved by a digest with DNase I (Fermentas) for 1 h at 37°C. In contrast to that, genomic DNA was removed by a precleaner column when the innuPREP RNA Mini Kit was used, thus an additional DNA digest was not necessary. RNA-concentration of the samples was determined with the aid of the photometer Nanodrop 2000 (Thermo Scientific). The RNA was stored at -80°C.

Reverse Transcription (RT) was conducted to transcribe single stranded mRNA into double stranded, more stable cDNA. In contrast to genomic DNA of eukaryotes, cDNA is characterized by the lack of introns. To retranscribe total mRNA of a sample the fact that a poly-A-tail is attached to the 3' end of eukaryotic mRNA as a protection against degradation by exoribonucleases was exploited by using oligo(dT) primers. For reverse transcription 1 µg of RNA per sample was used. The reaction was performed with RevertAid H Minus M-MuLV Reverse Transcriptase (Fermentas). cDNA was produced by a two-step RT-PCR protocol as follows.

Total RNA	1 µg
Oligo(dT) (100 µM)	0.5 µg
RNase free water	To 12.5 µL

The premix was mixed gently and incubated for 5 min at 65°C and then chilled on ice before the bellow mentioned components were added.

5× Reaction Buffer	4 µL
RNase Inhibitor	0.5 µL (20 U)
dNTP Mix, 10 mM each	2 µL
RevertAid H Minus Reverse Transcriptase	1 µL (200 U)

Reverse transcription was performed at 42°C for 60 min followed by heat induced inactivation of the enzyme at 70°C for 10 min. cDNA samples were stored at -20°C.

2.1.2 Polymerase Chain Reaction (PCR)

PCR is a commonly used method for the amplification and detection of specific DNA/cDNA segments of up to 6 kb. Standard PCR occurs generally in three steps: denaturation, annealing and elongation. First single stranded DNA (ssDNA) is produced by heating the sample to 95°C, followed by a temperature reduction which allows the annealing of oligonucleotide primers which are complementary to the flanking sites of the DNA region of interest. Thus a thermostable DNA polymerase can bind to the primer/ssDNA hybrid and elongate the primer according to the template sequence by incorporation of the corresponding dNTPs [137]. For PCR cDNA was diluted 1:10 in ddH2O and the DFS-TAQ DNA Polymerase from Bioron with the appendant buffer was used to prepare the following reaction mixture:

10× complete Buffer	1.2 µL
dNTP (2 mM)	0.6 µL
Primer forward (10 µM)	0.5 µL
Primer reverse (10 µM)	0.5 µL
TAQ DNA Polymerase	0.1 µL
H_2O	6.1 µL
cDNA (1:10)	1.0 µL
Total	10 µL

The general cycling conditions were:

TEMPERATURE [°C]	TIME	REPEATS
95	3 min	1×
95	30 s	34×
(60) adaption according to primer pair	30 s	
72	45 s	
72	5 min	1×
4	∞	1×

For analysis the PCR products were loaded on 1-2 % agarose gels containing 10 % Nancy-520, a fluorescent stain for dsDNA. The gels were run in a chamber filled with TAE and electrophoresis was performed at 130 V for 30 min. DNA bands were visualized with the aid of Intas UV Systems N-90m and documented by photographing.

2.1.3 Quantitative Real-Time PCR (qRT-PCR)

qRT-PCR allows the simultaneous amplification and detection of PCR products. By the use of dsDNA intercalating dyes a fluorescent signal is generated, which enables the quantification of the amount of PCR product during each PCR cycle in the exponential phase of DNA amplification. The resulting fluorescence signal is measured and plotted as a function of the cycle number by a sequence detection system. It is possible to extrapolate back in order to calculate the amount of template prior to the start of the PCR [138]. For normalization of the template amount in the PCR, it is necessary to include an internal control, at which housekeeping genes are used. In the following analyses gene expression was calculated in relation to β-Actin [139].

Prior to qRT-PCR, template cDNA was diluted 1:40 in ddH_2O, mixed with forward and reverse primer (2 µM) of the gene of interest, as well as SyBRGreen Master Mix (Applied Biosystems) according to the manufacturer's protocol. Besides the fluorescent dye the master mix contains buffer, dNTPs and a thermostable hot-start DNA polymerase. The PCR was run under standard conditions with an MX3000P sequence detection system (Stratagene).

2.1.4 Protein isolation and modified Lowry assay

For protein isolation eukaryotic cells were harvested and washed as described before (compare to 2.1.1 RNA Isolation). Cell pellets were resuspended in cell lysis buffer, for subsequent immunoblot analysis RIPA buffer was used, whereas DISC buffer was applied in the case of sample processing for immunoprecipitation (IP). The samples were incubated on ice for 20 min and centrifuged at 4°C at 14 000 g for 10 min to remove cellular debris. The protein containing supernatant was transferred to a new collection tube.

Colorimetric quantification of protein concentration was then determined by DC™ Protein Assay (Bio Rad), which is a method based on Lowry-Assay. In brief, in an alkaline medium copper-treated proteins reduce Folin reagent resulting in the development of a characteristic blue colour, which shows strong absorbance at λ=650 nm. In order to determine the protein concentration with colorimetric means, a standard curve had to be measured. For this purpose, a seven-point standard curve was prepared using bovine serum albumin (BSA) diluted in the corresponding lysis buffer with a range from 10 mg/mL to 0.16 mg/mL.

2.1.5 SDS PAGE

SDS PAGE facilitates the separation of proteins according to their molecular weight. The polyacrylamide gels were casted just before use. First the resolving gel was prepared, whereat the concentration of polyacrylamide and thus the resulting pore size of the gel was varied according to the molecular weight of the protein of

interest. During polymerization the resolving gel was covered carefully with isopropanol to avoid drying up.

RESOLVING GEL

	10 %	12 %
dH_2O	5.9 mL	5.0 mL
30 % Bisacrylamide	5.0 mL	6.0 mL
1.5 M Tris, pH=8.8	3.8 mL	3.8 mL
10 % SDS	0.15 mL	0.15 mL
10 % APS	0.15 mL	0.15 mL
TEMED	6 µL	6 µL

When the polymerization of the resolving gel was completed, the isopropanol was demounted and the stacking gel was casted on top of the resolving gel and a comb was inserted.

STACKING GEL

dH_2O	1.72 mL
30 % Bisacrylamid	0.5 mL
0.5 M Tris, pH=6,8	0.76 mL
10 % SDS	0.03 mL
10 % APS	0.03 mL
TEMED	3 µL

Protein samples were mixed with Laemmli Buffer. This buffer does not only serve as a loading dye, but it also contains β-mercaptoethanol and SDS. These ingredients crack up the protein tertiary structure. While β-mercaptoethanol splits disulphide-bridges, SDS leads to denaturation of the protein and a constant relation between negative charge and molecular weight is achieved. The samples were boiled in Laemmli at 95°C for 5 min. The SDS-gels were placed in electrophoresis chambers and covered with TAE buffer. Equal protein amounts were loaded on the gels, for the assignment of protein size PageRuler plus pre-stained protein ladder (Fermentas) was used. The samples were then subjected to gel electrophoresis at 20 mA at room temperature. The proteins migrated from cathode to anode due to their negative charge, in which smaller proteins are able to travel the gels faster than bigger ones hence separation occurred according to protein size [140].

2.1.6 Western Blot

Subsequently, the proteins were transferred horizontally to nitrocellulose or PVDF membranes. Blotting was performed either in a wet chamber overnight at 4°C and 180 mA or in a semi-dry manner for 35 min at 0.45 A (limit 25 V) in the Trans-Blot Turbo device (Bio Rad). After blotting, the membranes were blocked for 1 h at room temperature in PBS containing 5 % skimmed milk powder. Then, the membranes were incubated with the desired primary antibodies diluted in 5 % milk either at room temperature for at least 2 h or overnight at 4°C. Afterwards the blots were washed thoroughly three times with PBS. Meanwhile a suitable horseraddish-peroxidase (HRP)-conjugated secondary antibody was diluted in PBS + 5 % skimmed milk powder. HRP is a reporter protein that catalyzes the oxidation of luminol. The secondary antibody was added on top of the membrane and incubated for 1 h at room temperature on a shaker. After washing again thrice for 10 min with PBS, the membranes were treated with Luminate Forte Western HRP Substrate for 3 min. The luminescent signal was then detected by exposing the blots to high performance chemiluminescence films (Amersham) and the films were developed in the autoprocessor Curx 60 (Agfa).

2.1.7 Immunoprecipitation (IP)

This method allows the purification of specific proteins from crude protein lysates as well as from cell culture supernatants. For this purpose, an affinity matrix is used which is composed of protein G cross linked to agarose. Protein G is a component of the bacterial wall capable of binding the F_c domain of IgG antibodies from different species.

One day prior to immunoprecipitation, the cells were washed once and complete growth medium was replaced by starvation medium (cell culture medium without FCS). On the following day, the cells were harvested as described previously. The cell pellet was lysed for 30 min on ice using DISC lysis buffer. Cellular debris were removed by centrifugation at 14 000 g for 5 min, the protein containing supernatant was transferred to a new tube and the protein concentration was determined (see also 2.1.4 Lowry Assay). Concentrations of the samples were adjusted with DISC buffer in such a way that 4 mg/mL protein per sample were obtained. The antibody of interest was added, at which 1-2 µg antibody per 4 mg protein sample were applied. Meanwhile, the affinity matrix Protein G agarose (Roche) was prepared. For this purpose, 40 µL of the matrix stock solution were used per 4 mg protein sample. The matrix was spun down for 1 min, 1500 g and 4°C, the supernatant was discarded and the matrix was resuspended in 1 mL DISC buffer. The washing procedure was repeated three times. Finally, the matrix was diluted in DISC buffer such that an amount of 100 µL Protein G agarose per 4 mg protein sample resulted. The combination of antibody, protein sample and Protein G agarose was incubated overnight at 4°C on a rotor. Subsequently, the matrix was washed

with DISC buffer at least three times (400 g, 1 min, 4°C) to remove unbound proteins. Samples were boiled for 10 min at 95°C in 1× Laemmli buffer and loaded to SDS-polyacrylamide gels and subjected to analysis by western blot or Coomassie staining.

2.1.8 Deglycosylation digest

As the protein of interest, Lyve-1, is a highly glycosylated protein a deglycosylation digest was performed in order to remove N- and O-linked glycosylation side chains of the protein.

For deglycosylation total cell lysates were obtained from Lyve-1$^+$ transgenic cells lines. The digest was performed with the EDEGLY enzymatic protein deglycosylation kit (Sigma-Aldrich), which includes the following proteins: PNGase F, O-Glycosidase, α-(2→3,6,8,9)-Neuraminidase (Sialidase A), β-(1→4)-Galactosidase and β-N-Acetylglucosaminidase. The digest was performed according to the manufacturer's instructions at 37°C for 3 h.

2.1.9 Enzyme-linked immunosorbent assay (ELISA)

Prior to ELISA, cell culture supernatants were centrifuged to obtain cell-free culture media. After collection human blood samples were allowed to clot at room temperature for 15–30 min. The precipitate was removed by centrifugation at 1000 g. Immediately after the centrifugation step, the resulting supernatant or plasma was transferred to a new tube. All ELISAs were performed according to the manufacturer's instructions.

ELISA is a robust and sensitive method that facilitates the detection and quantification of specific soluble antigens, e.g. secreted cytokines or proteins. In this case, the ELISA method was used for the analysis and characterization of cell culture supernatants and plasma samples. The performed ELISAs were based on the principal of sandwich ELISA. Shortly, a primary capture antibody was passively immobilized onto the plastic surface of 96-well plate. Samples were added in the appropriate dilutions, so the antigen of interest could be bound whereas unbound components were removed by washing. A second primary antibody, the so called detection antibody, against another epitope of the antigen was added. Finally, an enzyme-linked antibody, e.g. a secondary HRP-antibody, was applied that in turn binds the detection antibody. The amount of antigen was then determined by assessing the enzyme activity by conversion of its substrate to a measurable product. For evaluation of the experimental outcome, sample values had to be correlated to measurements of a standard curve.

2.1.10 Fixation

For immunohistochemical analyses different samples types were used and prepared in different ways for optimal outcome.

Cells were either grown to confluency on coverslips or centrifuged onto microscopic glass slides as cytospins. Dependent on the desired primary antibody, the cells were either fixed with ice-cold acetone for 10 min or with PFA. For PFA-fixation, the cells were washed first with PBS, then treated with 2 % PFA for 10 min and then washed with 0.5 % Triton X-100 in PBS for 15 min. After fixation with 4 % PFA for 10 min, the cells were again washed thoroughly three times with PBS.

After cutting, paraffin sections were dried overnight at 37°C. In order to remove the surrounding paraffin, the sections were rinsed twice in xylene and then rehydrated by incubation in a decreasing alcohol series (100 %–70 % EtOH) and finally the sections were washed with water twice. For antigen-retrieval the sections were heated to 95°C for 20 min either in EDTA pH9 or citrate pH6 buffer (Leica).

Cryo-sections were air-dried overnight after preparation. Fixation was performed with ice-cold acetone for 10 min at room temperature.

2.1.11 Immunohistochemistry

Fixed samples were washed twice in PBS and once in PBS + 0.01 % Tween20 (PBST). To block intrinsic peroxidase, the samples were treated with 0.3 % peroxide in PBS for 10 min. Afterwards the samples were washed as before and protein block was performed by addition of 2 % BSA in PBS for 30 min. Next, the protein block was removed and the samples were incubated with the desired primary antibodies, which were diluted in Antibody Diluent (Dako) for 2 h. To remove unbound antibodies, the samples were again washed as before and incubation with the appropriate HRP-coupled secondary antibody (in Antibody Diluent) was performed for 45 min. The specimens were first washed as previously described, before AEC chromogen (Dako) was used for the visualization of the HRP-labelled target-molecules by the formation of an insoluble red dye. The staining was stopped by rinsing of the samples in water and counter-staining was conducted with Mayer's Haemalaun (Merck). The stained samples were embedded in faramount aqueous mounting media (dako). Pictures were taken with the Nikon Eclipse NI microscope with the Clara interline CCD camera (Andor) NIS-Elements Advanced software (Nikon). Images were arranged using Adobe Photoshop 6.0 software.

2.1.12 Sequential staining

Paraffin embedded tissue samples were dewaxed as described before with the aid of a xylene/alcohol series. For antigen retrieval specimen were treated with proteinase K (Dako) for 5 min. After rinsing once in water and TBS, the samples were blocked for 10 min in 5 % skimmed milk in TBS. Primary antibodies were diluted

in antibody diluent (Dako) and applied for 1 h at 37°C or overnight at 4°C. Surplus primary antibodies were removed by washing thrice in TBS before the specimen were incubated with peroxidase blocking solution (Dako) for 7 min. The samples were washed again as before and were covered with HRP-labelled secondary antibody for 30 min at room temperature. For detection of HRP-labelled cells the substrate VECTOR NOVARED Peroxidase solution (Vector Laboratories) was used for 10 min at 37°C. After rinsing in water for 5 min counterstaining was performed with 10 % Haemalaun-solution for 6 min. The specimens were then placed successively into 80 %, 96 % and 100 % ethanol and twice in xylene for 2 min each, before they were mounted with eukitt. After documentation of the staining per microscopy, the cover slips and mounting medium were removed by placing the samples into xylene overnight. On the following day the samples were re-hydrated by the descending xylene/alcohol series and de-stained in stripping buffer at 50°C for 1 h. The samples were washed consecutively in water (5 min), 95 % ethanol (2 min), water (2 min) and finally in TBS (2 min). Thus, the samples were completely de-stained and could be stained for another antigen of interest.

2.1.13 Immunofluorescence

For immunofluorescent staining the samples were fixed as described before. The samples were washed twice in PBS and once in PBST. Blocking was performed with 2 % BSA in PBS. Primary antibody was diluted in Antibody Diluent and incubated with the specimens for at least 2 h. After washing as before, the samples were treated with the corresponding secondary antibody labelled with a fluorochrome. In the case of double staining, primary antibodies were mixed and incubated simultaneously with the samples. Appropriate secondary antibodies were used which were labelled with different fluorochromes. Specimens were embedded in fluorescent mounting media (dako) and pictures were taken with the Nikon Eclipse NI microscope with the Clara interline CCD camera (Andor) NIS-Elements Advanced software (Nikon). Images were arranged using Adobe Photoshop 6.0 software.

2.1.14 Fluorescent associated cell sorting (FACS) analysis

FACS is a method based on the simultaneous measurement of different physical characteristics of cells. For this purpose, the cells are transported in a fluid to pass a laser beam as single cells. By detection of the emerging scattered and transmitted light as well as emitted fluorescence the relative granularity or intern complexity, the size of the cell and the fluorescence intensity can be determined. Thus, the method allows the characterization of expression levels of specific proteins through tagging cells with fluorochrome coupled antibodies.

For FACS surface staining the cells were prepared as a single cell suspension. The cells were washed once in FACS surface buffer. The samples were then treated with 1.5µL F_c block (BD bioscience) per 1×10^6 cells for 10 min. Next, the fluorochrome coupled antibody was added for further 20 min at room temperature. After washing twice with FACS surface buffer, the cells were resuspended in approximately 300µL FACS surface buffer and analyzed with FACS-Canto™ II (BD Biosciences) and data was analyzed using FlowJo V10.1 software.

2.1.15 Detection of reactive oxygen species and nitric oxygen species

$CD14^+$ cells were stimulated for seven days either with M-CSF or M-CSF/dexamethasone/IL-4 and washed once in PBS. The cells were incubated for 30 min either with HPF (Cell Technology) at 37°C for the detection of ROS or with DAF-2DA for NOS detection (Cell Technology) at 4°C. Both reagents are non-fluorescent by themselves. In the presence of hROS and NOS respectively they are readily converted to emit a strong dose-dependent fluorescent signal (excitation λ=488 nM and emission λ=515 nm). After cell loading, excess dyes were washed away with FACS surface buffer and the cells were subjected to flow cytometric analysis with FACS-Canto™ II (BD Biosciences) and data was analyzed using FlowJo V10.1 software.

2.1.16 Expression Vectors

As a vector construct the previously described lentiviral 3rd generation pHAGE vector was used. This vector was modified by Mostoslavsky et al. by insertion of the human promoter sequence of EF1α and a StemCCA (stem cell cassette). The StemCCA was then replaced by a multiple cloning site (MCS), also called ADR3, an internal ribosomal entry site (IRES), the sequence of red fluorescent protein (RFP) and a puromycin resistance gene (Puro). The resulting construct constitutes the empty vector (EV) backbone, which will be called ADR3 EV in the following.

In order to generate a DNA insert which can be cloned into the vector constructs, cDNA of mmLyve-1 (clone IRAVp968E0743D, Genome CUBE) and hsLyve-1 (clone IRAUp969G0386D, Genome CUBE) was amplified with primers that add the restriction sites for the endonucleases Xba I and Mlu I to one end of the insert sequence each. The PCR amplification was performed with κ-HiFi HotStart PCR kit (VWR / formerly Peqlab). The included κ-DNA-polymerase enables high fidelity PCR amplification while proofreading is optimized with error rates approximately 100 times lower than commonly used wild-type TAQ. PCR was performed according to the manufacturer's recommendations:

COMPONENT	50 µL FINAL VOLUME
PCR-grade water	Up to 50 µL
5× κ-HiFi Buffer	10.0 µL
10 mM dNTP Mix	1.5 µL
10 µM Forward Primer	1.5 µL
10 µM Reverse Primer	1.5 µL
1 U/µL κ-Polymerase	1 µL
Template cDNA	1 ng

The following thermo cycler conditions were applied:

STEP	TEMPERATURE	TIME	CYCLES
Hot Start	95°C	3 min	1
Denaturation	98°C	20 s	18 or 22
Annealing	Tm of Primer 60-75°C	15 s	
Extension	72°C	60 s	
Final extension	72°C	5 min	1

The obtained PCR product was purified with the aid of purification kit omnipure-OLS (Omni life science). Both PCR product and the vector construct were digested in parallel with the restriction enzymes XbaI and Mlu (Fermentas) for at least 3 h at 37°C. During the last 30 min of digest, the enzyme CIAP (Fermentas) was added to the vector DNA. CIAP removes the 5'-phosphate group of the DNA backbone, thus preventing religation of the linearized vector. After the digest, DNA was again purified as before (omnipure-OLS Kit). In order to ligate the insert with the linearized vector, T4 DNA ligase (Thermo Scientific) was used in the following reaction set up. Ligation was performed either for 1 h at room temperature or overnight at 4°C.

COMPONENT	20 µL FINAL VOLUME
Linear vector DNA	20-100 ng
Insert DNA	molar ratio 3:1 over vector
10× T4 Ligase Buffer	2 µL
T4 DNA Ligase	1 U
nuclease-free water	to 20 µL

For transformation, the chemically competent *E.coli* cloning strain DH5α (Invitrogen) was used. 50 µL bacteria culture were thawed slowly on ice and 3 µL of the ligation mixture was added and mixed thoroughly. After incubation for 10 min on ice, the plasmid containing bacteria suspension was heat shocked at 42°C for 45 s. The mixture was cooled on ice again and 500 µL SOC medium was added. The bac-

teria solution was then incubated for 1 h at 37°C on a shaker with 800 rpm. A part of the bacteria solution was plated on LB agar plates containing 100 µg/mL ampicillin (Fluka) for selection of positive clones. Bacterial colonies were allowed to grow over night at 37°C in an incubator.

After transformation single colonies were picked from the LB agar plates. The colonies were used to inoculate ampicillin containing LB-medium. Bacteria were allowed to grow over night while being incubated at 37°C with gentle agitation. On the following day bacteria were harvested by centrifugation and plasmid DNA was purified with QIAGEN Plasmid Midi Kit. After disruption of bacteria, the lysate was cleared by centrifugation. The plasmid DNA was purified with the aid of a DNA binding column. After elution, isopropanol was added for DNA precipitation. Isopropanol was removed and the DNA pellet was air-dried before being resolved in DNase-free water. The DNA concentration was determined by Nanodrop and the sequence identity was confirmed by sequencing (Sequencing was performed by Source Bioscience).

2.2 *In vitro* assays

2.2.1 Cell culture methods

For cell culture experiments different human and murine cell lines were used. Characteristics and culture methods of the individual cell lines according to ATCC are described in the following. All cell lines were cultured at 37°C in an atmosphere enriched with 5 % carbon dioxide. Assessment of cell lines was accomplished by observation of morphological changes and growth curve analyses. Both cell lines and produced transgenic clones were tested regularly for mycoplasma infection by PCR.

2.2.2 Human cell lines

1. U937 (ATCC® CRL-1593.2™) The monocytic cell line was established from malignant cells which were derived from a caucasian male patient suffering from histiocytic lymphoma. The cells were cultured in RPMI-1640 Medium supplemented with 10 % fetal calf serum (FCS), 100 U Penicillin, as well as 100 µg/mL Streptomycin (Pen/Strep) (RPMI Complete). As the cells grow in suspension, cultures were maintained either by the addition of fresh medium or by complete replacement of medium. The latter required centrifugation of the cell suspension for 5 min at 300 g, the supernatant was discarded and the cell pellet resuspended in PBS for a washing step. Cells were seeded at approximately 1×10^5 cells/mL.

2. HT144 (ATCC® HTB-63™) The cells were obtained from the metastatic site of malignant melanoma from a male caucasian patient. Morphologically the tumorigenic cells resemble fibroblasts. The adherent cells were grown in RPMI complete. For subculturing, the medium was removed and the cellular monolayer was rinsed with PBS in order to remove residual medium. Cell detachment was achieved by incubation with Trypsin-EDTA solution for several minutes, the status of loosening was observed with an inverted microscope. To stop trypsin activity complete growth medium was added and the cells were spun down at 300 g for at least 5 min. The supernatant was removed and the pellet resuspended in complete growth medium. Cells were routinely splitted with a subcultivation ratio of 1:10.

3. A375 (ATCC® CRL-1619™) The cells originate from malignant melanoma of a female patient. Cultivation procedures were performed as for the HT144 cell line.

4. 293T/17 [HEK 293T/17] (ATCC® CRL-11268™) The cells originate from fetal kidney. The clone 17 is descended from the highly transfectable 293T cell line, which itself is a derivative of the cell line 293. For transfection experiments 293T/17 cells were used due to their ability to produce high retrovirus titers. The fast growing adherent cells were cultivated in Dulbecco's Modified Eagle's Medium (DMEM) supplemented with 10 % fetal calf serum (FCS), 100 U Penicillin and 100 µg/mL Streptomycin (Pen/Strep) (DMEM complete) in combination with 10 mM sodium-pyruvate. Subcultivation was achieved by trypsin treatment, as described above. The splitting ratio was 1:4 to 1:8.

5. HUMAN UMBILICAL VEIN ENDOTHELIAL CELLS (HUVEC; PROMOCELL HEIDELBERG) Human primary cells are isolated from the vein in the umbilical cord. The adherent cells were grown in endothelial growth medium (EGM, Promocell) mix 1:2 with Medium 199, supplemented with 10 % FCS, 50 µg/mL gentamycin, 50 µg/mL heparin and 2.5 µg/mL amphotericin B. Cells were splitted after trypsin treatment and subcultured with a ratio of 1:3.

2.2.3 Murine cell lines

1. RAW264.7 (ATCC® TIB-71™) The adherent macrophage cell line was derived from a tumour induced by Abelson murine leukaemia virus in the mouse strain BALB/C. The cells were grown in DMEM complete. For subcultivation, medium was removed from the cellular monolayer and the cells were rinsed with DPBS. New complete growth medium was added and cells were dislodged from the culture vessel surface with a cell scraper. The cell suspension was aspirated and an appropriate amount was transferred to a new cell culture vessel. The cells were regularly subcultivated at 1:6.

2. B16-F1 (ATCC® CRL-6323™) B16-F1 is a melanoma derived cell line that originates from the mouse strain C57BL/6J. In a syngeneic mouse model the cell line is tumorigenic. As growth medium DMEM complete was used. Subcultivation was accomplished by trypsin treatment as described before. Subcultivation ratio was at least 1:10.

3. B16-F10 LUC (BIOWARE, CALIPER) Like B16F1, B16F10 is a tumorigenic cell line derived from melanoma bearing C57BL/6J. The cells were stably transfected with the North American firefly luciferase gene under the control of the SV40 promoter. The cells produce a bioluminescent signal when the substrate luciferin in administrated. The cells were cultured in RPMI complete. For subcultivation (1:10), the cells were loosened by trypsin treatment.

2.2.4 Cryopreservation of cell lines

For cryopreservation, the cells were prepared as single cell suspensions in freezing medium, which consisted of complete growth medium supplemented with 10 % anti-freezing agent DMSO and aliquoted into cryo-vials. To avoid the formation of large ice crystals, the cells were frozen slowly at 1°C/min. For this purpose, the cryo-vials were put into isopropanol insulated freezing containers, which were placed into a -80°C freezer. For long-term storage, the frozen cells were then transferred to liquid nitrogen tanks.

The frozen cells were thawed quickly in a 37°C water bath until only a small ice crystal was left. The cell suspension was diluted rapidly in complete growth medium and cells were spun down by centrifugation at 300 g for 5 min. The DMSO-containing supernatant was removed and the cells were resuspended and seeded in complete growth medium. On the following day, the medium was renewed.

2.2.5 Isolation of $CD14^+$ cells from human peripheral blood

Buffy coat samples from healthy donors were obtained from German Red Cross Blood Donation Service, Baden-Württemberg. By density gradient centrifugation it is possible to separate cellular components of the blood according to their weight. The buffy coats were diluted 1:1 with sterile PBS. With a volume ratio of 2:1 the diluted blood samples were slowly layered over biocoll separation solution. For the formation of the density gradient the samples were centrifuged without break at 1200 g for 30 min. Biocoll solution contains polysucrose, a highly branched polymer of approximately 400 kDa and a density of 1.077 g/mL. During the gradient centrifugation only blood cells that are dense enough are able to transmigrate the biocoll layer, thus after centrifugation layers with different cell types are formed. The lowermost layer is mainly composed of erythrocytes, which aggregate upon contact with the polymer component of the separation solution. On top of the red blood cells, granulocytes accumulate. In contrast to these cell types mononuclear

cells do not penetrate the biocoll layer, so that a concentrated band consisting of lymphocytes, monocytes and thrombocytes appears right between the biocoll layer and the uppermost layer which is the blood plasma.

After formation of the density gradient the layer of mononuclear cells was transferred to a new collection tube using a sterile Pasteur pipette and the tube was filled with PBS. The cell suspension was spun down at 300 g for 10 min. The supernatant was discarded and the cell pellet was again resuspended in PBS, the washing step was repeated twice. A second density gradient centrifugation was performed, at which the cell suspension was layered over a continuous gradient formed by silica colloid medium Percoll© to achieve improved fractioning of lymphocytes and monocytes. Centrifugation was performed at 1200 g for 30 min without break. The white layer consisting of monocytes and thrombocytes was transferred to a new collection tube with a sterile pipette. The cells were washed three times with PBS as described above. After the last washing step, the cells were resuspended in MACS (magnet associated cell sorting) buffer and labelled for 20 min with magnetic microbeads that are conjugated to monoclonal anti-human CD14 antibodies. CD14 is a co-receptor of the LPS receptor complex; it is commonly used as a marker of monocytes and macrophages. After washing once with MACS buffer, the cell suspension was loaded onto LS MACS Columns, which were clipped into the MACS Separator Magnet. The columns were washed thrice with MACS buffer. Due to the labelling with the magnetic beads, $CD14^+$ cells were restrained, whereas the negative cell fraction was washed out of the columns. Finally, the columns were removed from the magnetic field of the MACS Separator and the $CD14^+$ cells were eluted in MACS buffer. To remove MACS buffer, cells were washed with PBS and resuspended in X-Vivo medium. The cell concentration was determined and 1×10^6 cells/mL were seeded for cultivation and stimulation experiments.

STIMULUS	CONCENTRATION
M-CSF	100 ng/mL
Dexamethasone	1×10^{-7} (1000 U/mL)
IL-4	10 ng/mL
TGF-β	100 ng/mL
SB203580	50 µM
NFκB inhibitor	5 µM
Mifepristone	100 nM
APMA	50 µM
GM6001	50 µM
MMP-9/13 Inhibitor	50 µM
Tapi-1	50 µM

2.2.6 Production of lenti virus for transduction of eukaryotic cells

Lenti viruses are a subset of retroviruses which are derived from HIV-1. The advantage of lentiviral vectors is their ability to transduce both dividing and non-dividing cells. Moreover, the transduction of cells results in the integration of the transgene into the host genome and thus stable expression is achieved.

To produce lenti viruses HEK293/T17 cells were used. The cells were seeded and grown until a confluency of 80 % was reached. The cells were transfected with 3rd generation lentiviral plasmids (pMD2.G L1, pRSV rev L2, pMDLg/pRRE L3 and pCDNA3.1/p35 E 71) in combination with the transfer vector (ADR3) carrying the transgene of interest. Transfection was achieved with X-tremeGENE 9 DNA Transfection Reagent (Roche), a non-liposomal multicomponent reagent. In order to increase efficacy of transfection, 100 mM Na-pyruvate was added to the complete growth medium which supports plasmid uptake by HEK293/T17 cells. On the following day, the culture medium was supplemented with 10 mM Na-butyrate. The stimulation for 8 h with Na-butyrate increases the release of newly produced viruses by the producer cells. Subsequently, the medium was replaced by harvesting medium (DMEM + 1 % Pen/Strep), which was collected and filtered after 8 h of virus production. To obtain sufficient virus, harvesting procedure was repeated three further times, at which the cells were cultured in the harvesting medium for 8-12 h before it was collected and filtered. The virus containing medium was concentrated via Vivaspin Columns (MWCO=100,000 PES), the suspension was stored in aliquots at -80°C.

2.2.7 Production of transgenic cell lines

The lentiviral vector system was used for production of eukaryotic transgenic cell lines. For this purpose, 1×10^6 cells were seeded in 10 cm-dishes in 10 mL complete growth medium and 100 µL concentrated virus suspension per transduction was added dropwise. After two days the virus containing medium was replaced by selection medium (complete growth medium + 2 µg/mL puromycin). As a control, virus untreated cells were cultured in selection medium as well. As soon as these control cells died due to the selection pressure, the surviving transduced cells were expanded in complete growth medium. The expression of the transgene was verified by western blot analysis, qRT-PCR and fluorescence microscopy.

2.2.8 Proliferation-Assay

To estimate the proliferative capacity of cells, a 5-bromo-2'-deoxy-uridine (BrdU) based assay was performed. BrdU is a pyrimidine analogue that is stably integrated into newly synthesized genomic DNA of proliferating cells as a substitute of thymidine. The incorporated BrdU can be tracked by a fluorochrome labelled mono-

clonal antibody. Thus the amount of BrdU positive cells can be determined by means of FACS analyses and provides information about the proliferation rate of the cell lines.

For the proliferation-assay, the cells were seeded at low concentrations of about 1×10^5 cells/mL in 10 cm Petri-dishes. On the following day, the cells were pulsed with 25 µg/mL BrdU for 1 h. The labelling medium was removed and the cells were harvested and washed once with PBS. Cell suspensions were spun down at 300 g for 5 min. The cells were fixed in ice-cold 70 % ethanol (100 µL/1×10^6 cells), which was added drop-wise while the cells were vortexed. After 20 min incubation at RT, cells were washed with PBS + 0.5 % BSA and 2 M HCl was added for denaturation for 20 min. The cells were washed again as before; remaining HCl was neutralized by the addition of 0.1 M sodiumborat buffer. For the detection of incorporated BrdU, the cells were then incubated with mouse anti-BrdU or a mouse IgG isotype control antibody, both labelled with fluorescein isothiocyanate (FITC). The amount of $BrdU^+$ cells was then measured by flow cytometry (FACS-Canto™ II). Data was analyzed using FlowJo V10.1 software.

2.2.9 Scratch Assay

To examine the migratory behaviour of different cell lines, scratch assays or so called wound healing experiments were performed. The cells were seeded in 6-well culture plates with a concentration of 2×10^5 cells per well. The cells were allowed to grow until 100 % confluency was reached. An artificial wound was caused to the monolayer with the aid of a 10 µL pipette tip. Floating cells were washed away by several medium replacements. Scratches were photographed every two hours in a period from 0-10 h and 24 h after the initial scratch with Axio Vert.A1 microscope from Zeiss. The area of the scratch was determined with the aid of ImageJ macro MRI wound healing tool.

2.2.10 Apoptosis Assay

To study the mortality rate of cells, a hydrogen peroxide induced apoptosis assay was performed. Stimulating cells with hydrogen peroxide leads to oxidative stress which results in the intracellular accumulation of ROS. Excessive ROS are detrimental to cellular integrity and cause cell injury like e. g. DNA damage. High doses of hydrogen peroxide initiate apoptosis by stimulating the release of cytochrome C from mitochondria and the activation of caspase 3 [141].

96-well culture plates were coated with 0.2 % gelatine. In the following 5×10^4 cells/well were seeded in complete growth medium. The cells were allowed to grow overnight or until a confluency of 90 % was reached. The supernatant was removed and the cellular monolayer was washed once with PBS. The cells were then incubated for 3 h with complete growth medium containing 0-20 mM hydrogen peroxide. Removal of dead cells was achieved by washing the cells carefully

with water. The remaining attached cells were fixed and stained with 5 % crystal violet and 20 % methanol in H_2O for 15 min at room temperature. The culture plates were rinsed thoroughly with water before they were air dried. To evaluate the amount of survived cells, the stained cells were re-suspended in 100 % methanol and photometrically quantified with the TECAN Infinity M200 Pro.

2.2.11 Adhesion Assay

To study cell adhesion to components of the ECM, a 96-well plate was coated with either 1 µg/mL fibronectin or 0.2 % gelatine. After 24 h at 37°C the plate was washed twice with PBS and 2×10^4 cells/well were seeded in 50 µL culture medium. The cells were allowed to settle for 30 min at 37°C, before the plate was shaken for 10-15 s at 2000 rpm. Non-adherent cells were removed by careful washing with H_2O twice. Adherent cells were fixed and stained with crystal violet and photometrically quantified with the TECAN infinity M 2000 Pro (see also 2.2.10 Apoptosis assay).

2.3 *In vivo* experiments

2.3.1 Mouse Models

C57BL/6 wild type mice were purchased from Elevisier Janvier, Le Genest Saint Isle, France. B6.129P2-Lyz2$^{tm1(cre)Ifo}$/J (also known as LysMcre) and B6.129S1-Lyve-1^{tm1Lhua}/J (Lyve-1$^{-/-}$) were purchased from the Jackson Laboratory. GRflox mice were provided by Prof. Dr. Günther Schütz [199].

All mice are housed under specific pathogen-free conditions at the animal facility Mannheim. All animal experiments were filed at the local authorities Regierungspräsidum Karlsruhe under the numbers G213/12, G42/14 and G119/15.

2.3.2 Murine tumour models

For *in vivo* tumour experiments the murine melanoma cell line B16F1 or B16F10 LUC were used. The cells were loosened from the culture vessel surface by treatment with Trypsin/EDTA. Afterwards the cells were washed at least three times with PBS. To ensure single cell suspension, the cells were run through a 70 µM cell strainer. The cell concentration was adjusted to 10×10^6 cells/mL. 8-weeks old mice were anesthetized by intraperitoneal injection of a ketamine/xylazine combination. The right flanks were shaved and 100 µL of the cell suspension (1×10^6 cells) was injected sub-cutaneously. Mice were sacrificed after at least ten days of tumour growth. The tumours were weighed and shock frosted in liquid nitrogen. The tissue samples were stored at -80°C.

2.3.3 *In vivo* imaging

To monitor tumour growth *in vivo* imaging was performed. 150 µL of D-Luciferin potassium salt 30 mg/mL (Biovision) in PBS were injected intraperitoneal into B16F10 LUC tumour bearing mice. Mice were anesthetized in an isoflurane gas chamber and luminescence pictures were taken three min after substrate injection with IVIS Lumina; exposure time was set to 15 s (PerkinElmer, Living Image 4.3).

2.3.4 Isolation of CD11$^+$ from murine tumours

Tumor bearing mice were sacrificed 14 days after s. c. injection of tumour cells. The tumours were excised and rinsed in PBS, before being homogenized by pressing through a 100 µm cell strainer. The separated tumour cells were washed with pre-cooled PBS and centrifuged for 10 min at 300 g. The cell pellet was resuspended in 10 mL RPMI supplemented with collagenase IV (190 U/mL, Genaxxone) and DNAse I (500 U/mL, Sigma) and digested at 37°C for at least one hour. The samples were washed again as before with PBS. The cells were transferred into MACS buffer and after determination of the cell number, CD11b micro beads (Miltenyi) were added to magnetically label tumour associated macrophages. Following 20 min incubation at 4°C on a rotor the cells were washed once in MACS buffer and magnetic associated cell separation was performed to isolate CD11b$^+$ cells from the crude cell mixture (compare to 2.2.5 isolation of CD14$^+$ cells).

2.4 Statistics

Statistical analyses of all data was calculated by using GraphPad Prism 6.0 (GraphPad Software, USA). Statistical significance was examined by using standard Student's t-test or by one-way ANOVA and Bonferroni as a post-test. The level of significance is indicated by asterisks (*** ≤ 0.001; ** ≤ 0.01 and * ≤ 0.05). Error bars depict SEM of each experiment. All experiments were performed at least in triplicates.

3. MATERIALS

Table 1: Chemicals

CHEMICALS AND REAGENTS	COMPANY
30 % Acrylamide mix	Bio-Rad
4-Aminophenylmercuric acetate (APMA)	Sigma
5-bromo-2'-deoxy-uridine (BrdU)	Sigma
Acetic Acid	Roth
Acetone	Roth
Agarose	Sigma
Ammonium persulfate (APS)	Sigma
Ampicillin	Fluka
Biocoll	Biochrom
β-Mercaptoethanol	Sigma-Aldrich
Bovine Serum Albumin (BSA)	Fitzgerald
CD14 Dynabeads	Miltenyi
Hyperfilm ECL	Amersham
Coomassie Brilliant Blue	Serva
Crystal violet	Roth
Dexamethasone	Sigma
DMSO	Sigma
DNA Ladder	Thermo Scientific
dNTP	Fermentas
Escherichia coli	Invitrogen
Ethanol	Roth
Ethylenediaminetetraacetic acid (EDTA)	Sigma
Fc Block	BD Biosciences
Fibroblast growth factor-2 (FGF-2)	Peprotech
Fibronectin	Sigma
Gelatine	Sigma
High molecular weight hyaluronic acid	R&D Systems
Hydrogen-peroxide (H_2O_2)	Merck
Hydrochloric acid (HCl)	Merck
Ilomastat, MMP Inh., Galardin (GM6001)	US Biological
Immune-Blot PVDF Membrane	BioRad
Interferon-γ (IFN-γ)	Peprotech

CHEMICALS AND REAGENTS	COMPANY
Interleukin-4	Peprotech
Isopropanol	Roth
Ketamine 10 %	Medistar
Lipopolysaccharide (LPS)	Invitrogen
Low molecular weight hyaluronic acid	R&D Systems
Luciferin	BioVision
Lysogeny broth (LB) Agar	Roth
Lysogeny broth (LB) Medium	Roth
Macrophage colony-stimulating factor (M-CSF)	Peprotech
Methanol	Sigma
Mifepristone	Sigma
MMP-9/13 Inhibitor I	Merck
Nancy 520	Sgima
NFκB Activation inhibitor	Calbiochem
NP 40	Fluka
Oligo $(dt)_{18}$ Primer	Fermentas
PageRuler Prestained Protein Ladder	Fermentas
Paraformaldehyde	Roth
Penicillin/Streptomycin	Biochrom
Percoll	GE Healthcare
Protease Inhibitor Cocktail	Roche
Protein G Agarose	Roche (Sigma)
Puromycin	Invivogen
Ribolock inhibitor	Fermentas
Rompun 2 %	Bayer
SB203580	Calbiochem
skim milk powder	Roth
sLyve-1	R&D Systems
Sodium dodecyl sulphate (SDS)	Bio-Rad
sodium fluoride (NaF)	Sigma
Sodiumazide (NaN_3)	Sigma
Sodium-borat ($Na_2B_4O_7{\times}10H_2O$)	Fluka
Sodium-butyrate ($Na(C_3H_7COO)$)	Sigma-Aldrich
Sodium-chloride (NaCl)	Sigma
Sodiumdeoxychelat ($C_{24}H_{39}O_4Na$)	Sigma Aldrich
Sodiumpyruvate ($C_3H_3NaO_3$)	Sigma
SyBRGreen Master Mix	Applied Biosystems
TAPI-1	Calbiochem
Tetramethylethylenediamine (TEMED)	GenAxxon
Transforming growth factor-β (TGF-β)	Peprotech

CHEMICALS AND REAGENTS	COMPANY
Tris/HCl	Sigma
Triton X-100	Sigma
Trypsin/EDTA	Biochrom
Tumour necrosis factor-α (TNF-α)	Peprotech
Tween 20	Sigma
Vascular endothelial growth factor-α (VEGF-α_{165})	Peprotech
Xylene	Roth

Table 2: Enzymes

ENZYME	COMPANY
CIAP	Fermentas
Collagenase IV	Genaxxon
DFS TAQ	Bioron
DNase I	Fermentas
Kappa Polymerase	Invitrogen
Mlu I	Thermo Scientific
RevertAid H Minus M-MuLV Reverse Transcriptase	Thermo Scientific
T4 DNA Ligase	Thermo Scientific
Xba I	Thermo Scientific

Table 3: Kits

KIT	COMPANY
VECTOR NOVARED Peroxidase (HRP) Substrate Kit	Vector laboratories
Selective Indicators for Highly Reactive Oxygen Species	Cell technology
RNeasy Kit	Qiagen
Plasmid Midi Kit	Qiagen
omnipure-OLS	Omni Life Science
Nitric Oxide Synthase (NOS) Detection Kit	Cell technology
κ-HiFi HotStart PCR kit	VWR/Peqlab
innuPREP RNA Mini Kit	Analytik Jena
Human Lyve-1 DuoSet ELISA	R&D
FITC Mouse Anti-BrdU Set	BD Biosciences
DC™ Protein Assay	Bio Rad
CD14 Microbeads	Miltenyi
CD11b Microbeads	Miltenyi

Table 4: Instruments

INSTRUMENT	COMPANY
Autoprocessor Curx 60	Agfa
Axio VER.A1 microscope	Zeiss
Centrifuge 5417R	Eppendorf
Centrifuge 5810R	Eppendorf
Cryotome CM3050S	Leica
Cytospin 3	Shandon
DS-U3 Digital Camera Control Unit	Nikon
FACS-Canto™ II	BD Biosciences
Freezer MDF U743V	Sanyo
HeraSafe KS Laminar Flow	Thermo Scientific
Incubator Heracell L50i	Thermo Scientific
infinite M200 Pro	Tecan
Kelvitron T	Heraeus
Microtome RM2065	Leica
Mupid-One Electrophoresis Chamber	Biozym
Nanodrop 2000	Thermo Scientific
pH Meter FG2/EL2	Mettler Toledo
PowerPac Basic	BioRad
QuadroMACS™ Separator	Miltenyi
Rotator SB2	Stuart
Shaker DRS12	Peqlab
TC20™ Automated Cell Counter	BioRad
Thermoblock Thermomixer	Eppendorf
Thermocycler T100	BioRad
Trans-Blot Turbo Device	BioRad
Upright motorized Microsope Eclipse Ni-E	Nikon
UV Systems N-90m	Intas
Vortex Genie-2	Scientific Industries
Waterbath	Memmet
Z2 Coulter Particle Count & Size Analyzer	Beckman Coulter

Table 5: Cell culture media

MEDIUM	COMPANY
RPMI-1640	Gibco
Dulbeccos's Modified Eagle Medium (DMEM)	Gibco
Endothelial Cell Growth Medium (EGM)	Lonza
Fetal calf serum (FCS)	Biochrom
Medium 199	Sigma
Minimum Essential Medium Eagle	Sigma
Non-Essential Amino Acid(NEAA)	Biochrom
Opti-MEM I reduced serum media	Gibco
SOC Medium	Invitrogen
Trypsin/EDTA	Gibco
Vivaspin Columns	Sartorisus
X-treme Gene 9 DNA transfection reagent	Roche
X-Vivo	Lonza

Table 6: Consumables

CONSUMABLE	COMPANY
Immune-Blot PVDF Membrane	BioRad
High Performance Chemiluminescence Film	Amersham
Cellculture flask 25 cm^2 (T25)	Greiner bio-one
Cellculture flask 75 cm^2 (T75)	Greiner bio-one
Cellculture flask 175 cm^2 (T175)	Greiner bio-one
6-well plates	Greiner bio-one
12-well plates	Greiner bio-one
24-well plates	Greiner bio-one
96-well plates	Greiner bio-one
Cell scraper	Greiner bio-one

Table 7: Software

Adobe Photoshop 6.0 software
NIS-Elements Advanced software (Nikon)
FlowCytomix Pro Software (ebioscience)
GraphPad Prism 6.00
Image J
Zeiss Software System
FlowJo V10.1

Table 8: Primer

KLONIERUNG	SEQUENCE
HS LYVE-1 XbaI Fw	GAT TCT AGA CAC GAT GGC CAG GTG CTT
HS LYVE-1 MluI Rev	GAT ACG CGT CTA AAC TTC AGC TTC CAG GCA
MM LYVE-1 XbaI Fw	TTA TCT AGA GGG ATC TGC ACA ATG CT
MM LYVE-1 MluI Rev	AAT ACG CGT TGC ATC TAA ACT TCA GCT T

qRT-PCR	SEQUENCE
HS CD163 Fw	GCC ACA ACA GGT CGC TCA TCC
HS CD163 Rev	GTG TGG CTC AGA ATG GCC TCC
HS CD206 Fw	TGG TTT CCA TTG AAA GTG CTG C
HS CD206 Rev	TTC CTG GGC TTG ACT GAC TGT TA
HS CD11B Fw	CCA GGG GGA GGG CTC GGT
HS CD11B Rev	CGT GCC CCT GGG CTC CTA
HS CD68 Fw	ATG ATG AGA GGC AGC AAF ATG G
HS CD68 Rev	GCT ACA TGG CGG TGG AGT ACA A
HS ARG-1 Fw	CGG AGA CCA CAG TTT GGC A
HS ARG-1 Rev	TAC AGG GAG TCA CCC AGG AG
HS ACTIN Fw	GGC ACC ACA CCT TCT ACA ATG A
HS ACTIN Rev	TCT CCT TAA TGT CAC GCA CGA T
HS LYVE-1 Fw	CTT GCA GCT ATG GCT GGG TT
HS LYVE-1 Rev	TAA GGG GAT GCC ACC GAG TA

Table 9: Antibodies

1st ANTIBODY	APPLICATION	DILUTION	COMPANY
PE anti-hs CD163	FACS	1/5	BD Bioscience (#556018)
APC anti-hs CD11b	FACS	1/5	BD Bioscience (#550019)
PE-Cy5 anti-hs CD206	FACS	1/5	BD Bioscience (#551136)
APC-Cy7 anti-hs HLA-DR	FACS	1/100	BD Bioscience (#561358)
biotin anti-hs Lyve-1	Western Blot	0.08 µg/mL	R&D (BAF2089)
anti-hs Lyve-1	IHC (PFA Fixation, Antigen retrieval Proteinase K)	10 µg/mL	Abcam (ab36993)
anti-hs CD68	IHC (Antigen retrieval Proteinase K)	1/200	Dako (M087629-2)
anti-hs CD163	IHC (Antigen retrieval Proteinase K)	1/500	Abcam (ab111250)
anit-mm/hs GAPDH	Western Blot	0.08 µg/mL	Santa Cruz (SC25778)
anti-mm CD68	IHC/IF (Acetone Fixation)	2 µg/mL	ABD (MCS1957)
anti-mm CD31	IHC/IF (Acetone Fixation)	0.5 µg/mL	BD Bioscience (#550274)
anti-mm/hs Ki67	IHC/IF (PFA Fixation)	1/50	Abcam (ab16667)

2nd ANTIBODY	APPLICATION	DILUTION	COMPANY
Strepta HRP	Western Blot	1/10000	Dianova (016-030-084)
Strepta FITC	FACS	1/200	eBioscience (11-4317-87)
anti-rabbit IgG HRP	IHC	1/200	Santa Cruz (2031)
anti-rat IgG HRP	IHC	1/200	Santa Cruz (2956)
anti-rabbit IgG HRP	Western Blot	1/5000	GE Healthcare (NA934V)

2nd ANTIBODY	APPLICATION	DILUTION	COMPANY
anti-rabbit IgG DL-488	IF	1/200	Dianova (711-486-152)
anti-rat IgG Cy3	IF	1/200	Dianova (712-165-153)

Table 10: Buffers

BUFFER	COMPANY
0.5 M Tris (pH 6,8)	Bio-Rad
1.5 M Tris (pH 8,8)	Bio-Rad
10× Tris Glycine Buffer (TGS)	Bio-Rad
AEC Chromogen Substrate	Dako
AG Retrieval Solution pH6	Leica
AG Retrieval Solution pH9	Leica
Antibody Diluent	Dako
DPBS	Gibco
Eukitt	Kindler
Faramount Aqueous Mounting Medium	Dako
Fluorescent Mounting Medium	Dako
Laemmli Buffer	Bio-Rad
Luminate Forte Western HRP Substrate	Millipore
Mayer's Haematoxylin	Merck
Peroxidase Blocking Solution	Dako
Phosphate buffered saline	Invitrogen
Proteinase K	Dako
Rotiophorese Buffer TAE	Roth

Table 11: Buffer recipes

RIPA-P BUFFER	
Sodium chloride	150 mM
NP-40	1 %
Sodium deoxychelate	0.50 %
SDS	0.10 %
Tris/HCl (pH 8,0)	50 mM
Sodium fluoride	10 mM
EDTA	2 mM
Protease inhibitor cocktail (Roche)	4 %

BLOTTING BUFFER (WET CHAMBER)	
TGS	1×
Methanol	20 %

BLOTTING BUFFER (SEMI-DRY)	
TGS	2×
Methanol	20 %
SDS	0.10 %

DISC	
TrisHCl pH07	30 mM
NaCl	120 mM
Glycerol	10 %
Triton X-100	1 %

MACS BUFFER	
PBS	1×
BSA	0.50 %
EDTA	2 mM

FACS SURFACE BUFFER	
PBS	1×
BSA	10 %
Sodium azide	0.05 %

TBS	
Tris	20 mM
NaCl	150 mM
pH	7.6

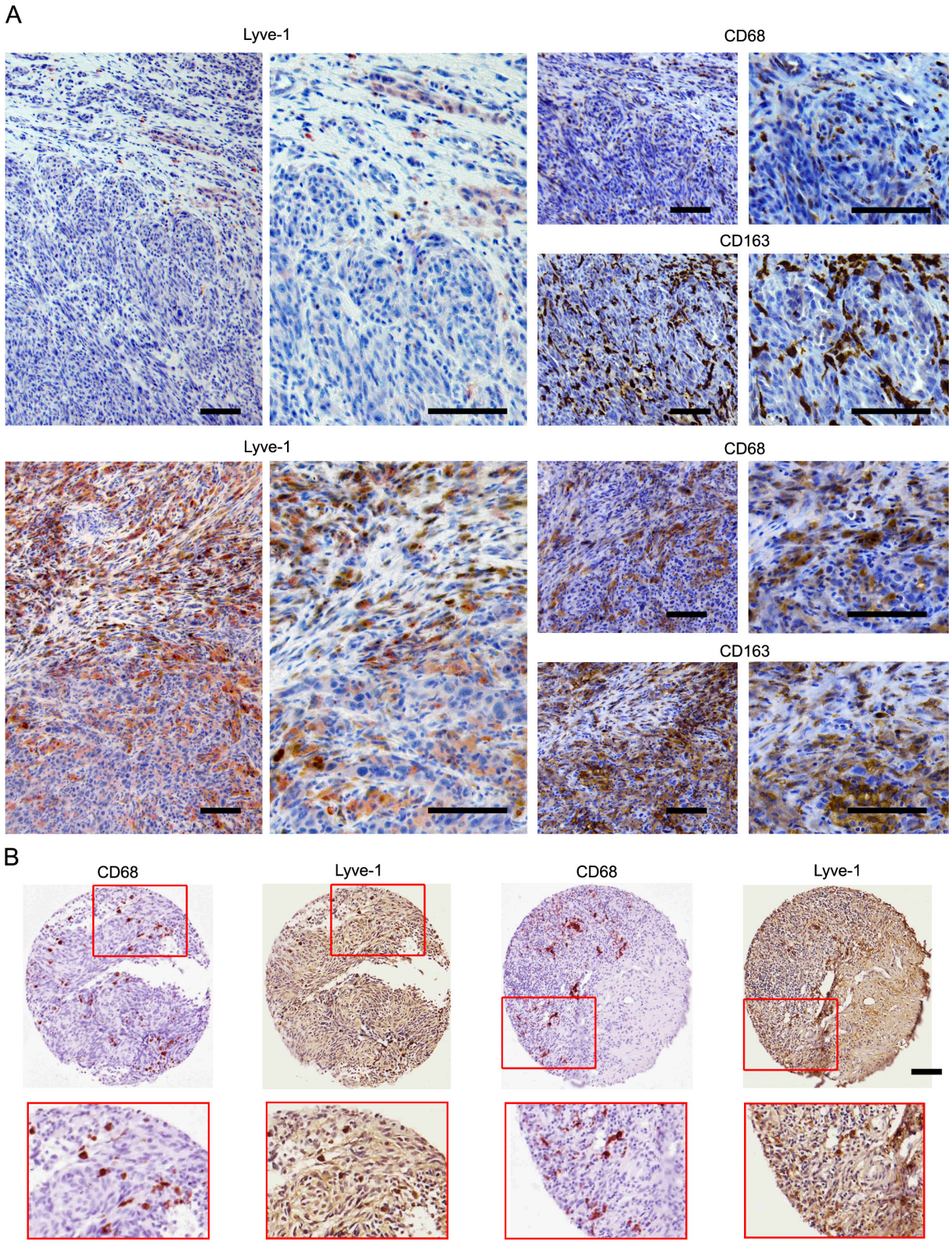
A
Lyve-1
CD68
CD163
Lyve-1
CD68
CD163
B
CD68
Lyve-1
CD68
Lyve-1

4. RESULTS

4.1 Lyve-1$^+$ macrophages are present in human melanoma

Lyve-1 has been found not to be expressed exclusively by lymphatic endothelial cells as previously thought, but also by macrophages. Our group has identified Lyve-1$^+$ TAM in murine B16 melanoma *in vivo*. In addition, Lyve-1 expression could be induced *in vitro* in bone marrow derived macrophages by the combined stimulation with B16 tumour conditioned medium in combination with dexamethasone (dexa) and IL-4 [116].

To determine if Lyve-1$^+$ macrophages are also present in human melanoma, serial sections from paraffin embedded specimens were prepared and stained for Lyve-1, the pan-macrophage marker CD68 and CD163, which is a marker of M2-like macrophages. Histopathological analyses identified Lyve-1$^+$ cells as endothelial cells and macrophages. Compared to Lyve-1$^+$ TAM more CD68$^+$ and CD163$^+$ TAM were found in human melanomas. (Fig. 5 A).

To further substantiate the existence of Lyve-1$^+$ macrophages in human melanoma samples, tissue microarrays with melanoma samples have been stained sequentially. In a first step, the samples were stained with anti-CD68 and after a destaining procedure the same samples were stained with an anti-Lyve-1 antibody. Thus, expression of Lyve-1 in CD68$^+$ cells could be clearly demonstrated. However, Lyve-1 expression has been observed to variable extent only in a subpopulation of CD68$^+$ cells (Fig. 5 B).

FIGURE 5: Identification of Lyve-1$^+$ macrophages is human melanoma. (A) *Immunhistological stainings of serial sections of melanoma specimens derived from two different patients. The 1.5 µM sections were stained with antibodies against Lyve-1, CD68 and CD163. Whilst Lyve-1$^+$ cells were visualized using AEC chromogen (red), CD68$^+$ and CD163$^+$ were stained with DAB (brown), scale bars = 100 µM.* (B) *Two tissue microarrays with 250 melanoma derived specimens were sequentially stained against CD68 with Nova Red for visualization first, after a destaining procedure the TMA were stained again with anti-Lyve-1 (visualized with DAB in brown). Two representative specimen are depicted, scale bar = 100 µM.*

4.2 Characterization of the *in vitro* induction of Lyve-1 in pBMC

4.2.1 M-CSF, dexamethasone and IL-4 induce a M2-like phenotype of pBMC *in vitro*

As already shown by Schönhaar, LYVE-1 expression can be induced *in vitro* in pBMC by the combined stimulation with MDI after seven days of stimulation. The expression of a combination of macrophage markers was examined to describe the phenotype of these MDI treated cells in more detail. The results were compared to M-CSF (M) treated pBMC. Besides analysis of the macrophage differentiation marker CD11b, expression levels of the scavenger receptor CD163 and mannose receptor CD206 were evaluated, as their expression is associated with a M2-like phenotype. In addition, human leukocyte antigen-antigen D related (HLA-DR) protein surface expression was studied.

Both qRT-PCR and FACS analysis confirmed the significant induction of LYVE-1 in pBMC by the combined stimulation with M-CSF dexa/IL-4 after seven days of stimulation (Fig. 6) In general, expression analyses on protein and mRNA level showed similar trends for MDI-induced macrophage markers. The macrophage marker expression profile revealed significant up-regulation of the M2 associated markers CD163 and CD206 in response to MDI treatment, likewise on mRNA and protein level, whereas changes in the expression level of CD11b were not significant. However, a slight down-regulation of CD11b was observed in MDI-treated pBMC. Finally, examination of HLA-DR expression on the protein level by FACS analysis showed comparable expression levels in M and MDI treated pBMC (Fig. 6).

FIGURE 6: Expression analysis of macrophage marker in M-CSF and MDI stimulated pBMC. *pBMC were stimulated for seven days with M-CSF or M-CSF/dexa/IL4 (MDI) as indicted. (A) Expression of macrophage markers was analyzed by FACS, overlay histograms show a representative experiment; MCSF (silver) MDI (red). (B) To compare marker protein expression levels the median fluorescence intensities (MFI) of the FACS analyses were compared, n=10, (C) qRT-PCR analysis determined mRNA expression relative to β-actin mRNA levels. MDI values are given as fold-induction over expression levels for M-CSF treated control, (n=6).*

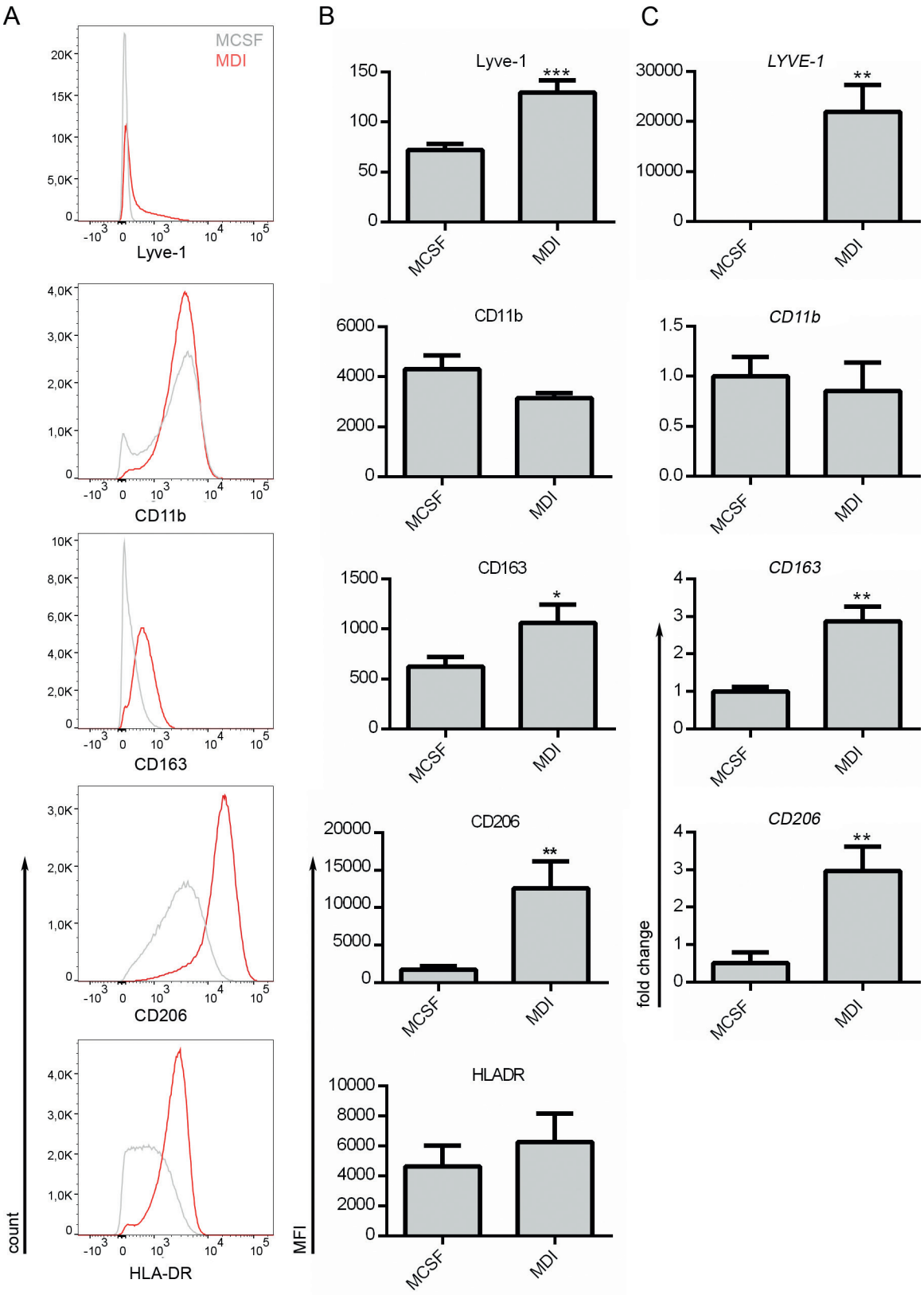
A
B
C
MCSF
MDI
Lyve-1
CD11b
CD163
CD206
HLA-DR
count
MFI
fold change
LYVE-1
HLADR
MCSF
MDI

In addition, arginine metabolism and production of ROS and NOS in M-CSF and MDI treated PBMC were examined by means of FACS and qRT-PCR. In TAM and M2-like macrophages arginase-1 is up-regulated promoting the hydrolysis of L-arginine to urea and ornithine, whereas in pro-inflammatory M1-like macrophages conversion of L-arginine by iNOS to NOS is prevailing and high abundance of ROS is characteristic.

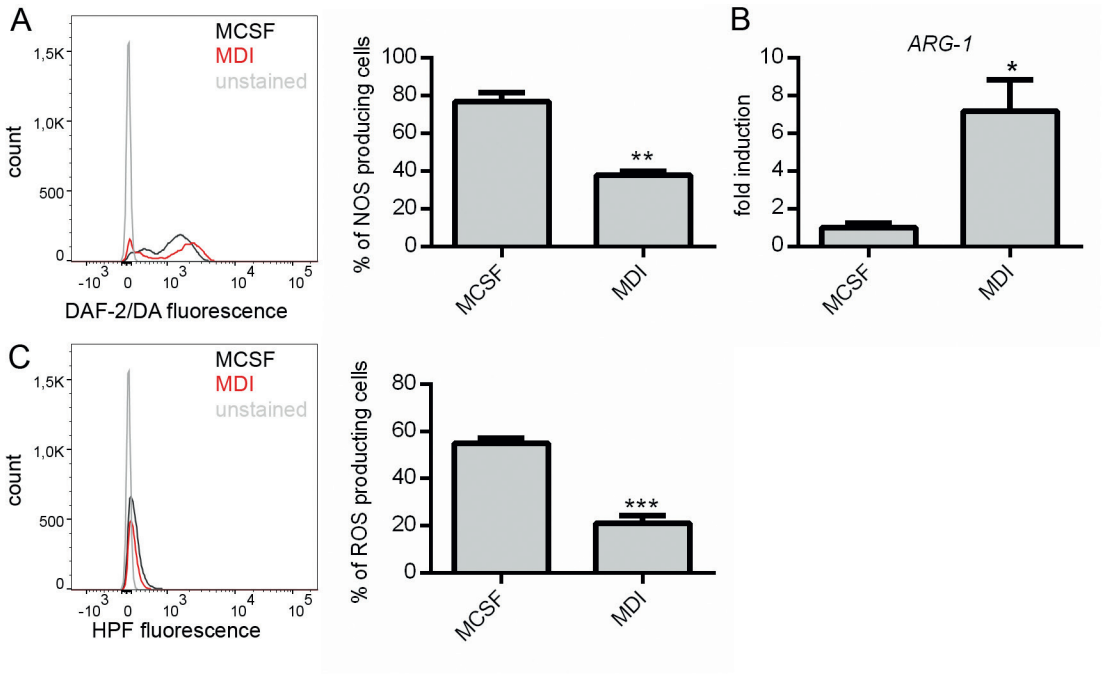

FIGURE 7: NOS and ROS production is impaired in MDI stimulated PBMC. PBMC were stimulated for seven days with M-CSF or MDI as indicted. (A) Presence of NOS was detected by loading cells with DAF-2/DA, overlay histogram (left) shows a representative experiment; MCSF (black), MDI (red) and control (grey). The number of NOS producing cells was assessed by FACS analysis, (n=3). (B) mRNA expression of ARG-1 relative to β-actin mRNA levels was determined by qRT-PCR. MDI values are given as fold-induction over expression levels for M-CSF treated controls, (n=6). (C) Presence of ROS was detected by loading cells with HPF. Overlay histogram (left) shows a representative experiment, MCSF (black), MDI (red) and control (grey). The number of ROS producing cells was assessed by FACS analysis, (n=3).

In MDI treated PBMC the number of NOS producing cells was significantly reduced compared to MCSF stimulated control cells (Fig. 7A). These findings are in line with the observation that the mRNA-expression of the iNOS counteracting enzyme Arg-1 was up-regulated in response to MDI treatment (Fig. 7B). Moreover, it was asserted that significantly fewer MDI-treated cells contain ROS (Fig. 7C). Taken together the results demonstrate that seven days of MDI stimulation induce an M2-like phenotype in PBMC.

4.2.2 Characterization of the Lyve-1$^+$ PBMC subset

Only a subpopulation of PBMC treated with MDI express Lyve-1. By FACS analysis the Lyve-1$^+$ PBMC subset could be quantified and again the macrophage marker expression profile was analyzed to assess the differences between the Lyve-1$^+$ and Lyve-1$^-$ MDI-stimulation derived cell populations.

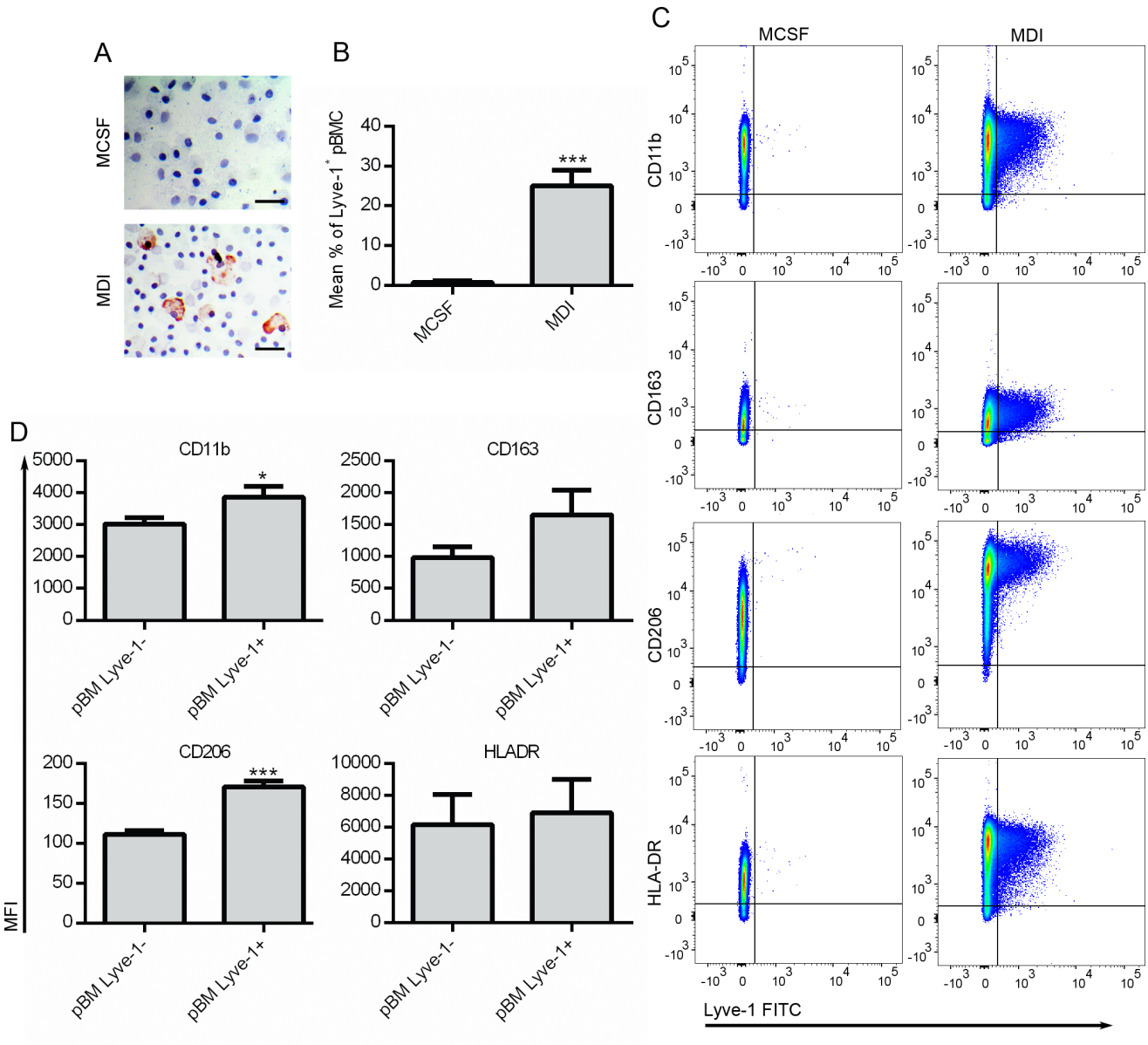

FIGURE 8: Expression analysis of macrophage marker in Lyve-1$^+$ and Lyve-1$^-$ MDI stimulated PBMC. PBMC were stimulated for seven days with M or MDI as indicated. (A) Cytospins were fixed with PFA and stained with anti-Lyve-1, scale bars = 20 µM. (B) Flow cytometric quantification of Lyve-1 surface expression in M or MDI treated cells, (n=8). (C) FACS analysis was performed to determine co-expression of Lyve-1 and diverse macrophage markers, representative experiments are shown. (D) Comparison of marker expression levels between Lyve-1$^+$ and Lyve-1$^-$ MDI treated PBMC by evaluation of MFI, (n=10).

Even after seven days of treatment with MDI, we observed Lyve-1 expression only in a minor subset of stimulated PBMC (Fig. 8 A). With regard to this finding, flow cytometric analysis revealed that Lyve-1 is expressed in approximately 25 % of the MDI-treated PBMC, though expression levels varied between different donors (Fig. 8 B). Furthermore, Lyve-1 was found to be co-expressed with all examined macrophage markers. In the Lyve-1^{+} PBMC subpopulation CD206 and CD11b were significantly up-regulated and CD163 showed a slight up-regulation too, whereas HLA-DR levels were comparable to the Lyve-1^{-} subpopulation (Fig. 8 C + D).

4.2.3 Dexamethasone is crucial for *in vitro* induction of LYVE-1 in PBMC

In vitro, LYVE-1 could already be induced by stimulation of PBMC with M-CSF and dexa, though the addition of IL-4 boosted the effect and yielded higher expression levels of LYVE-1. Moreover, inhibition of the glucocorticoid receptor (GR) by its antagonist mifepristone led to the inhibition of LYVE-1 expression in PBMC [136]. Yet, it remained unknown at which time point during the seven day lasting MDI treatment GR activation is required for the induction of LYVE-1. To address this question, time course experiments with dexamethasone and mifepristone were performed. For this purpose, PBMC were stimulated with MDI for seven days. The first sample was additionally stimulated with 100 nM mifepristone for all seven days, to the second sample mifepristone was added on the second day of MDI stimulation, to the third sample on the third day and so on. In a similar manner a time course experiment for dexamethasone stimulation was accomplished. In this case, PBMC were stimulated for seven days with M-CSF in combination with IL-4 and dexamethasone was added on consecutive days to the cell culture medium for a total of seven days.

Immunohistological staining of PFA-fixed cytospins from MDI stimulated PBMC showed that the addition of 100 nM mifepristone efficiently blocked Lyve-1 expression in the cells, whereas the expression of Lyve-1 in the control group (PBMC treated with MDI/EtOH) remained unaffected (Fig. 9 A).

First, LYVE-1 gene expression could already be detected after five days of MDI treatment and peaked after nine days of stimulation (Fig. 9 B).

Further characterization of the influence of GR-activation on Lyve-1 expression revealed that 24 h of MF treatment prior to expiration of the seven days lasting MDI stimulation was sufficient to block LYVE-1 gene expression completely (Fig. 9 C). These findings brought into question if dexamethasone stimulation might be just required during the last days of the stimulation. However, the sequential addition of dexamethasone to M-CSF/IL-4 primed cells experiment demonstrated that this was not the case. In fact, it could be confirmed that dexamethasone stimulation is necessary for all seven days in combination with M-CSF/IL-4 to significantly induce LYVE-1 expression in the PBMC model (Fig. 9 D).

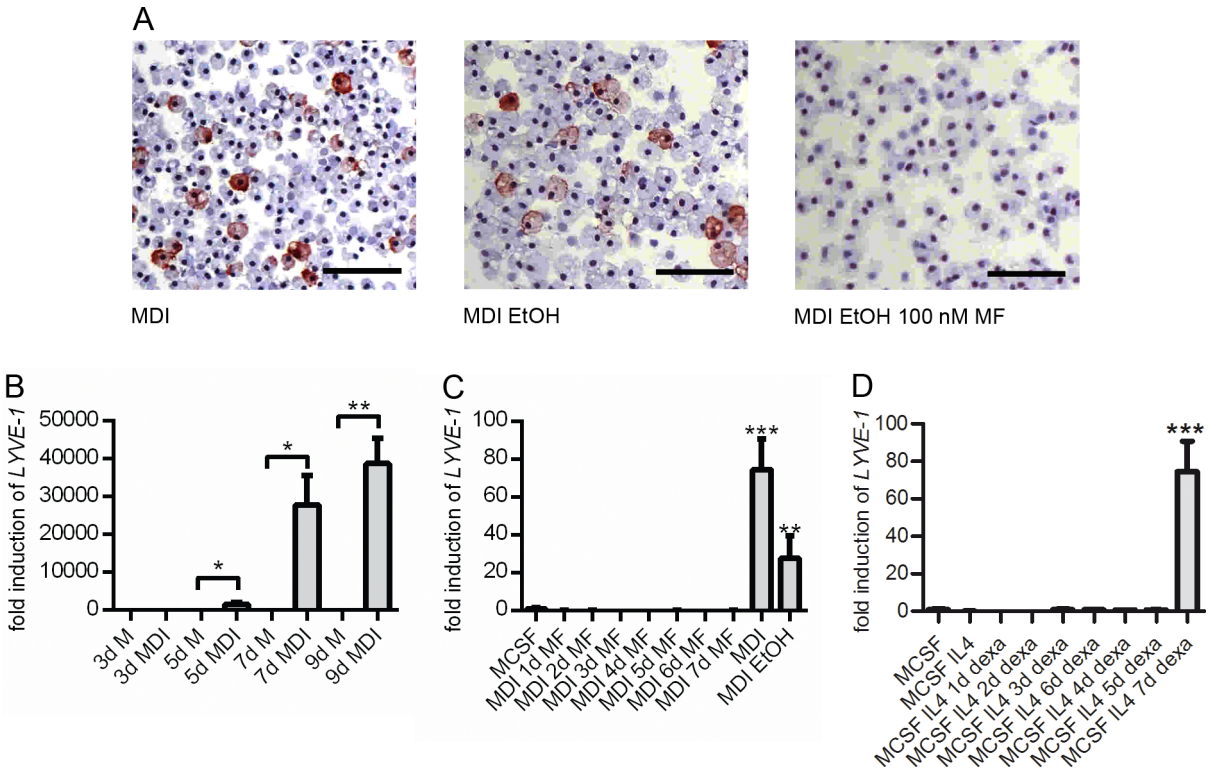

FIGURE 9: Expression of LYVE-1 in human PBMC is dexamethasone dependent. (A) Immunohistological staining of Lyve-1 in PBMC following treatment with MDI in combination with GR antagonist mifepristone (MF) or ethanol (EtOH) as control, scale bars = 100 µM. (B) PBMC were stimulated for 3, 5, 7 or 9 days with M or MDI, expression of LYVE-1 was examined on mRNA level by qRT-PCR, (n=3). (C) qRT-PCR analysis of LYVE-1 expression after 100 nM MF was added to the MDI treated PBMC. The addition of MF was accomplished on consecutive days, at which the indicated time of MF stimulation is in relation to the experimental endpoint, (n=4). (D) Time course experiment with dexamethasone being added at different time points to MCSF/IL-4 stimulated PBMC, (n=4). All qRT-PCR values were normalized to an internal β-actin control and MDI values are given as fold-induction over expression levels for M-CSF treated control.

4.2.4 Activation of p38 MAPK is relevant for LYVE-1 induction in PBMC

In an attempt to deepen our knowledge about the *in vitro* induction of LYVE-1, we used different pathway inhibitors of major signalling pathways involved in the generation of various TAM phenotypes to study their influence on LYVE-1 induction in MDI stimulated PBMC. After priming of the PBMC for three days with MCSF or MDI, the stimulation cocktail was supplemented with the p38 MAPK inhibitor SB203580 for the remaining stimulation time.

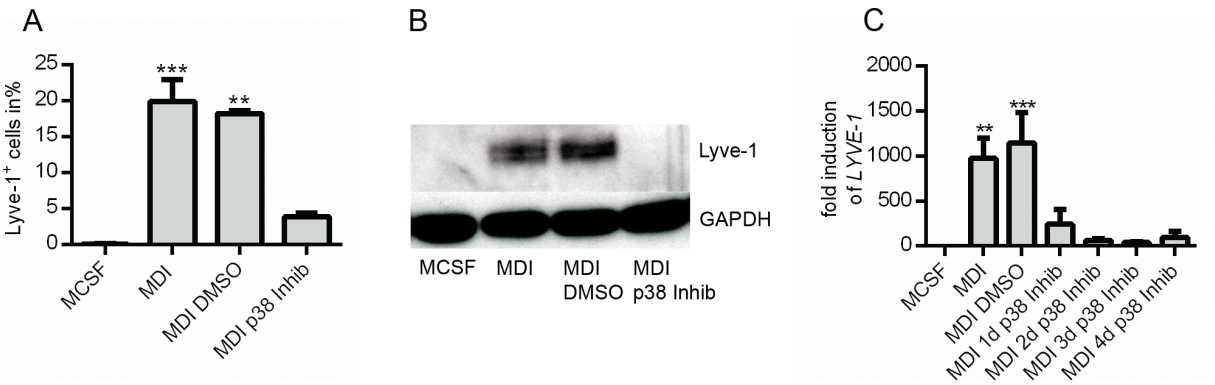

FIGURE 10: p38 inhibition suppresses MDI-mediated LYVE-1 induction in PBMC. *(A) Flow cytometric analysis, (n=3) and (B) western blot of Lyve-1 expression in PBMC which were stimulated for seven days with M-CSF and MDI respectively; on the third day of the stimulation a p38 inhibitor (50 µM) or DMSO (control) were added for the remaining stimulation time to MDI primed cells. (C) Gene expression of Lyve-1 was assessed via qRT-PCR in MCSF/MDI stimulated PBMC with subsequent addition of p38 inhibitor at different time points. Values were normalized to an internal β-actin control and MDI values are given as fold-induction over expression levels for M-CSF treated control, (n=4).*

The suppression of p38 MAPK signalling resulted in the blockade of Lyve-1 expression in MDI-stimulated PBMC on the protein level (Fig. 10 A + B). To determine the kinetics of this inhibition a time course experiment was performed by adding the p38 inhibitor to the MDI treated cells on day 3 (MDI 4 d p38 inhibition), 4, 5 and 6 of the stimulation. Evaluation of the fold induction of the gene expression revealed that 24 h of treatment with the p38 MAPK inhibitor were sufficient to block LYVE-1 induction significantly, though not completely (Fig. 10 C).

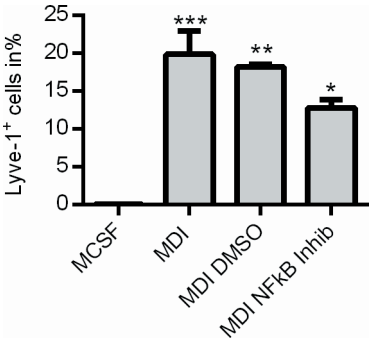

FIGURE 11: Inhibition of NFκB has no influence on LYVE-1 expression in MDI stimulated PBMC. *PBMC were stimulated for seven days with M-CSF and MDI respectively; on the third day of the stimulation a NFκB inhibitor (5 µM) or DMSO (control) were added for the remaining stimulation time to MDI primed cells. Flow cytometry was performed to determine the number of Lyve-1+ cells (n=3).*

NFκB inhibition with a specific inhibitor did not significantly influence expression of Lyve-1 in MDI-stimulated pBMC on the protein level (Fig. 11). Thus, NFκB signalling is not required for the regulation of LYVE-1 gene transcription in M2-like differentiated pBMC.

4.2.5 Activation of p38 MAPK signalling via TGF-β does not induce LYVE-1 in pBMC

A well-studied activator of intracellular p38 MAPK signalling is the cytokine TGF-β, which is also involved in the polarization of macrophages towards a M2-like phenotype. To study the role of p38 MAPK activation for Lyve-1 expression, we used different cytokines in combination with TGF-β.

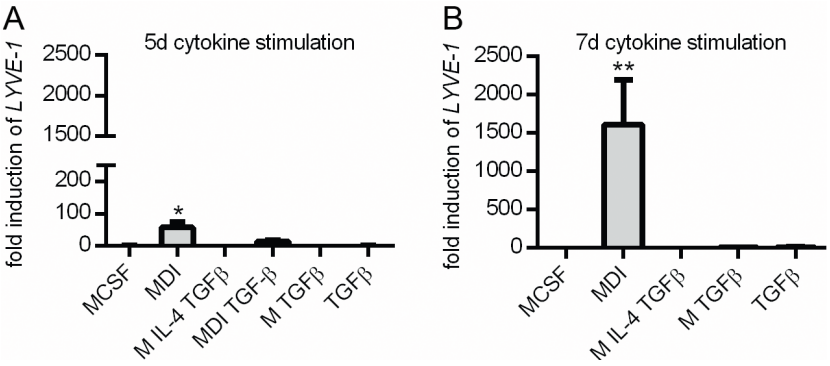

FIGURE 12: Stimulation with TGF-β does not influence LYVE-1 expression in pBMC. *qRT-PCR analysis of Lyve-1 gene expression in stimulated pBMC. Values were normalized to an internal β-actin control and MDI values are given as fold-induction over expression levels for M-CSF treated controls, (n=4). (A) Stimulation for 5 days as indicated. (B) Seven days of cytokine stimulation as indicated.*

To test whether the addition of TGF-β to our pBMC model might lead to differences in the induction of LYVE-1 as a result of the simultaneous activation of the p38 MAPK signalling cascade and GR several combinations were tested. After five days of stimulation a slight, but significant induction of LYVE-1 could be observed by exposure to MDI as seen before. The addition of TGF-β to MDI reduced LYVE-1 expression, thus no synergistic effect of GR and p38 MAPK signalling could be observed to this point. Moreover, (M-CSF+)TGF-β alone, were not sufficient to induce gene expression of LYVE-1 (Fig. 12 A). After seven days of stimulation, LYVE-1 expression could not be detected, when dexamethasone was removed from the stimulation mixture and was substituted by TGF-β (Fig. 12 B). Consequently, activation of GR is crucial for induction of LYVE-1 and stimulation of p38 MAPK activity via TGF-β does not contribute to the induction of LYVE-1 expression. Lyve-1 expression in macrophages seems to require long time of periods of stimulation indicating more fundamental regulatory mechanisms as for example chromatin modifications rather than fast direct expression switches.

4.3 Functional analyses of Lyve-1 overexpression in U937 and B16F1

4.3.1 Highly glycosylated Lyve-1 in transgenic U937 binds the ligand HA

Previous studies have shown that Lyve-1 has got various sites for post-translational modifications by N- and O-linked glycosylation. Interestingly, the glycosylation status of the protein varies depending on the cell type in which Lyve-1 is expressed. In order to determine the glycosylation status of Lyve-1 in macrophages and to perform functional assays, we transduced the monocytic cell line U937 with the LYVE-1 containing expression vector ADR3 and the empty vector (EV) construct as a control.

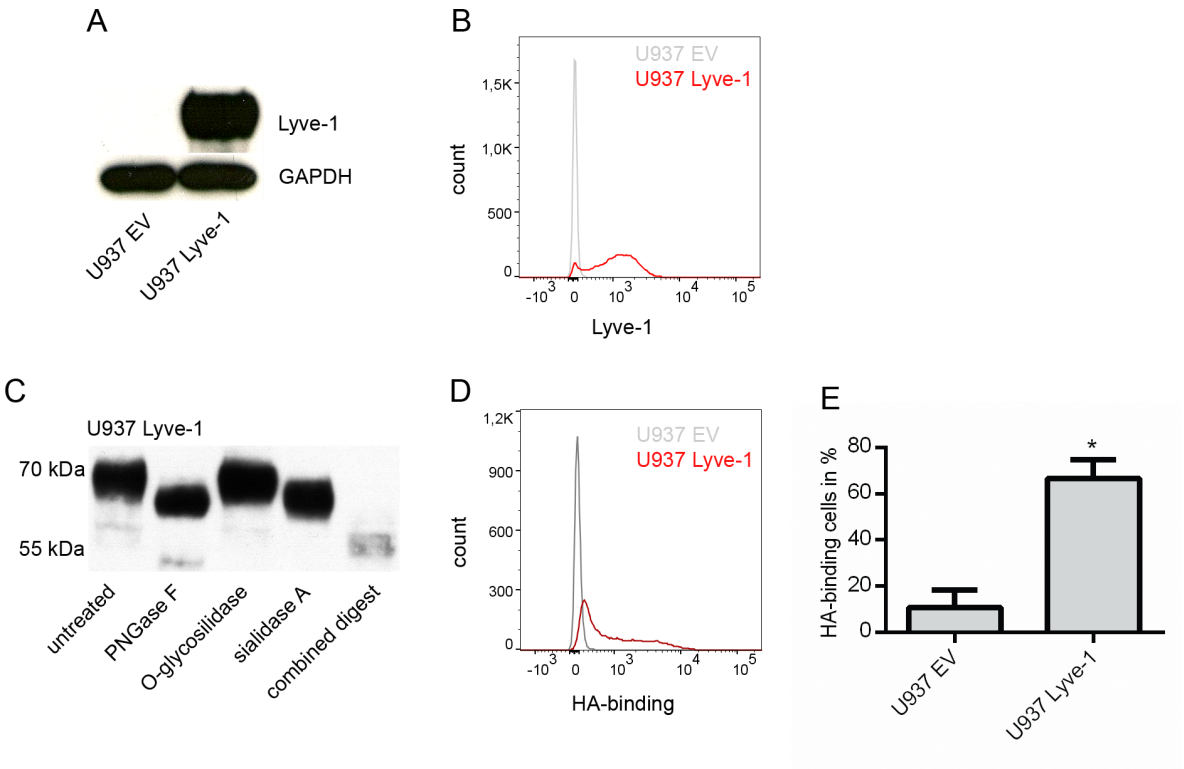

FIGURE 13: U937 Lyve-1 express glycosylated Lyve-1 which is able to bind HA. (A) Expression of Lyve-1 in transgenic U937 was verified on the protein level by Western blot and (B) flow cytometry. (C) Protein lysates derived from U937 Lyve-1 were digested for 3 h at 37°C with different deglycosylating enzymes as indicated and Lyve-1 was detected by immunoblot. (D) Overlay histogram of mock transduced U937 EV and U937 Lyve-1 stained for surface bound HA, representative experiment. (E) Ligand binding capability of U937 Lyve-1 was examined by incubation with biotinylated HA. Percentage of HA-binding cells was determined by flow cytometry using strepta-FITC to detect bound HA, (n=3).

The U937 cell line was transduced with pLenti-ADR3 EV and Lyve-1, respectively. Expression of Lyve-1 was verified by western blot and flow cytometry (Fig. 13 A + B). U937 derived Lyve-1 had a protein molecular weight of approximately 70 kDa, whereas the 322 AA sequence predicts a mass of 35.2 kDa. By treatment with PNGase F and sialidase A, post-translational modifications in the form of glycosylation could be removed resulting in a reduction of the protein weight to approximately 65 kDa. Digest with O-glycosilidase did not show any effect on the Lyve-1 protein weight, even though O-glycosylation sites have been described for the protein. The combined digest with all three enzymes yielded in a deglycosylated 55 kDa protein form, indicating that removal of glycosylation sites could not be achieved completely (Fig. 13 C). To assess the functionality of transgenic expressed Lyve-1 in U937, the cells were incubated with biotinylated HA, which could be detected in FACS by streptavidin-FITC. These experiments demonstrated enhanced binding of HA to U937 Lyve-1 in comparison to mock transfected U937 EV cells (Fig. 13 D + E).

4.3.2 Ligand binding does not influence proliferation rate of U937 Lyve-1

It has been described that in endothelial cells interactions of Lyve-1 with the ligands FGF-2 and low molecular weight hyaluronic acid (LMW-HA) induce cell proliferation, whereas stimulation with high molecular weight hyaluronic acid (HMW-HA) has an anti-angiogenic effect on endothelial cells [125, 132, 133, 151]. To assess the impact of Lyve-1 overexpression and ligand interactions on the proliferation rate of macrophages, U937 Lyve-1 and U937 EV were seeded in RPMI medium containing 0.2 % FCS and allowed to adapt to the culture conditions for 4 h. In the following the U937 Lyve-1 were stimulated with 20 ng/mL FGF-2 and 10 µg/mL LMW-HA or HMW-HA respectively. 24 h later, the proliferation rate was determined in a BrdU based proliferation assay. As a positive control, the cells were incubated overnight in cell culture medium supplemented with 2 % FCS.

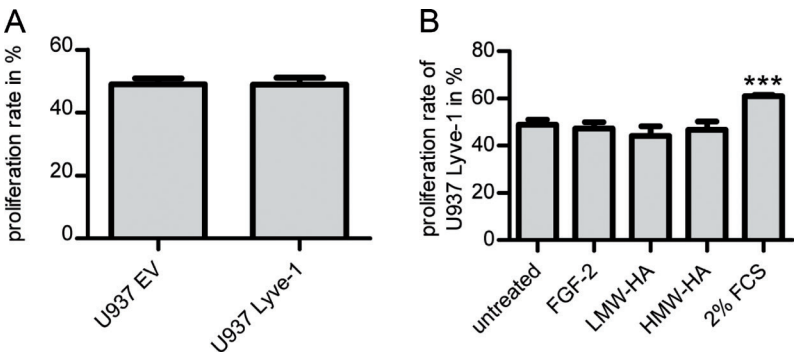

FIGURE 14: The proliferation rate of U937 Lyve-1 could not be affected by FGF-2 or HA stimulation. (A) *Proliferation rate of U937 EV and U937 Lyve-1 after culturing for 24 h in medium supplemented with 0.2 % FCS.* (B) *U937 EV and U937 Lyve-1 were stimulated overnight with ligands of Lyve-1 as indicated in culture medium containing 0.2 % FCS and the proliferation rate was measured in a BrdU assay. To induce proliferation in U937, control cells were incubated simultaneously in RPMI + 2 % FCS (n=5).*

Comparison of the proliferation rate of untreated transgenic U937 cells revealed that overexpression of Lyve-1 *per se* did not affect the proliferation rate of the monocytic cell line (Fig. 14 A). Furthermore, stimulation with the Lyve-1 ligands FGF-2 and HA did not induce significant changes in the proliferation rate of U937 Lyve-1. As a control, U937 Lyve-1 were incubated in medium supplemented with 2 % FCS which resulted in a significantly increased proliferation rate by 12.18 ± 2.308 % compared to cells which were cultured in medium with 0.2 % FCS (Fig. 14 B). Hence, in macrophages ligand binding to Lyve-1 does not influence cell proliferation.

4.3.3 Overexpression of Lyve-1 in B16F1 increases adhesion to fibronectin coated surfaces

For further functional analyses the murine melanoma cell line B16F1 was transduced with the ADR3 expression vector containing murine LYVE-1 or the EV construct as a control. We decided to use this model for two reasons. First, in contrast to U937, B16F1 are not suspension cells but do grow adherently in monolayers, which facilitates and simplifies the accomplishment of several basic assays to evaluate the impact of Lyve-1 overexpression on cellular functions. Secondly, we planned to perform *in vivo* experiments using a melanoma mouse model, thus evidently a murine melanoma cell line was selected, as experimental outcomes might provide first hints for the possible role of Lyve-1 in a tumour environment.

It has already been demonstrated that Lyve-1 is capable of binding to surfaces coated with immobilized HA, so the effect of Lyve-1 overexpression on cellular adhesion was examined [112].

For this purpose, a 96-well plate was coated either with 0.2 % gelatine or fibronectin (1 µg/mL). B16F1 EV and B16F1 Lyve-1 were seeded and allowed to adhere for 30 min. Afterwards, the plates were shaken for 10-15 s at 2000 rpm. Non-adherent cells were removed by washing carefully, while adherent cells were stained with crystal violet.

Transgenic surface expression of Lyve-1 in B16F1 was confirmed by flow cytometric analysis (Fig. 15 A). In a simple adhesion assay, B16F1 showed in general stronger connection to fibronectin coated surfaces compared to gelatine layered ones. Furthermore, the overexpression of Lyve-1 in B16F1 significantly enhanced the adhesion specifically to fibronectin, whereas adhesion to gelatine remained comparable between B16F1 EV and B16F1 Lyve-1 (Fig. 15 B).

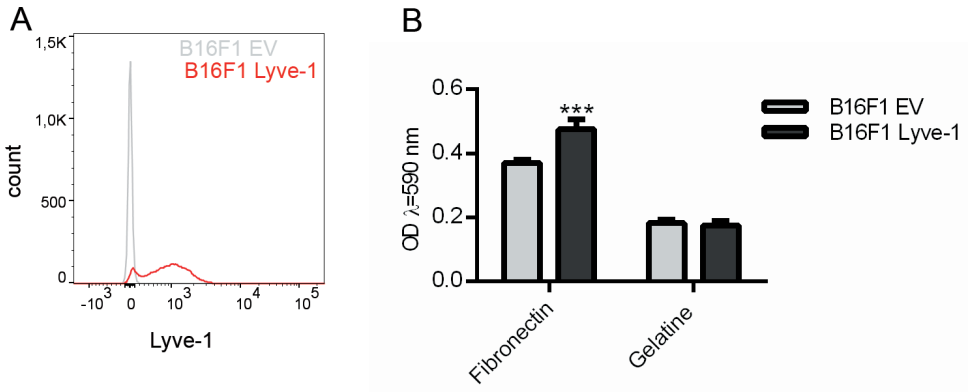

FIGURE 15: B16F1 Lyve-1 adhere more firmly to fibronectin coated surfaces. (A) Expression of murine Lyve-1 in B16F1 was verified by flow cytometry. (B) Cell culture vessels were coated either with fibronectin or with gelatine, after removal of non-adherent cells by subsequent shaking and washing, adherent cells were stained with crystal violet and colourimetrically quantified (n=9).

4.3.4 Lyve-1 overexpression does not influence migratory behaviour or cell death in B16F1

As the adhesion quality of cells also influences cellular migration, a simple wound healing assay was performed to test whether overexpression of Lyve-1 has an influence on migration. B16F1 EV and B16F1 Lyve-1 cells were grown until confluency was reached and a scratch was applied to the cell monolayer. The migration rate of the cells into the scratch was assessed by regular two-hour scratch measurements from 0 h-10 h and 24 h after wounding. To determine the migration rate, the area of the scratch was photographed and analyzed with the MiToBo (Microscope Image Analysis Tool Box) plug-in for ImageJ. The operator 'scratch assay analyzer' was used for the segmentation of scratch images by the detection of the scratch boundaries. The photographs were thus converted to binary images facilitating the computation of the scratch area.

By measuring the area of the wound, it could be demonstrated that B16F1 EV and B16F1 Lyve-1 migrated into the artificial scratch in comparable time. After 24 h, complete closure of the wound was neither achieved by B16F1 EV nor by B16F1 Lyve-1 and the gaps between the cell boarders remained at similar magnitude. Representative pictures of the time course are shown from the starting point (0 h) and during the closure of the wound after 4 h, 10 h and 24 h, indicating no differences in the amount of cells populating the scratch area (Fig. 16). Therefore, migration rate of B16F1 was not influenced by Lyve-1 overexpression.

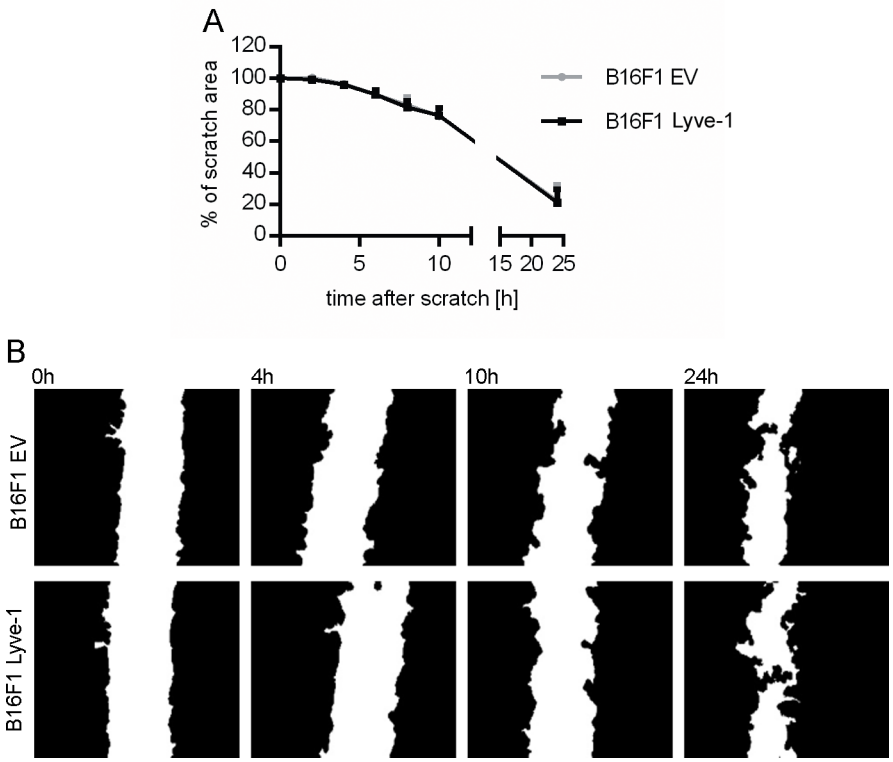

FIGURE 16: Overexpression of Lyve-1 does not affect motility of B16F1. *An artificial wound was caused to a confluent monolayer of transgenic B16F1 cells allowing the indirect assessment of the migration rate by measurement of the reduction of the scratch area over time. (A) Results are shown as percentages of four independent experiments with 100 % indicating total scratch area. (B) Representative pictures of the scratch experiment are shown. The phase contrast microscopic pictures were converted by ImageJ in such a way, that the scratch area could be calculated.*

Moreover, the transgene B16F1 cell lines were exposed to different concentrations of peroxide to study an eventual role of Lyve-1 in cellular response to apoptotic stimuli.

After three hours of peroxide stimulation, no differences in the amount of surviving cells between the lineages B16F1 EV and Lyve-1 respectively have been asserted. While 2.5 mM peroxide were not adequate to induce apoptosis, stimulation with 5 mM peroxide promoted cell death in 3.1 % of B16F1 EV and 6.8 % of B16F1 Lyve-1, however the difference was statistically not significant. In addition, exposure to 10 nM peroxide led to cell death in 41.7 % of B16F1 EV and 43.2 % of B16F1 Lyve-1 and in the case of stimulation with 20 mM in both cells only about 24 % of the cells survived the treatment (Fig. 17). In summary, transgenic expression of Lyve-1 did not affect the apoptosis rate of B16F1.

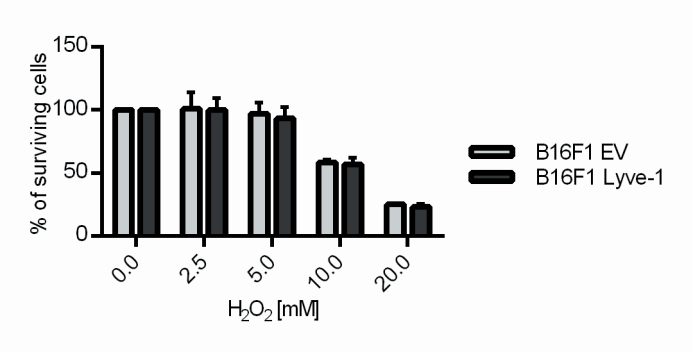

FIGURE 17: Apoptosis rate of B16F1 is not influenced by Lyve-1 overexpression. *Transgenic B16F1 cells were stimulated with varying concentrations of peroxide for 3 h. Dead cells were removed by washing and surviving cells were quantified following crystal violet staining. The percentage of surviving B16F1 EV and B16F1 Lyve-1 is given in relation to untreated cells (0 mM H_2O_2). Results of three independent experiments are shown.*

4.4 Functional implications of sLyve derived from macrophages

4.4.1 Identification of a soluble form of Lyve-1 in cell culture supernatant of U937

Lyve-1 is a structural homolog of the hyaluronan receptor CD44, which can be secreted by metalloproteinase-mediated shedding. It was not until recently that shedding of Lyve-1 has been reported to occur in lymphatic endothelial cells catalyzed by ADAM17 and MT1-MMP (MMP-14). To investigate if Lyve-1 is secreted from macrophages in a similar manner, the cell culture supernatant of U937 Lyve-1 cells was used for immuno-precipitation (IP).

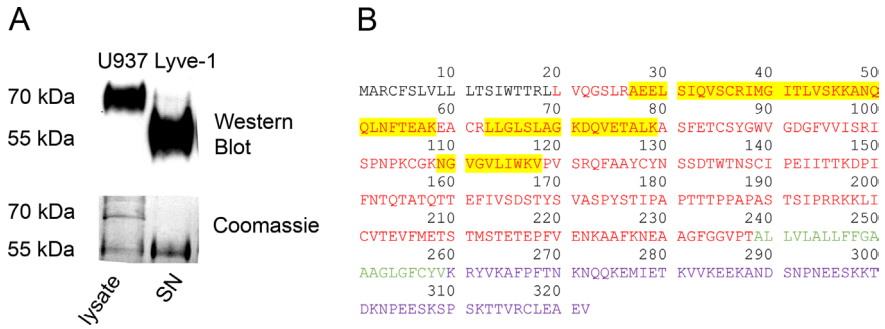

FIGURE 18: Confirmation of the existence of macrophage derived soluble Lyve-1. *(A) Lyve-1 was detected in western blot after Lyve-1 directed immunoprecipitation of lysates and culture supernatant (SN) derived from U937 Lyve-1. IP-samples were also stained with Coomassie brilliant blue, protein bands were excised and analyzed by mass spectrometry. (B) The amino acid sequence of Lyve-1 is depicted: signalling peptide – black, extracellular domain – red, transmembrane domain – green, intracellular domain – violet. Lyve-1 was purified from U937 Lyve-1 SN and analyzed by mass spectrometry. Identified tryptic peptides are highlighted in yellow.*

Detection of Lyve-1 after IP in western blot showed the full length version (70 kDa) of the protein in the samples derived from U937 Lyve-1 lysates, whereas a 15 kDa shorter version was found to be present in the cell culture supernatant (SN). After purification of Lyve-1 from the lysate and the SN and separation by SDS-PAGE, the polyacryl-amide gels were also stained by Coomassie brilliant blue (Fig. 18 A). The protein bands of Lyve-1 were broadly excised from the Coomassie gel and digested in-gel with trypsin. Such generated tryptic peptides were analyzed by MALDI-TOF. The tryptic peptides identified by mass spectrometry confirmed our assumption that the 55 kDa protein is the extracellular Lyve-1 domain (Fig. 18 B).

In lymphatic endothelial cells a soluble form of Lyve-1 is produced by MMP-mediated shedding. In order to examine if processing of Lyve-1 in macrophages occurs in a similar way, U937 Lyve-1 and transgenic HUVEC Lyve-1 were stimulated for 24 h with different shedding modulators. U937 Lyve-1 were stimulated directly after seeding, whereas HUVEC Lyve-1 were grown until a confluency of 70-80 % was reached before stimulants were added.

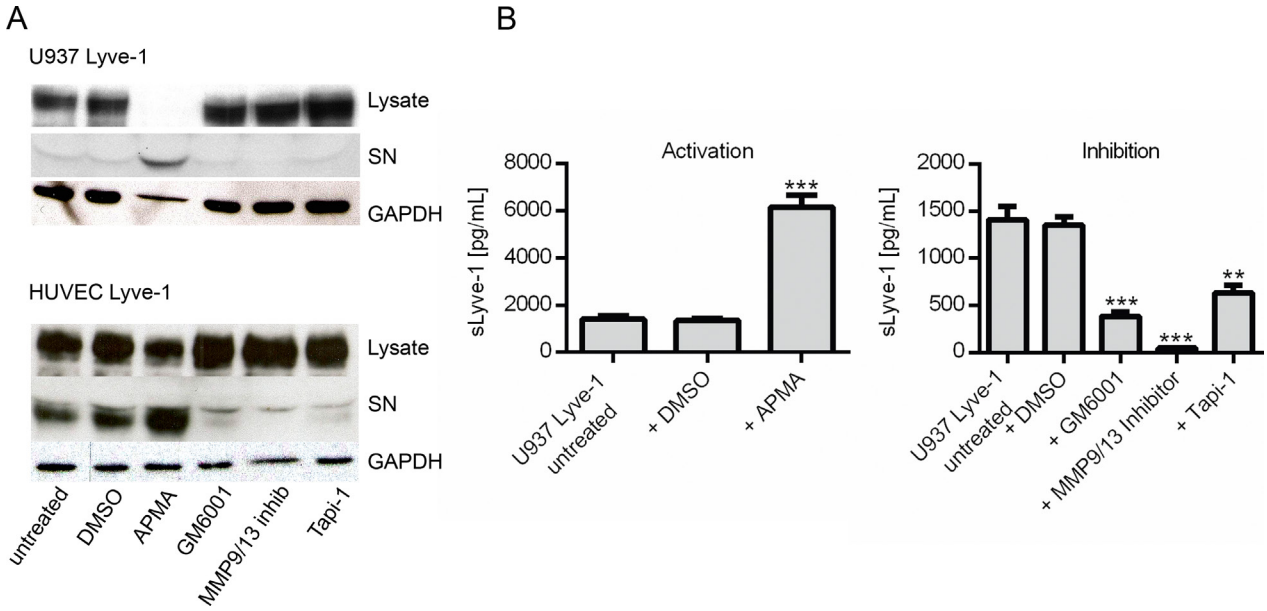

FIGURE 19: sLyve-1 is generated by metalloproteinase-mediated shedding. *U937 Lyve-1 and HUVEC Lyve-1 were stimulated with APMA, GM6001, MMP9/13 inhibitor, Tapi-1 and DMSO as a control (50 µM each) for 24 h. (A) Lyve-1 was detected by western blot, both in the cell lysates and in the supernatants (SN). (B) SN of U937 Lyve-1 were analyzed by ELISA facilitating the quantification of sLyve-1 after treatment with shedding modulators (n=3).*

Stimulation of the transgenic cell lines U937 Lyve-1 and HUVEC Lyve-1 with the shedding activator APMA resulted in the accumulation of sLyve-1 in the supernatant, whereas reduced amounts of full-length Lyve-1 were detected in the cell lysates. The opposite was true when the cells were stimulated with the shedding

inhibitors GM6001, MMP-9/13 inhibitor and Tapi-1 resulting in reduction of Lyve-1 shedding (Fig. 19 A). Quantification of sLyve-1 by ELISA in the supernatants of U937 Lyve-1 following stimulation with the shedding modulators confirmed the western blot finding revealing that MMP-9/13 inhibitor has the strongest inhibitory effect (Fig. 19 B). Besides MMP-9 and MMP-13, this small molecule inhibitor also targets metalloproteinases 1, 3 and 7. Hence, Lyve-1 secretion in macrophages occurs via a shedding process that is orchestrated by metalloproteinases similar, but less efficient if compared to shedding in endothelial cells.

4.4.2 sLyve-1 reduces the proliferation rate of melanoma cell lines

We hypothesized that the shedded ectodomain of Lyve-1 might function as a decoy receptor for the respective ligands such as HA and FGF-2. To test this assumption in the connection with possible implications of Lyve-1 shedding for tumour growth, we assessed the proliferation rate of melanoma cell lines after exposure to soluble Lyve-1 (sLyve-1) *in vitro*. 1×10^6 U937 Lyve-1 or EV were seeded per millilitre FCS-free cell culture medium. After 24 h cells were removed by centrifugation and the conditioned medium was again centrifuged to remove remaining cellular debris. HT144 were seeded in the conditioned medium mixed with fresh FCS-free culture medium 3:1. The melanoma cell line was cultured for 24 h and the proliferation rate was determined in a BrdU assay. In addition, HT144 and A375 were seeded in a 96-well plate and stimulated for 48 h with different concentrations of synthesized sLyve-1 (amino acids 24-238) cell growth was assessed by crystal violet staining.

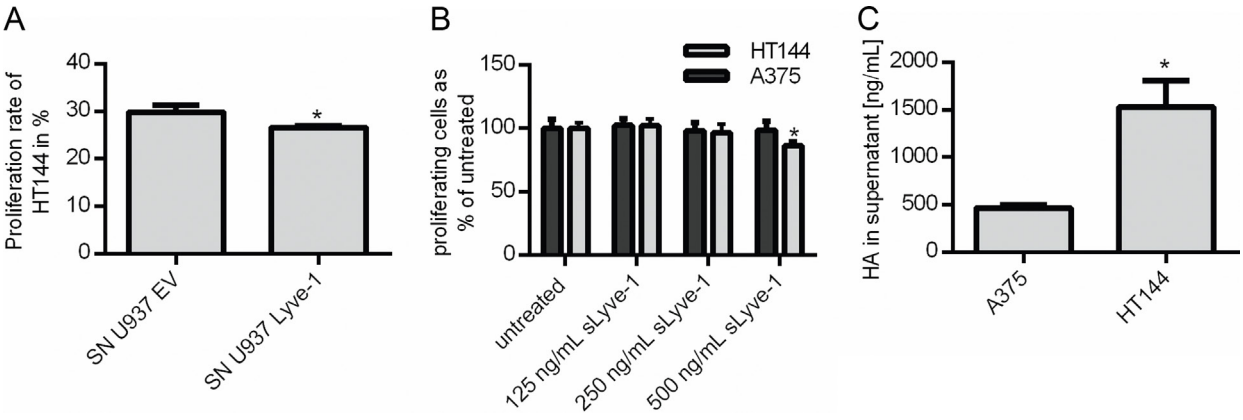

FIGURE 20: sLyve-1 inhibits growth of melanoma cell line HT144. (A) *Proliferation rate of* HT144 *cultured for 24 h in U937 EV/Lyve-1 conditioned* FCS*-free medium mixed 3:1 with fresh* FCS*-free culture medium.* (B) *Different concentrations of sLyve-1 were added to* HT144 *and* A375 *cultured in medium supplemented with 2 %* FCS*, number of cells was determined by crystal violet staining in relation to untreated control cells, (n=8).* (C) *Quantification of* HA *in supernatant of* A375 *and* HT144 *cells after 24 h of cultivation in* FCS*-free medium by* ELISA*, (n=3).*

Cultivation of HT144 in U937 conditioned medium resulted in a significant inhibition of the proliferation of the cancer cell line specifically in medium derived from U937 Lyve-1 (Fig. 20 A). To confirm that this was due to the presence of sLyve-1 in the culture supernatant, proliferation of HT144 and additionally A375 cells was assessed after treatment with synthesized sLyve-1. Whereas no effect of sLyve-1 was observed on A375 cells, 500 ng/mL sLyve-1 significantly inhibited cell proliferation of HT144 cells after 48 h (Fig. 20 B). Finally, conditioned FCS-free medium from A375 and HT144 cells was examined for the presence of HA and quantification by ELISA showed enhanced production of HA by the HT144 (477.6 ± 29.35 ng/mL) cell line compared to A375 cells (1352 ± 168.2 ng/mL) (Fig. 20 C). Taken together, these results indicate that sLyve-1 interferes with melanoma cell proliferation by interacting with autocrine HA stimulation.

4.4.3 sLyve-1 is significantly elevated in blood plasma of psoriasis patients

To test whether circulating Lyve-1 exists in human blood and may qualify as a potential prognostic marker in human diseases, we measured levels of sLyve-1 in plasma samples derived from patients suffering from skin disorders.

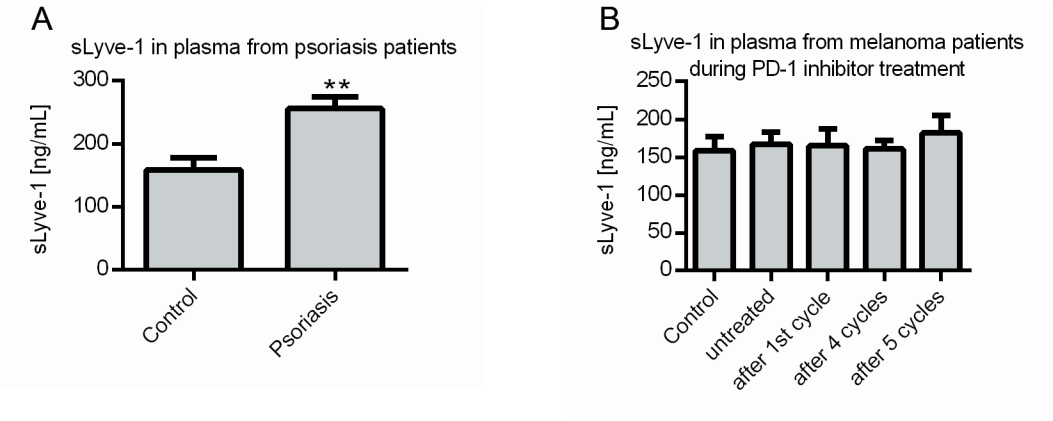

FIGURE 21: sLyve-1 is detectable in human blood plasma. *The amount of sLyve-1 was determined by* ELISA *in blood plasma of healthy donors, (n=20) compared to (A) plasma derived from psoriasis patients, (n=42) and (B) patients suffering from melanoma, (n=11) before and at different time points of* PD-1 *inhibitor treatment.*

sLyve-1 could be detected in blood plasma samples derived from healthy donors with concentrations of 158.8 ± 18.67 ng/mL. In the plasma of patients suffering from psoriasis, which is Th1 cytokine dominated skin disease, sLyve-1 levels were found to be significantly elevated (256.1 ± 18.03 ng/mL) (Fig. 21 A). In addition, the concentration of sLyve-1 was determined in plasma from melanoma patients, which were comparable to the control group of healthy donors. All melanoma patients received a PD-1 inhibitor treatment; monitoring of sLyve-1 levels during different time points of the treatment revealed no relevant differences in the plasma concentration of Lyve-1 (Fig. 21 B).

4.5 Relevance of dexamethasone dependent proteins for tumour growth

4.5.1 *In vivo* Lyve-1 deficiency leads to increased tumour growth

As already shown in 2006 by Schledzweski et al., Lyve-1$^+$ TAM are present in subcutaneously (s.c.) grown B16F1 tumours in mice [116].

We examined the growth of melanoma tumours in C57BL/6 Lyve-1$^{-/-}$ knockout mice and compared it to the tumour growth in wild type control mice. For this purpose, 1×10^6 B16F1 cells were injected s.c. into the flank of the mice.

After ten days, tumour growth of B16F1 in C57BL/6 Lyve-1$^{-/-}$ and wild type control mice, the mice were sacrificed and the tumours were harvested and analyzed. Immunohistological staining of tumour intersections with the markers for macrophages CD68 and for endothelial cells CD31 revealed in both cases a minor, not significant reduction of positive cells in the tumours derived from Lyve-1 knockout mice (Fig. 22 A + B). In contrast, significantly more cells were stained positive for the proliferation marker Ki-67 in tumours grown in C57BL/6 Lyve-1$^{-/-}$ (Fig. 22 C). The higher proliferation rate of the tumour cells also correlated with the finding that the tumour end weight of B16F1 tumours was increased in the knockout mice, thus Lyve-1 deficiency resulted in a higher tumour end weight (Fig. 22 D).

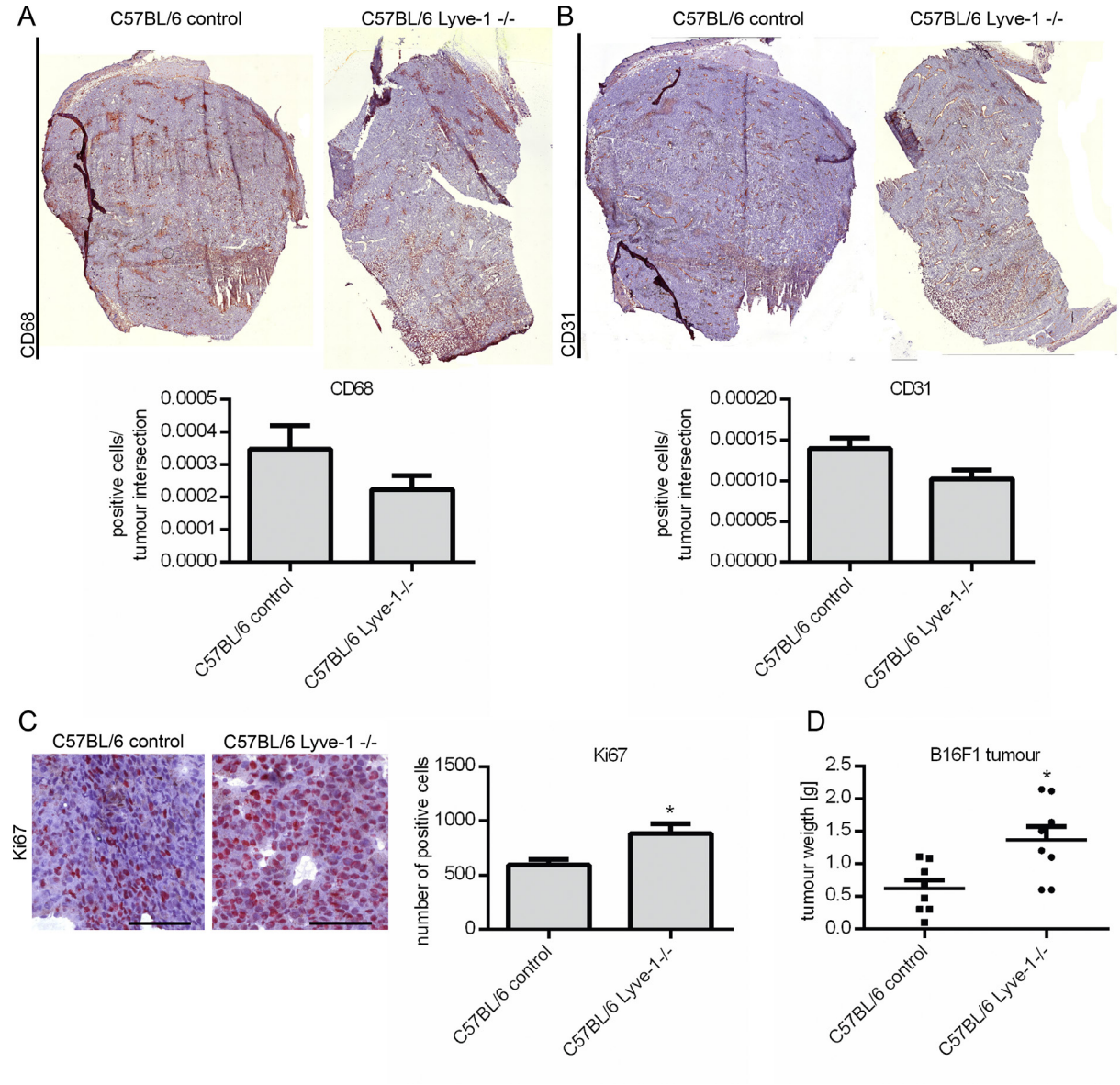

FIGURE 22: Tumour growth is enhanced in Lyve-1$^{-/-}$ mice. 1×10^6 B16F1 melanoma cells were injected s.c. into the flank of the mice and after ten days of growth, the mice were sacrificed and the tumours were harvested for analysis. (A) Immunohistological staining of 7 µm acetone-fixed cryosection of CD68 and (B) CD31. The number of positively stained cells was assessed in relation to the area of the tumour intersection, representative stainings are shown, (n=7). (C) Staining of the cryosections with anti-Ki67, scale bars = 100 µm. The positive cells of five representative pictures per tumour sample were counted, (n=7). (D) Tumour end weight after 10 days of growth (n=8).

Further in *vivo* tumour growth experiments were accomplished with B16F10 LUC cells. These cells express luciferase derived from the North American firefly. This cell line was used for the *in vivo* monitoring of tumour growth in C57BL/6 Lyve-1$^{-/-}$ and wild type control mice by measuring a bioluminescence signal which is produced by the tumour cells after the administration of the luciferase substrate luciferin. 150µL of D-Luciferin potassium salt (30mg/mL) in PBS were injected intraperitoneal into the B16F10 LUC tumour bearing mice. The mice were anesthetized in an isoflurane gas chamber and luminescence pictures were taken three minutes after substrate injection with IVIS Lumina (PerkinElmer, Living Image 4.3).

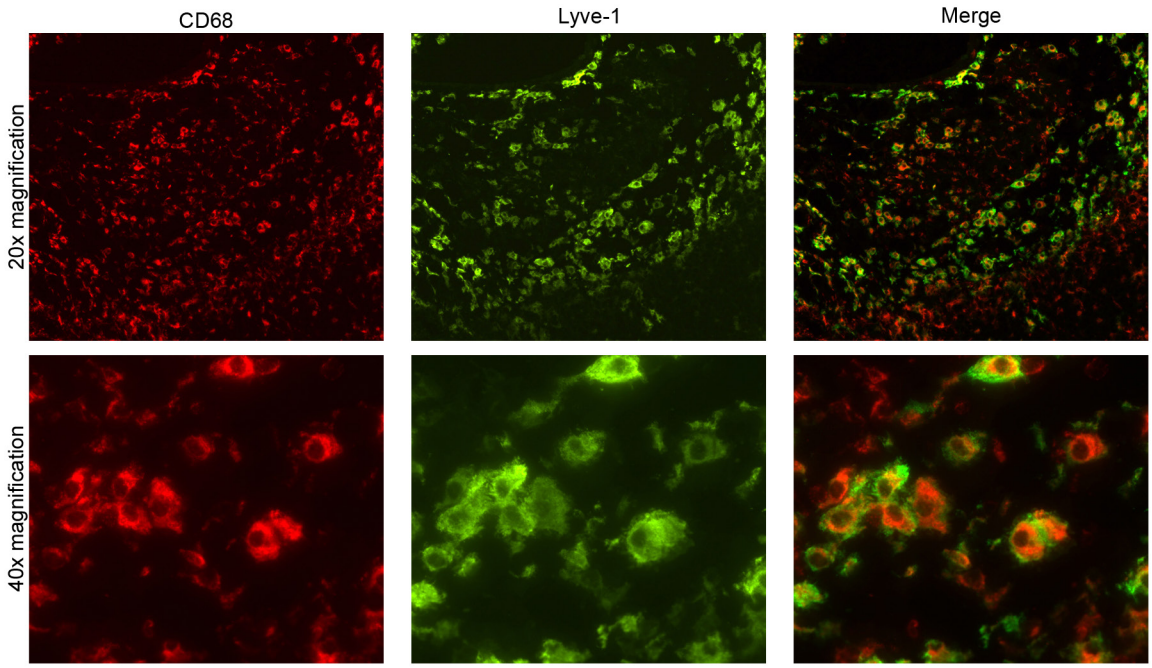

FIGURE 23: Lyve-1$^+$ TAM are present in the periphery of B16F10 tumours. 1×10^6 B16F10 LUC *melanoma cells were injected s. c. into the flank of the* C57BL/6 *wild type mice. 11 days after tumour cell injection, mice were sacrificed and tumours were snap frozen in liquid nitrogen. Immunofluorescent staining of 7 µm acetone fixed cryosection with anti-*CD68 *(red) and anti-Lyve-1 (green) of tumours derived from wild type mice was accomplished, representative pictures are shown.*

By immunofluorescent double staining with anti-CD68 and anti-Lyve-1 of B16F10 LUC tumours derived from wild type mice the existence of Lyve-1$^+$ macrophages in the tumour stroma could be confirmed. Lyve-1$^+$ TAM were found mainly in the tumour periphery, whereas they occurred only sporadically in the tumour centre (Fig. 23).

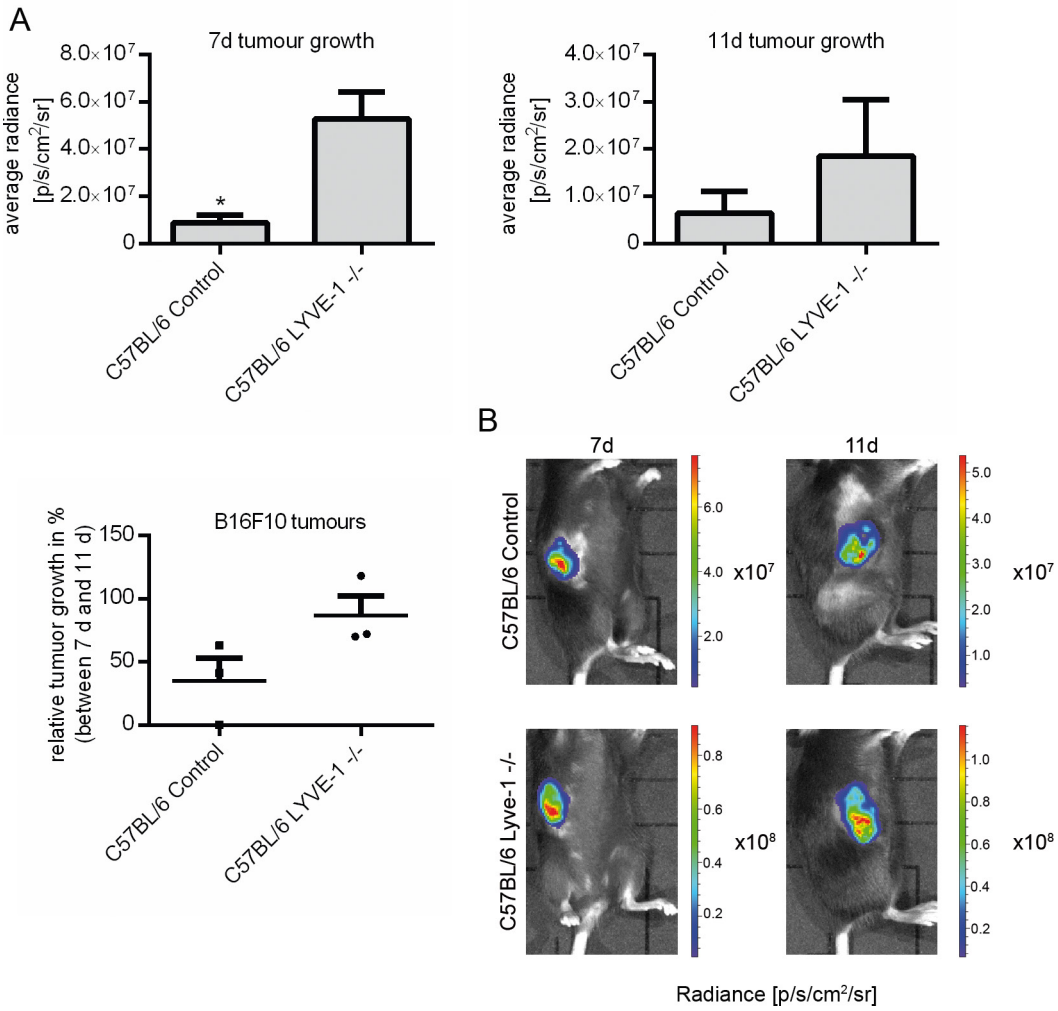

FIGURE 24: Tumour growth is accelerated in Lyve-1$^{-/-}$ mice. 1×10^6 B16F10 LUC melanoma cells were injected s.c. into the flank of the C57BL/6 Lyve-1$^{-/-}$ and wild type mice respectively. (A) Monitoring of tumour growth via luminescence measurement following luciferin injection after 7 days and 11 days of B16F10 LUC tumour growth following tumour cell injection; assessment of average photon flux and relative tumour growth, (n=3). (B) Representative pictures of tumour bearing mice after luminescence injection at the indicated time points after tumour cell injection.

Luminescence measurement on day 7 and day 11 after tumour cell injection facilitated the *in vivo* monitoring of tumour growth in Lyve-1 knockout mice and wild type controls. The average photon flux, which strongly correlates with the tumour volume, was assessed. On day 7 we measured an enhanced average photon flux in the knockout mice, while on day 11 differences between the experimental groups were more balanced. Regarding the relative tumour volume gain between day 7 and day 11, tumours in the knockout mice grew faster by trend (Fig. 24). Overall these analyses reveal that Lyve-1 deficiency accelerates tumour cell proliferation during the early phases of tumour growth.

4.5.2 Myeloid specific depletion of the glucocorticoid receptor accelerates tumour growth

The *in vitro* experiments have highlighted the central role of glucocorticoids for the induction of Lyve-1. To define the role of glucocorticoids for Lyve-1 expression and tumour growth *in vivo* a new mouse model was generated. A strain of mice (LysMcre) that express nuclear localized-Cre recombinase under the control of myeloid specific, endogenous Lyz2 promoter/enhancer elements was crossed with mice (GR fl) having loxP sites adjacent to exon 3 of the NR3C1 gene which encodes for the GR. Descendants of this breeding strategy show a myeloid specific knockout of GR. Recombination of NR3C1 was confirmed by PCR-based genotyping. B16F10 LUC cells (1×10^6) were injected s.c. into the flank of female $GR^{LysMcre}$ mice and tumour growth was documented during 12 days. Tumour growth was monitored by luminescence measurement as described above by administration of luciferin to the tumour bearing mice.

Measurement of the average luminescent radiance of B16F10 tumours of $GR^{LysMcre}$ and wild type controls showed no significant differences on day 4 and day 8 after the injection of the tumour cells. A significant greater average flux was measured on day 12 in the $GR^{LysMcre}$ experimental group which implied increased tumour volumes (Fig. 25 B). Furthermore, relative gain of tumour volume was significantly increased in the $GR^{LysMcre}$ mice between day 8 and day 12 (Fig. 25 B). After two weeks, the tumours were harvested and weighed at which it was found that the tumours from $GR^{LysMcre}$ were considerably bigger compared to the tumours which grew in the wild type controls (Fig. 25 C).

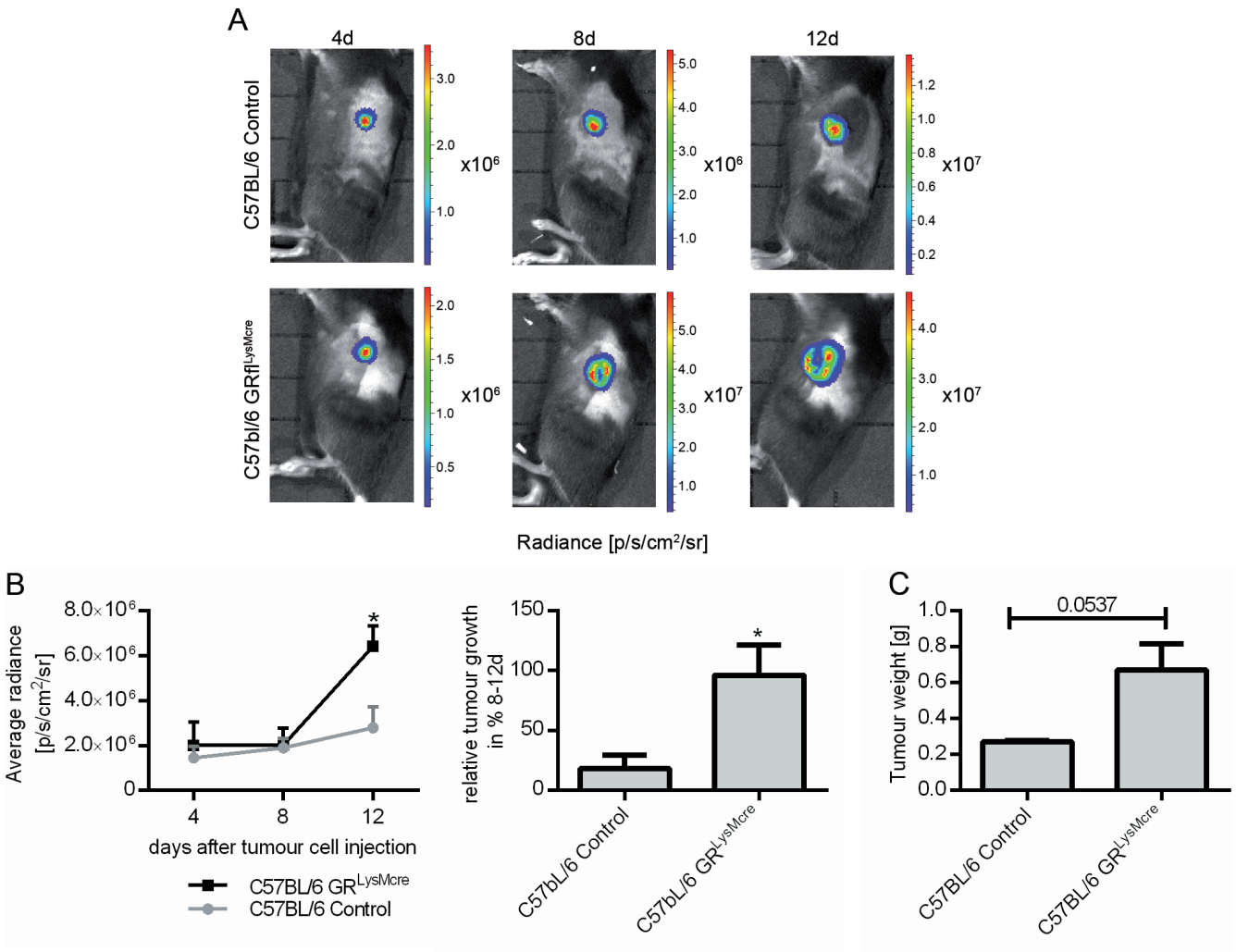

FIGURE 25: Tumour growth is enhanced in $GR^{LysMcre}$ mice. 1×10^6 B16F10 LUC *melanoma cells were injected s.c. into the flank of the* $GR^{LysMcre}$ *and wild type mice, respectively. (A) Monitoring of tumour growth via luminescence measurement after luciferin injection at 4 d, 8 d and 12 d after tumour cell injection. (B) Assessment of average photon flux and relative gain of tumour area between day 8-12 (n=5). (C) On day 14 of tumour growth mice were sacrificed and the tumour end weight was determined (n=3).*

Cryosections of the melanoma tumours grown in wild type and $GR^{LysMcre}$ mice were analyzed by immunofluorescent staining. CD68/Lyve-1 double positive cells could be detected in the periphery of B16 tumours which were grown in $GR^{LysMcre}$ mice. Therefore, ablation of GR expression in macrophages did not suppress Lyve-1 expression in TAM. Evident differences regarding distribution and quantity of $CD68^{+}$/$Lyve\text{-}1^{+}$ cells between tumours from control mice and the mutant mice strain were not observed (Fig. 26). Although, GR signalling seems to be a key regulator of Lyve-1 expression *in vitro*, during tumour growth conditions *in vivo* other factors, which remain to be determined, play a role in the regulation of Lyve-1 expression. In summary, myeloid specific knockout of GR had an accelerating effect on tumour growth, but had no effect on Lyve-1 expression in TAM.

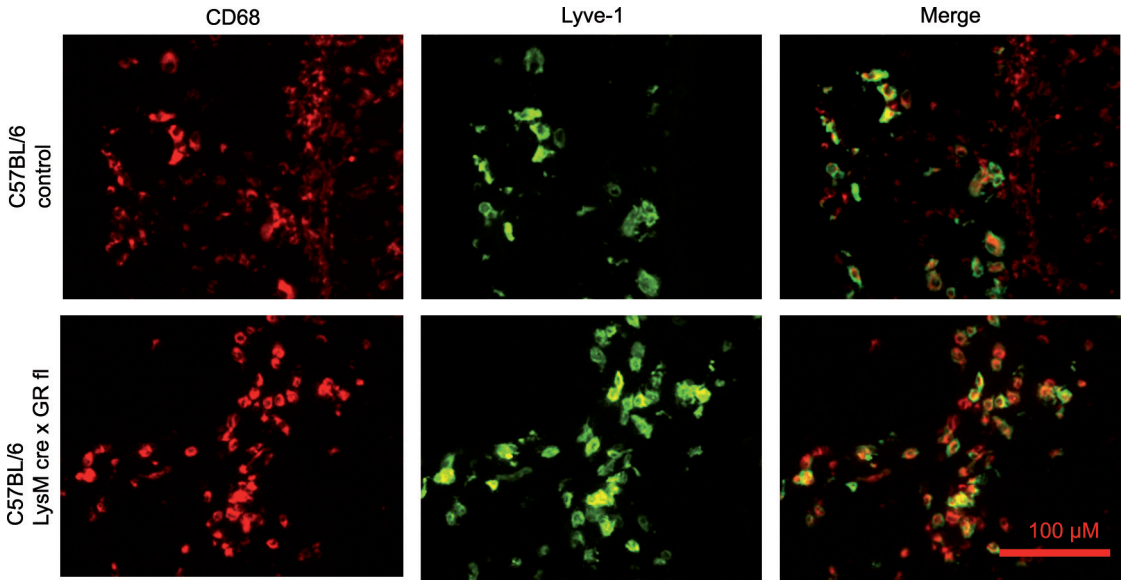

FIGURE 26: Knockout of GR in macrophages does not suppress Lyve-1 expression in TAM. 1×10^{6} B16F10 LUC melanoma cells were injected *s.c.* into the flank of the $GR^{LysMcre}$ and wild type mice respectively after 12 days of growth, mice were sacrificed and tumours were snap frozen in liquid nitrogen. Immunofluorescent staining of 7 µm acetone fixed cryosection with anti-CD68 (red) and anti-Lyve-1 (green) was performed, representative pictures are shown, scale bar = 100 µM.

5. DISCUSSION

5.1 Characterization of Lyve-1$^+$ macrophages *in vivo* and *in vitro*

Immunohistological staining of human primary melanoma revealed the existence of Lyve-1$^+$ cells within the tumour stroma which were identified by histopathological analyses as endothelial cells and macrophages. The existence of Lyve-1$^+$ macrophages was further substantiated by the observation that these cells do also express the macrophage markers CD68 and CD163. By sequential staining, CD68$^+$/Lyve-1$^+$ cells could be identified for the first time. This novel staining method, which has recently been established in our lab, allows successive staining of the same slide with different antibodies and therefore is really helpful to study the inflammatory environment of tumours. The staining revealed that these double positive cells mainly accumulate in the periphery of the tumours.

In vitro, Lyve-1 expression could be induced in murine BMDM by the stimulation with tumour conditioned medium (TCM)/dexa/IL-4. To transfer this to a human setting, we stimulated PBMC isolated from Buffy coat samples and detected Lyve-1 expression after seven days of stimulation with MDI. Besides Lyve-1 the combined stimulation wit MDI induces genes, such as GLDN, EPS8, GPR91 and CLEC10A which were also found to be expressed by TAM *in vivo*. Hence, this stimulation of PBMC was used as a model for the differentiation of human TAM *in vitro* [136]. However, the activation status and phenotype of the MDI-induced macrophages has yet not been further characterized.

Due to the high heterogeneity of macrophages their classification represents a serious obstacle. Diverse models exist that aim at the classification of macrophage phenotypes. Most commonly macrophages were separated into pro-inflammatory M1 macrophages induced by Th1 derived cytokines such as IFN-γ and TNF-α, and microbial antigens like LPS and anti-inflammatory M2 macrophages shaped amongst others by Th2 cytokines like e.g. IL-4 or IL-13, IL-10 and glucocorticoids. Still, this division only represents two extremes of a continuum of various phenotypes lying in between. *In vivo*, macrophages are exposed to complex microenvironments composed of a mixture of pro- and anti-inflammatory stimuli and hence develop a rather mixed M1/M2 phenotype. Leading researchers in the field of macrophages recently formulated guidelines to describe macrophage activation and polarization more specifically in the corresponding experimental set up by delineation of the macrophage source, the activators used for macrophage stimu-

lation and marker expression profiling to describe the macrophage activation status [42]. Taking this into account expression analyses of well-studied macrophage markers on MDI-induced macrophages was accomplished and compared to control cells which were stimulated by M-CSF only. The expression levels of pan-macrophage marker CD11b, mannose receptor CD206, scavenger receptor CD163 and MHC class II protein were examined. The analysis revealed up-regulation of the scavenger receptors CD206 and CD163 in MDI-treated PBMC, both are commonly used markers for M2-like macrophages and TAM [37]. Furthermore, TAM are characterized by impaired antigen-presentation abilities as a result of reduced expression of MHC molecules. Yet, an influence of MDI on MHC class II expression was not observed in MDI stimulated PBMC.

Further expression analyses of the MDI-induced macrophages indicated a shift of the arginine metabolism towards the production of ornithine and urea accompanied by decreased production of NOS and ROS. Enhanced degradation of L-arginine as a result of arginase up-regulation in myeloid cells constitutes a central mechanism of tumour immunoescape. Depletion of L-arginine leads to the suppression of the anti-tumour response mediated by T cells through the down-regulation of TCR ζ chain. In different neoplasms such as prostate cancer, non-small lung cancer and different myelomas involvement of arginase mediated immune suppression of tumour infiltrating leukocytes has been shown [142]. Immunosuppressive qualities of MDI-induced macrophages are thus conceivable. Taken together, our results clearly demonstrate that the combined stimulation of MDI induces a M2-like phenotype in PBMC. As this stimulation induces many different genes which also been described to be expressed by TAM our model might constitute a novel *in vitro* differentiation method to induce a TAM-like phenotype in PBMC.

Stimulation of murine BMDM with TCM, dexa and IL-4 induced Lyve-1 expression in approximately 40 % of the treated cells. In a similar manner, cytokine stimulation of human PBMC resulted in the formation of a Lyve-1 expressing subpopulation comprising a minor fraction of 25 % of the stimulated cells. Protein expression profiling of the above mentioned macrophage markers was repeated to determine specific differences between the Lyve-1$^+$ and Lyve-1$^-$ MDI-derived distinct subsets. Lyve-1 expression in MDI-treated PBMC was accompanied by increased expression of CD11b and CD206. A similar macrophage marker expression profile has already been described in a subpopulation of TAM derived from TS/A tumours. Lyve-1 was differentially expressed in a subpopulation of macrophages displaying high expression of ARG-1, CD206, CD163, STAB-1 and low expression of MHC class II [73]. In connection with our results, we assume that the *in vitro* cytokine stimulation with MDI induces the shaping of a phenotype mirroring specific characteristics of Lyve-1$^+$ TAM. Moreover, Lyve-1$^+$ macrophages are a distinct subpopulation which is more oriented towards a M2-like phenotype.

5.2 Critical pathways for Lyve-1 induction *in vitro*

MDI treatment induces Lyve-1 expression in PBMC in a time-dependent manner showing progressively increasing Lyve-1 expression between day 5 and day 9 of MDI stimulation. This raised the question if Lyve-1 is a direct target of dexamethasone induced glucocorticoid receptor (GR) activation. Successive addition of either GR inhibitor mifepristone to MDI treated cells or dexamethasone to M-CSF/IL-4 stimulated cells demonstrated the crucial dependency of Lyve-1 expression on GC during the complete stimulation time. Impairment of dexamethasone stimulation at any time reduced Lyve-1 expression significantly. The GR is a member of the hormone receptor transcription factor family, which is expressed almost ubiquitously. Upon ligand binding GR is liberated from a multiprotein complex and translocates from the cytoplasm to the nucleus to modulate gene expression via binding to GR responsive elements (GRE) in the regulatory region of its target genes. Transactivation of genes requires the dimerization of GR whereas transrepression can also be mediated by monomers. Anti-inflammatory effects of GR are mediated by the transcription of anti-inflammatory genes like IL-10 and by inhibiting the action of key-regulators of inflammation such as NFκB and AP-1 [143, 144]. In macrophages, GC greatly influence gene expression. On the one site immunomoldulators are downregulated such as GM-CSF, TNF-α, IL-1, IL-6, iNOS and COX-2 [145]. On the other site, a recent study which examined gene expression during monocyte to macrophage differentiation under the influence of glucocorticoids demonstrated activation of diverse genes associated with increased cell motility, decreased adhesion and enhanced phagocytosis [146]. In general, glucocorticoid receptor activation in macrophages is associated with the formation of a M2-like phenotype. Such macrophages are mainly involved in homeostatic processes, wound healing and resolution of the inflammatory response. TAM resemble M2-like macrophages in many ways as they promote immunoescape, as well as tumour growth and progression. Therefore, it is tempting to speculate that the dependency on GC of Lyve-1 expression is suggestive of a possible pro-tumour role of Lyve-1.

In the course of expression profiling of murine Lyve-1$^+$ BMDM induced by the combined stimulation with TCM/dexa/IL-4, Ms4a8a was identified as a novel marker of murine M2 macrophages. Examination of regulatory mechanisms of Ms4a8a expression *in vitro* revealed that impairment of either GR, p38 MAPK or NFκB signalling inhibited Ms4a8a expression. In analogy to these observations the eventual contribution of these signalling pathways on Lyve-1 induction was assessed. While Lyve-1 expression in MDI-treated PBMC remained unperturbed under the influence of a NFκB inhibitor, treatment with the p38 MAPK inhibitor SB203580 diminished Lyve-1 induction significantly. The physiological role of p38 MAPK activation comprises stress and immune responses as well as regulation of apoptosis and differentiation [147]. TGF-β is a well characterized inducer of the p38

MAPK signalling via SMAD independent activation of a MAPK signalling cascade involving the subsequent activation of TRAF6, TAK1, as well as MMK4 and MKK3/6 following the formation of a TGF-β receptor complex [148]. In macrophages TGF-β stimulation is involved in the induction of M2-associated genes. Therefore, TGF-β was used for PBMC stimulation in different combinations with M-CSF, dexa and IL-4 to examine its effect on Lyve-1 induction *in vitro*, at which TGF-β showed no influence on Lyve-1 induction.

p38 MAPK signalling has also been identified to be involved in IL-4 mediated differentiation of M2 macrophages. The first stimuli which were identified to induce alternative activation of macrophages were IL-4 and IL-13 inducing enhanced expression of CD206 and diminished expression of pro-inflammatory cytokines. Classically, IL-4 binding to its corresponding receptor activates the JAK/STAT6 pathway or PI3KC downstream signalling. In murine peritoneal macrophages, activation of p38 MAPK signalling in response to IL-4 stimulation has been observed and was related to the expression of M2 marker genes, such as ARG-1, YM-1 and FIZZ-1 [149]. Further evidence for this connection was provided by the description of p38 MAPK dependency of APRIL induction in murine macrophages following exposure to IL-4 [150]. In human PBMC, stimulation with M-CSF and dexa suffices to induce Lyve-1 expression, but the addition of IL-4 boosts this effect probably through indirect mechanisms mediated by the activation of p38 MAPK. This is also in line with the observation that mifepristone mediated suppression of Lyve-1 induction proved to be more efficient compared to treatment with SB203580. Considering the strong dependency of Lyve-1 induction on dexamethasone we concluded that Lyve-1 induction in PBMC is subjected to GR activation by direct or indirect mechanisms and is augmented by p38 MAPK signalling.

5.3 Functional implications of Lyve-1 expression

Both MDI-induced PBMC and transgenic U937 express Lyve-1 in a highly glycosylated form. In the area of the link domain two sites for N-linked glycosylation have been identified which are involved in the HA-binding capacity of Lyve-1. Further multiple sites for O-linked glycosylation are located in the membrane proximal region which is characterized by numerous serine and threonine residues. Lately, it was demonstrated that HA-binding to Lyve-1 depends on the surface density of the receptor and cluster formation or higher order complexation of HA accordingly. Lyve-1 monomers show only weak affinity to HA thus it is conceivable that several receptors are required for stable binding of HA on the cellular surface in primary lymphatic endothelial cells. In our expression model of lenti-

viral overexpression Lyve-1 expression levels were sufficient to bind biotinylated HA efficiently on the cell surface. Interactions of endogenously expressed Lyve-1 in macrophages with HA still need examination.

HA is a linear non-sulphated polymer component of the extracellular matrix build by repetitive assembly of [β(1,4)D-glucuronic acid-β(1,3)N-acetyl-D-glucosamine]. HA is subjected to constant turn-over which is mainly accomplished by local uptake and degradation by macrophages and fibroblast or transport via the lymph to lymph nodes for final degradation. HA exerts a wide range of different functions which are mediated by diverse receptors with distinct properties, at which the size of the polymer is relevant, too. While HMW-HA exerts anti-inflammatory functions, LMW-HA promotes inflammation and angiogenesis [151]. Excessive production of HA due to upregulated expression of HA-synthases is associated with the formation of aggressive, metastatic tumours. High HA levels further correlate with tumour progression in different tumour entities, such as breast, ovarian, prostate and colorectal cancer [152, 153]. *In vivo*, inhibition of HA synthesis in prostate cancer cells attenuated tumour growth [154]. A possible explanation for these findings was provided by a study demonstrating that inhibition of HA production within the tumour stroma resulted in decreased recruitment of TAM and thus diminished formation of a tumour vasculature. Notably, aggregation of HA by versican, a member of the HA-binding chondroitin sulphate proteoglycan family, was found to be necessary for successful TAM recruitment and enhanced tumour growth [155]. The underlying mechanism of the interaction of TAM with stromal HA has not been examined yet, though involvement of Lyve-1 is conceivable.

Lyve-1 possesses dual ligand binding activity. Besides HA, different growth factors such as PDGF-bb, VEGF-a and FGF-2 have been identified as ligands of Lyve-1. Their binding occurs outside of the HA-binding link domain. Deglycosylation of Lyve-1 impaired interactions with FGF-2 demonstrating the importance of glycosylation for growth factor interactions. The impact of receptor density on growth factor bindings has not been under investigation yet. However, it seems to be likely that interactions between Lyve-1 and its growth factor ligands occur independently from receptor clustering, as interactions between Lyve-1 and FGF-2 were shown in lymphatic endothelial cells both *in vitro* and *in vivo*. In lymphatic endothelial cells interactions with either LMW-HA or FGF-2 with Lyve-1 induced proliferation and migration. Thus, these interactions induce lymphangiogenesis [125, 132].

While the majority of TAM differentiate from chemokine recruited tumour infiltrating monocytes, recent findings suggest expansion of TAM by local proliferation in mammary tumours [156, 157]. In this context, cell surface retention of macrophage produced growth factors could also induce proliferation in an autocrine manner [124]. In our transgenic macrophage cell line however neither overexpression of Lyve-1 *per se* nor stimulation with its ligands HA or FGF-2 induced cell proliferation.

Further functional analyses were performed using the murine melanoma cell line B16F1, which was transduced to establish lentiviral overexpression of Lyve-1. We used this artificial model to gain insights into principal cellular functions of Lyve-1 expression regarding effects on cellular adhesion and migration as well as on apoptosis. As it is well established that Lyve-1 interacts with HA and thereby mediates adhesion to HA coated surfaces [112, 118], we examined Lyve-1 mediated cellular adhesion to fibronectin and gelatine. In fact, Lyve-1 overexpression significantly increased adhesion to fibronectin, whereas no such effect was observed when cellular adhesion to gelatine coated surfaces was assessed. CD44, the closest homologue of Lyve-1, shows similar adhesion characteristics. Besides HA, further components of the extracellular matrix have been identified as ligands of CD44 such as laminin, type I collagen fibrils and also fibronectin, while binding to gelatine was not observed [158]. In this context, macrophages direct tumour cell migration in a lock-step manner towards blood vessels by moving along collagen fibres and thus facilitate intravasation of tumour cells and promote the formation of metastasis at distant sites [95]. Lyve-1 might therefore play a role in mediating adhesion and migration of tumour associated macrophages along components of the extracellular matrix and directing tumour cell migration. To evaluate a possible role of Lyve-1 for cell migration a simple wound healing assay was performed. Closure of an artificial wound introduced to a cellular monolayer in the form of a scratch occurred at comparable velocity between Lyve-1 overexpressing and mock transfected control cells. Hence, cell migration was not influenced directly by Lyve-1 overexpression. However, a possible role of Lyve-1 in chemotaxis induced migration should not be disregarded and needs further evaluation.

Both signalling pathways identified to be relevant for the *in vitro* induction of Lyve-1 are regulators of cell survival. Glucocorticoids are widely used in cancer therapies based on their apoptosis promoting effect on cancer cells. However, GR signalling regulates the expression of both pro- and anti-apoptotic proteins and induction of apoptosis occurs in a cancer type specific way [159]. p38 MAPK signalling too is involved in regulation of cell death in a cell-type and stimulus dependent manner [160]. Hence, functional relevance of Lyve-1 was examined in the context of cell survival. Transgenic expression of Lyve-1 did not influence the apoptosis rate of cells which were challenged with increasing concentrations of cytotoxic peroxide.

5.4 Processing of Lyve-1

The high sequence homology of Lyve-1 and CD44 imply possible functional similarities between the HA-receptors at least to some extent. CD44 is a type I transmembrane protein which is expressed almost ubiquitously in malignant and benign cells with diverse functions mediating proliferation, differentiation and migration. Interactions with HA and further ligands such as osteopontin, collagens, fibronectin and matrix metalloproteinases (MMP) influence cell-cell and cell-matrix adhesion. Various different splicing variants plus extensive post-translational modifications by glycosylation determine cell-type specific functions of CD44. The protein is encoded by a single gene consisting of 20 exons. While the constant N-terminal link domain is the region of highest homology to Lyve-1, differential splicing results in a variable membrane proximal stalk region. On the other site, the transmembrane and intracellular domains are conserved amongst CD44 isoforms. Binding motifs in the intracellular tail mediate interactions with proteins like ankyrin and ERM (for ezrin, radixin and moesin) proteins which brace CD44 to the cytoskeleton and influence cellular shape and motility [161, 162]. A soluble form of CD44 is produced by shedding of the ectodomain. Proteolytic cleavage in the membrane proximal stalk region is regulated by the activation of several membrane associated metalloproteinases. CD44 has been identified as a substrate of ADAM10 which is activated as a consequence of cellular Ca^{2+} influx. In addition, activation of PKC or of the GTPase family members Rac and Ras induce ADAM17 activity which in turn cleaves CD44. MT1-MMP and MT3-MMP are additional proteases involved in shedding of CD44. The residual C-terminal part of CD44 experiences further proteolytic processing. Intramembranous cleavage by presenilin (PS)-dependent γ-secretase liberates the C-terminal fragment (CTF) from the membrane anchor. The CD44-CTF readily translocates to the nucleus and induces gene expression via interaction with TPA-responsive elements, amongst others inducing expression of CD44 by self-regulation [163, 164].

In analogy to CD44 shedding, we examined cell culture supernatants of genetically engineered U937 Lyve-1 for the presence of a soluble form of Lyve-1. Western blot analysis facilitated the identification of an approximately 55 kDa version of Lyve-1. The molecular weight and the identified tryptic peptides in mass spectrometry allowed the conclusion that we detected the soluble ectodomain of Lyve-1 in the cell culture supernatant. Stimulation with a sheddase activator and different protease inhibitors revealed that sLyve-1 is produced by metalloprotease mediated shedding in macrophages and in HUVEC in a comparable fashion.

Independent from our observations evidence for Lyve-1 shedding in lymphatic endothelial cells came from two further studies published in March 2016. VEGF-A binding to its corresponding receptor VEGFR-2 induced ERK-dependent activa-

tion of ADAM17 which in turn cleaved Lyve-1. In a migration assay it was further demonstrated that VEGF-A induced shedding of Lyve-1 promoted migration of LEC across HA-coated membranes [128]. The second study demonstrated MT1-MMP (also known as MMP-14) mediated shedding of Lyve-1 in LEC and macrophages. In MMP-14 deficient mice spontaneous lymphangiogenesis occurred as a result of augmented Lyve-1 surface expression on lymphatic endothelial cells in combination with increased expression of lymphangiogenic growth factor VEGF-C in pro-angiogenic macrophages. Loss of MMP-14 expression and thus reduced Lyve-1 shedding increased the proliferation and migration of LEC in response to FGF-2 and HA stimulation. A functional analysis on MMP-14 dependent cleavage of Lyve-1 expressed in macrophages has not been performed [127]. In humans, MMPs comprise a family of 23 different zinc dependent endonucleases. Under physiological conditions these enzymes are mainly involved in organ development and tissue remodelling. MMPs were found to be up-regulated in various cancer types, which often correlated with shortened patient survival due to increased invasiveness of the tumour. Substrates of MMPs are ECM components and cell surface proteins mediating cellular adhesion, growth and growth factor surface retention. Hence, increased expression of MMPs by cancer cells and cancer associated stromal cells like e.g. macrophages promotes cancer progression by numerous mechanisms affecting cell proliferation and migration, angiogenesis, as well as tumour invasion and the development of metastasis [165, 166]. Mammary gland specific overexpression of MMP-14 led e.g. to extensive matrix remodelling and tumour development in transgenic mice [167]. Overexpression of MMP-14 in an adenocarcinoma cell line increased tumour cell proliferation *in vitro* and in a transplant tumour model elevated MMP-14 expression promoted the development of highly vascularized invasive tumours accompanied by elevated levels of VEGF [168]. In human breast cancer patients, high expression levels of MMP-14 and of VEGF-C correlated with increased lymphatic vessel density and lymph node metastasis resulting in decreased overall survival [169]. Closely related to MMPs is the family of 21 different ADAMs, which are also commonly up-regulated in cancers. These zinc dependent sheddases act during fertilization and development, but also promote cancer. By shedding, ADAMs regulate the autocrine and paracrine signalling activity of chemokines, cytokines which can be expressed in membrane bound forms. ADAMs also influence motility of cells by mediating proteolysis of adhesion proteins. ADAM induced shedding plays also an important role in the regulation intramembrane proteolysis, which liberates the intracellular domain from the membrane following ectodomain shedding of transmembrane proteins [170]. ADAM17 has first been identified as tumour necrosis factor-α converting enzyme (TACE) as it regulates paracrine TNF-α signalling by cleaving the membrane bound pro-form of the cytokine. Besides different cytokines, adhesion proteins and growth factors are substrates of ADAM17, which hence mediates a broad array of

cellular functions. In breast cancer ADAM17 overexpression is for example associated with elevated levels of TGF-α, tumour progression, metastasis and poor prognosis [171]. Thus expression of Lyve-1 converting enzymes has closely been linked to cancer and tumour progression. Extensive shedding of Lyve-1 in the tumour microenvironment is therefore imaginable.

In this context, our results demonstrated that macrophage derived sLyve-1 inhibited the proliferation of tumour cells probably by acting as a competitive inhibitor or decoy receptor for membrane-bound HA-receptors. By decreasing the interactions to HA, sLyve-1 might also influence migration of macrophages and by paracrine stimulation also migration and proliferation of tumour cells. Likewise, interactions between HA and CD44 have a major impact on cell adhesion and migration in physiological and pathological processes, like mediation of leukocyte adhesion to the endothelium and subsequent extravasation, but also on tumour cell migration and tumour growth. On the one site, co-expression studies of MT1-MMP and its substrate CD44 in tumour cells revealed that tumour cell migration required shedding of CD44 [172]. Another study demonstrated that in a malignant melanoma cell line transgenic expression of soluble CD44 resulted in reduced tumour cell proliferation and HA sequestration on the cell surface was inhibited. Using these cells in a tumour transplant model resulted in a significant reduction of the tumour volume due to forced expression of the soluble form of CD44 [173]. These opposing findings led to the formulation of the following model of CD44 mediated cell migration. Ectodomain shedding at the leading edge of motile cells enables detachment from HA components of the ECM and the formation of lamellipodia. Stretching of the cell opens mechanosensitive Ca^{2+} channels. Subsequently, ADAM10 is activated by the resulting Ca^{2+} influx and cleaves CD44 at the rear end of the crawling cell. Simultaneously, the CD44-CTF domain translocates to the nucleus and induces CD44 expression, thus promoting adhesion to HA via newly synthesized CD44. Shifting of this balance of shedding mediated CD44 turnover impairs cell migration [164]. Potentially, processing of Lyve-1 mediates migration of macrophages in a similar way.

Under physiological conditions soluble CD44 (sCD44) has been detected in the lymph, synovial fluid, branchoalveolar lavage and serum. Examination of plasma levels of sCD44 were found to be increased in mice during an inflammatory response and tumour growth, while immunodeficiency was associated with reduced plasma concentrations of sCD44 [174, 175]. In highly metastatic melanoma cell lines increased motility was associated with elevated CD44 expression and turnover [176]. By detection of the 25 kDa CD44-CTF protein by immunoblotting, evaluation of CD44 shedding in malignant cells derived from different cancer tissues was facilitated, thus sCD44 could be detected frequently in brain, breast, lung, colon and ovarian cancers [177].

We were able to detect sLyve-1 in plasma samples derived from healthy donors and found significantly increased levels of sLyve-1 in plasma from patients suffering from Psoriasis. Our observations were in line with the findings of Nishida-Fukuda et al. who demonstrated Lyve-1 shedding in human psoriatic lesion by double staining of the intracellular and extracellular portion of the protein [128]. Psoriasis is a frequent chronic inflammatory skin disease affecting 1-3 % of the population in the United States and Europe. Psoriasis vulgaris is the most common form of the disease which is characterized by the development of red coloured, scaly plaques with clear boarders occurring mainly in elbows, knees, scalp and the lumbosacral area. A histologic hallmark of psoriasis is a greatly thickened epidermis (acanthosis), which is caused by increased proliferation and accelerated movement of keratinocytes through the epidermis. Thus differentiation is impaired leading to hyperkeratosis and parakeratosis. In psoriatic lesions the number of mononuclear leukocytes is significantly increased and abnormal vascularization leads to the development of numerous dilated dermal blood vessels resulting in erythema. Mechanistically, psoriasis is a T cell mediated disease. Langerhans cells secrete IL-12 and IL-23 to activate the T cell subsets Th1, Th17 and Th22 which in turn produce the pro-inflammatory cytokines IL-17, IFN-γ, TNF and IL-22. The inflammatory milieu stimulates keratinocytes to sustain T cell activation and recruitment by inducing the expression of further inflammatory cytokines and chemokines [178]. Elevated plasma levels of Lyve-1 therefore imply that shedding could be induced under inflammatory conditions.

We further examined levels of sLyve-1 in plasma of melanoma patients before and during the treatment with the PD-1 inhibitor pembrolizumab. sLyve-1 levels in the plasma from melanoma patients were not increased and cancer immunotherapy did not influence the levels of Lyve-1. Yet, continuously increasing MT1-MMP expression has been associated with melanoma progression [179]. Therefore, it is also conceivable that extensive shedding indeed occurs during tumour growth, but consequently results in higher concentrations of sLyve-1 locally in interstitial fluid and the tumour draining lymph vessels, considering the predominant expression of Lyve-1 in lymphatic vessels. Examination of the composition of the tumour interstitial fluid (TIF) has gained more interest in the recent years as the TIF represents the microenvironment to which tumour cells are exposed. Extraction of the TIF is still an obstacle, though a centrifugation based method allowed TIF collection from excised solid tumour samples from animal models and from human ovarian cancer [180, 181]. Malignant melanoma is a highly aggressive skin cancer occurring with increasing incidence. Approximately 1.7 % of the population in the United States will be diagnosed with melanoma throughout their lifetime. Melanoma arises from transformed melanocytes which are melanin producing cells predominantly located in the skin but can also be found in

the uveal tract of the eye, as well as in the meninges and the angogenital tract [182, 183]. In the course of malignant transformation mutations lead to the expression of tumour-associated antigens which can elicit an anti-tumour immune response. Though, immuoescape mechanisms of the tumours lead to resistance against such host defence programs. Human melanoma cells frequently express ligands of PD-1 (programmed death receptor-1), which is expressed on activated T cells. Ligand binding limits T cell functions by inhibiting down-stream signalling of the TCR. By blockade of this so called immune-checkpoint antitumour effector functions of T cells in the tumour microenvironment are augmented and tumour regression can be achieved [184].

5.5 Lyve-1 deficiency promotes tumour growth

Our *in vivo* experiments demonstrated that in subcutaneously grown B16F1 and B16F10 melanoma Lyve-1$^+$ TAM were located in the marginal zone of the tumour whereas macrophages within the tumour mass did not express Lyve-1. In orthotopically grown mammary tumours similar observations were made revealing the expression of Lyve-1 in TAM which were located in the tumour periphery while this subpopulation was absent in tumour infiltrating macrophages [185]. These findings sustain the view that diverse TAM subpopulations with distinct functions exist. Expression profiling of TAM subsets derived from murine mammary TS/A tumours showed strong correlation between low expression of MHC II and elevated expression LYVE-1. Further analyses of the MHC II^{low} TAM subset revealed localization in hypoxic areas with potent pro-angiogenic functions [73]. A pro-angiogenic role of Lyve-1$^+$ TAM has also been demonstrated in adipose tissue, where Lyve-1$^+$ infiltrating macrophages orchestrate the formation of vascular networks in hypoxic regions [186].

Surprisingly, we detected enhanced tumour growth of B16 transplanted tumours in Lyve-1 knockout mice. As we and others identified a soluble form of Lyve-1 which can be secreted by endothelial cells and macrophages, we speculate that excessive production of sLyve-1 impairs tumour growth in wild type mice. Shedding of the ectodomain of cell surface receptors can have diverse effects. Lyve-1 possesses dual functionality as a surface protein mediating interactions with HA and as a growth factor binding protein. Processing of Lyve-1 might therefore decrease adhesion to the ECM and inhibit growth factor induced proliferation. Furthermore, Lyve-1 mediates cell surface retention of growth factors, therefore shedding also impairs autocrine growth stimulation. The shedded ectodomain of Lyve-1 could also act as a decoy receptor for the respective ligands. In a paracrine

manner sLyve-1 could also influence growth and migration of tumour cells. Our *in vitro* experiments support this hypothesis demonstrating reduced proliferation of melanoma cells in the presence of macrophage derived and synthesized soluble Lyve-1. The regulatory mechanism of Lyve-1 processing is not known so far. To gain a better understanding of the distinct functions of full length and soluble Lyve-1 for tumour growth, differential expression of the protein forms in a tumour model would be necessary.

Therefore, it should not be disregarded that our Lyve-1$^{-/-}$ model results in a global knockout of Lyve-1 expression such that obstruction of Lyve-1 expression is not restricted to macrophages but affects the whole organism and hence also lymphatic endothelial cells. Characterization of Lyve-1 null mice revealed morphological and functional changes in the lymphatic vessels marked by constitutive increased interstitial fluid flow [130]. Various studies highlight the critical involvement of the lymphatics in tumour growth and progression, not only as a possible route for tumour dissemination. The lymphatic vessel network constitutes the second circulatory system which collects interstitial fluid and macromolecules, which constantly leak from blood vessels, and transport it back to the blood vasculature. Under physiological conditions, the lymphatic system is involved in tissue fluid homeostasis, immune surveillance and fat absorption. Spatial restriction during the expansion of the tumour mass leads to the development of high intratumoural pressure. Simultaneously the amount of interstitial fluid in tumours is elevated due to increased leakage of permeable, malformed tumour blood vessels. Therefore, fluid flow especially in the tumour stroma and the peritumoural lymph vessels is enhanced. Elevated interstitial fluids flow (IF) and lymph flow have been associated with increased invasiveness of tumours in diverse *in vitro* and *in vivo* studies [187, 188]. In a model of xenografted breast cancer for example invasiveness of the tumours correlated with increased extravascular drainage [189]. Moreover, it was shown that interstitial fluid flow directed the migration of tumour cells towards the tumour draining lymph nodes by homing of autologous chemotaxis [190]. Interstitial flow activates mechanosensitive cancer associated fibroblasts mediating stiffening of the extracellular matrix which in turn promotes tumour progression and invasion [191]. Besides fluid flow has been shown to be critical for the formation of both blood and lymphatic vessels and IF precedes directed lymphangiogenesis [192, 193]. Changes in the interstitial fluid flow rate in Lyve-1 knockout mice might therefore contribute to enhanced tumour growth of the B16 melanoma.

5.6 The role of glucocorticoids for TAM *in vivo*

By establishment of the *in vitro* differentiation model of monocytes derived TAM by stimulation with MDI several genes were found to be up-regulated which were also expressed by TAM *in vivo*. In general glucocorticoids greatly influence gene expression in macrophages by mediating the down-regulation of pro-inflammatory genes, while simultaneously inducing expression of immunosuppressive mediators. Our *in vitro* data indicate a central role of GC for the induction of Lyve-1 expression and probably for further M2 associated marker proteins. To examine the role of GC for the shaping of TAM phenotypes *in vivo* we bred a mouse strain with specific deletion of functional glucocorticoid receptor in myeloid cells. For this purpose, we crossed mice carrying loxP sites flanking the third exon of the NR3C1 gene, which codes for the first zinc-finger of the GR DNA binding domain, with mice expressing the cre-recombinase under the control of the LysM promoter. The progeny of this breeding strategy shows efficient GR excision in macrophages and granulocytes, as well as partial deletion of the functional receptor in splenic dendritic cells [194, 195]. In spite of myeloid specific GR deletion, Lyve-1^{+} TAM were still present in the periphery of subcutaneously grown B16 tumours in GR^{LysMcre} mice. Therefore, Lyve-1 gene induction *in vivo* might be regulated differently by a yet unknown signalling pathway. In addition, we observed that the tumour growth was enhanced in GR^{LysMcre}. The myeloid specific GR deletion model has previously been used to study the particular effect of GR signalling on macrophage polarization. Due to impaired resolution of the inflammatory innate immune response the GR^{LysMcre} mouse showed greater mortality when being challenged with LPS. Mechanistically, GR deficiency led to impaired inhibition of MAPK signalling following LPS mediated activation of TLR-4 and hence sustained the pro-inflammatory expression profile of LPS-exposed macrophages [196]. Similar observations were made in a study examining the role of GC mediated anti-inflammatory effects in a murine model of skin contact allergy. Myeloid specific knockout of GR abrogated the curative effect of GC treatment by maintaining a pro-inflammatory macrophage phenotype [197]. Based on their anti-inflammatory effects glucocorticoids have been used as therapeutics in chronic and acute inflammations, like rheumatoid arthritis, multiple sclerosis, psoriasis and as immunosuppressive agents following organ transplantation. Furthermore, GC are administrated as adjuvants in chemotherapy to treat lymphoid malignancies as GR signalling induces cell death in cells of the lymphoid lineage [143, 198]. It has yet not been understood by which mechanism the ablation of GR signalling in myeloid cells in our murine tumour transplant model promotes tumour growth and needs further characterizations of the phenotype of GR^{-} TAM besides Lyve-1 expression.

5.7 Concluding remarks

In conclusion, we demonstrated the existence of Lyve-1$^+$ macrophage subset in murine and human melanoma.

A human PBMC model was established to study Lyve-1$^+$ macrophages *in vitro* and expression profiling of the MDI induced macrophages demonstrated M2-polarization of the Lyve-1$^+$ subset.

While *in vitro* Lyve-1 induction was crucially dependent on GR signalling we found Lyve-1$^+$ TAM in B16 tumours derived from GR^{LysMcre} mice, which lack GR specifically in myeloid cells. Further characterization of the phenotype of these Lyve-1$^+$ TAM by gene expression profiling will help to functionally range their phenotype and will bring new insights into the regulation of Lyve-1 induction *in vivo*. Moreover, this model can be used to gain a better understanding of the *in vivo* relevance of GR activation for tumour growth.

In macrophages Lyve-1 is subjected to processing by metalloproteinases which results in shedding of the ectodomain of the protein. Macrophage derived sLyve-1 diminishes the proliferation rate of melanoma cells *in vitro*; therefore, we speculate that sLyve-1 acts as decoy receptor.

The exact role of Lyve-1$^+$ macrophages for tumour growth could not be resolved completely within the Lyve-1 knockout model, as the global knockout affects expression of Lyve-1 also in the lymphatic vasculature and thus our findings cannot be attributed explicitly to macrophages. Therefore, it will be necessary to develop a mouse model with macrophage specific ablation of Lyve-1 expression to determine the particular net effect of Lyve-1$^+$ TAM.

Our *in vitro* findings and evidence from current literature links expression of Lyve-1 to motile pro-angiogenic macrophages, thus implications of Lyve-1$^+$ macrophages regarding tumour angiogenesis and formation of metastasis should be taken into consideration.

6. REFERENCES

1. Kaufmann, S. H., *Immunology's foundation: the 100-year anniversary of the Nobel Prize to Paul Ehrlich and Elie Metchnikoff.* Nat Immunol, 2008. **9**(7): p. 705-12.
2. van Furth, R., et al., *The mononuclear phagocyte system: a new classification of macrophages, monocytes, and their precursor cells.* Bulletin of the World Health Organization, 1972. **46**(6): p. 845-852.
3. Furth, R., *Cells of the Mononuclear Phagocyte System*, in *Mononuclear Phagocytes: Functional Aspects*, R. Furth, Editor. 1980, Springer Netherlands: Dordrecht. p. 1-40.
4. Lavin, Y., et al., *Regulation of macrophage development and function in peripheral tissues.* Nat Rev Immunol, 2015. **15**(12): p. 731-44.
5. Wynn, T. A., A. Chawla, and J. W. Pollard, *Macrophage biology in development, homeostasis and disease.* Nature, 2013. **496**(7446): p. 445-55.
6. Ginhoux, F., et al., *Fate Mapping Analysis Reveals That Adult Microglia Derive from Primitive Macrophages.* Science (New York, N. Y.), 2010. **330**(6005): p. 841-845.
7. Hoeffel, G., et al., *Adult Langerhans cells derive predominantly from embryonic fetal liver monocytes with a minor contribution of yolk sac–derived macrophages.* The Journal of Experimental Medicine, 2012. **209**(6): p. 1167-1181.
8. Schulz, C., et al., *A lineage of myeloid cells independent of Myb and hematopoietic stem cells.* Science, 2012. **336**(6077): p. 86-90.
9. Gautier, E. L., et al., *Gene-expression profiles and transcriptional regulatory pathways that underlie the identity and diversity of mouse tissue macrophages.* Nat Immunol, 2012. **13**(11): p. 1118-1128.
10. Okabe, Y. and R. Medzhitov, *Tissue biology perspective on macrophages.* Nat Immunol, 2016. **17**(1): p. 9-17.
11. Lawrence, T. and G. Natoli, *Transcriptional regulation of macrophage polarization: enabling diversity with identity.* Nat Rev Immunol, 2011. **11**(11): p. 750-761.
12. Boyle, W. J., W. S. Simonet, and D. L. Lacey, *Osteoclast differentiation and activation.* Nature, 2003. **423**(6937): p. 337-342.
13. Hussell, T. and T. J. Bell, *Alveolar macrophages: plasticity in a tissue-specific context.* Nat Rev Immunol, 2014. **14**(2): p. 81-93.
14. Naito, M., et al., *Differentiation and function of Kupffer cells.* Medical Electron Microscopy. **37**(1): p. 16-28.
15. Saijo, K. and C. K. Glass, *Microglial cell origin and phenotypes in health and disease.* Nat Rev Immunol, 2011. **11**(11): p. 775-787.

16. Murray, P. J. and T. A. Wynn, *Protective and pathogenic functions of macrophage subsets*. Nature reviews. Immunology, 2011. **11**(11): p. 723-737.

17. Junt, T., et al., *Subcapsular sinus macrophages in lymph nodes clear lymph-borne viruses and present them to antiviral B cells*. Nature, 2007. **450**(7166): p. 110-114.

18. Murphy, K., *Janeway's Immunobiology* Vol. 8th Edition. 2012, New York, United States of America: Garland Science, Taylor and Francis Group.

19. Iwasaki, A. and R. Medzhitov, *Control of adaptive immunity by the innate immune system*. Nat Immunol, 2015. **16**(4): p. 343-53.

20. Takeda, K. and S. Akira, *Toll-like receptors in innate immunity*. International Immunology, 2005. **17**(1): p. 1-14.

21. Aderem, A., *Phagocytosis and the Inflammatory Response*. Journal of Infectious Diseases, 2003. **187**(Supplement 2): p. S340-5.

22. Aderem, A., and D. M. Underhill, *Mechanisms of phagocytosis in macrophages*. Annual Review of Immunology, 1999. **17**(1): p. 593-623.

23. Vieira, O. V., R. J. Botelho, and S. Grinstein, *Phagosome maturation: aging gracefully*. Biochemical Journal, 2002. **366**(Pt 3): p. 689-704.

24. Vieire, O. V., R. J. Botelho, and S. Grinstein, *Phagosome maturation: aging gracefully*. Biochemical Journal, 2002. **366**(3): p. 689-704.

25. Underhill, D. M. and A. Ozinsky, *Phagocytosis of microbes: Complexity in Action*. Annual Review of Immunology, 2002. **20**(1): p. 825-852.

26. Iles, K. E. and H. J. Forman, *Macrophage signalling and respiratory burst*. Immunologic Research. **26**(1): p. 95-105.

27. Shi, C. and E. G. Pamer, *Monocyte recruitment during infection and inflammation*. Nat Rev Immunol, 2011. **11**(11): p. 762-74.

28. Deshmane, S. L., et al., *Monocyte Chemoattractant Protein-1 (MCP-1): An Overview*. Journal of Interferon & Cytokine Research, 2009. **29**(6): p. 313-326.

29. Auffray, C., et al., *Monitoring of blood vessels and tissues by a population of monocytes with patrolling behavior*. Science, 2007. **317**(5838): p. 666-70.

30. Szekanecz, Z. and A. E. Koch, *Macrophages and their products in rheumatoid arthritis*. Curr Opin Rheumatol, 2007. **19**(3): p. 289-95.

31. Ramachandra, L., D. Simmons, and C. V. Harding, *MHC molecules and microbial antigen processing in phagosomes*. Curr Opin Immunol, 2009. **21**(1): p. 98-104.

32. Burgdorf, S. and C. Kurts, *Endocytosis mechanisms and the cell biology of antigen presentation*. Curr Opin Immunol, 2008. **20**(1): p. 89-95.

33. Mackaness, G. B., *The immunological basis of acquired cellular resistance*. The Journal of Experimental Medicine, 1964. **120**(1): p. 105-120.

34. Nathan, C. F., et al., *Identification of interferon-gamma as the lymphokine that activates human macrophage oxidative metabolism and antimicrobial activity.* The Journal of Experimental Medicine, 1983. **158**(3): p. 670-689.

35. Stein, M., et al., *Interleukin 4 potently enhances murine macrophage mannose receptor activity: a marker of alternative immunologic macrophage activation.* The Journal of Experimental Medicine, 1992. **176**(1): p. 287-292.

36. Doyle, A. G., et al., *Interleukin-13 alters the activation state of murine macrophages in vitro: Comparison with interleukin-4 and interferon-γ.* European Journal of Immunology, 1994. **24**(6): p. 1441-1445.

37. Schmieder, A., et al., *Differentiation and gene expression profile of tumor-associated macrophages.* Seminars in Cancer Biology, 2012. **22**(4): p. 289-297.

38. Goerdt, S. and C. E. Orfanos, *Other Functions, Other Genes: Alternative Activation of Antigen-Presenting Cells.* Immunity, 1999. **10**(2): p. 137-142.

39. Mantovani, A., et al., *Macrophage polarization: tumor-associated macrophages as a paradigm for polarized M2 mononuclear phagocytes.* Trends in Immunology, 2002. **23**(11): p. 549-555.

40. Mantovani, A., et al., *The chemokine system in diverse forms of macrophage activation and polarization.* Trends in Immunology, 2004. **25**(12): p. 677-686.

41. Mosser, D. M. and J. P. Edwards, *Exploring the full spectrum of macrophage activation.* Nat Rev Immunol, 2008. **8**(12): p. 958-969.

42. Murray, P. J., et al., *Macrophage activation and polarization: nomenclature and experimental guidelines.* Immunity, 2014. **41**(1): p. 14-20.

43. Colotta, F., et al., *Cancer-related inflammation, the seventh hallmark of cancer: links to genetic instability.* Carcinogenesis, 2009. **30**(7): p. 1073-81.

44. Balkwill, F. and A. Mantovani, *Inflammation and cancer: back to Virchow?* Lancet, 2001. **357**(9255): p. 539-45.

45. Giovannucci, E., *The prevention of colorectal cancer by aspirin use.* Biomedicine & Pharmacotherapy, 1999. **53**(7): p. 303-308.

46. Oh, J. K. and E. Weiderpass, *Infection and cancer: global distribution and burden of diseases.* Ann Glob Health, 2014. **80**(5): p. 384-92.

47. Mantovani, A., et al., *Cancer-related inflammation.* Nature, 2008. **454**(7203): p. 436-44.

48. Borrello, M. G., D. Degl'Innocenti, and M. A. Pierotti, *Inflammation and cancer: The oncogene-driven connection.* Cancer Letters, 2008. **267**(2): p. 262-270.

49. Jang, S. and M. B. Atkins, *Which drug, and when, for patients with* BRAF*-mutant melanoma?* The Lancet Oncology, 2013. **14**(2): p. e60-e69.

50. Sumimoto, H., et al., *The BRAF-MAPK signalling pathway is essential for cancer-immune evasion in human melanoma cells*. The Journal of Experimental Medicine, 2006. **203**(7): p. 1651-1656.

51. Ernst, P. B. and B. D. Gold, *The disease spectrum of Helicobacter pylori: the immunopathogenesis of gastroduodenal ulcer and gastric cancer.* Annu Rev Microbiol, 2000. **54**: p. 615-40.

52. Maeda, H. and T. Akaike, *Nitric oxide and oxygen radicals in infection, inflammation, and cancer.* Biochemistry (Mosc), 1998. **63**(7): p. 854-65.

53. Coussens, L. M. and Z. Werb, *Inflammation and cancer.* Nature, 2002. **420**(6917): p. 860-7.

54. Balkwill, F., K. A. Charles, and A. Mantovani, *Smoldering and polarized inflammation in the initiation and promotion of malignant disease.* Cancer Cell. **7**(3): p. 211-217.

55. Klink, M., *Interaction of Immune and Cancer cells*. 2013: Springer.

56. Noy, R. and Jeffrey W. Pollard, *Tumor-Associated Macrophages: From Mechanisms to Therapy.* Immunity. **41**(1): p. 49-61.

57. Jung, K. Y., et al., *Cancers with Higher Density of Tumor-Associated Macrophages Were Associated with Poor Survival Rates*. Journal of Pathology and Translational Medicine, 2015. **49**(4): p. 318-324.

58. Medrek, C., et al., *The presence of tumor associated macrophages in tumor stroma as a prognostic marker for breast cancer patients*. BMC Cancer, 2012. **12**(1): p. 1-9.

59. Varney, M. L., S. L. Johansson, and R. K. Singh, *Tumour-associated macrophage infiltration, neovascularization and aggressiveness in malignant melanoma: role of monocyte chemotactic protein-1 and vascular endothelial growth factor-A.* Melanoma Res, 2005. **15**(5): p. 417-25.

60. Lin, E. Y., et al., *Colony-Stimulating Factor 1 Promotes Progression of Mammary Tumors to Malignancy.* The Journal of Experimental Medicine, 2001. **193**(6): p. 727-740.

61. Shand, F. H. W., et al., *Tracking of intertissue migration reveals the origins of tumor-infiltrating monocytes*. Proceedings of the National Academy of Sciences of the United States of America, 2014. **111**(21): p. 7771-7776.

62. Bottazzi, B., et al., *Monocyte chemotactic cytokine gene transfer modulates macrophage infiltration, growth, and susceptibility to IL-2 therapy of a murine melanoma.* The Journal of Immunology, 1992. **148**(4): p. 1280-5.

63. Nesbit, M., et al., *Low-Level Monocyte Chemoattractant Protein-1 Stimulation of Monocytes Leads to Tumor Formation in Nontumorigenic Melanoma Cells*. The Journal of Immunology, 2001. **166**(11): p. 6483-6490.

64. Mantovani, A., et al., *Chemokines in the recruitment and shaping of the leukocyte infiltrate of tumors.* Seminars in Cancer Biology, 2004. **14**(3): p. 155-160.

65. Dorsch, M., et al., *Macrophage colony-stimulating factor gene transfer into tumor cells induces macrophage infiltration but not tumor suppression.* European Journal of Immunology, 1993. **23**(1): p. 186-190.

66. Leek, R. D., et al., *Macrophage infiltration is associated with* VEGF *and* EGFR *expression in breast cancer.* The Journal of Pathology, 2000. **190**(4): p. 430-436.

67. Murdoch, C., A. Giannoudis, and C. E. Lewis, *Mechanisms regulating the recruitment of macrophages into hypoxic areas of tumors and other ischemic tissues.* Blood, 2004. **104**(8): p. 2224-2234.

68. Wang, B., et al., *Transition of tumor-associated macrophages from* MHC *class* II^{hi} *to* MHC *class* II^{low} *mediates tumor progression in mice.* BMC Immunology, 2011. **12**(1): p. 1-12.

69. Berg, D. J., et al., *Enterocolitis and colon cancer in interleukin-10-deficient mice are associated with aberrant cytokine production and* CD4(+) TH1*-like responses.* J Clin Invest, 1996. **98**(4): p. 1010-20.

70. Deng, L., et al., *A Novel Mouse Model of Inflammatory Bowel Disease Links Mammalian Target of Rapamycin-Dependent Hyperproliferation of Colonic Epithelium to Inflammation-Associated Tumorigenesis.* The American Journal of Pathology. **176**(2): p. 952-967.

71. Lawrence, T., *The Nuclear Factor* NF-κB *Pathway in Inflammation.* Cold Spring Harbor Perspectives in Biology, 2009. **1**(6): p. a001651.

72. Greten, F. R., et al., IKKβ *Links Inflammation and Tumorigenesis in a Mouse Model of Colitis-Associated Cancer.* Cell. **118**(3): p. 285-296.

73. Movahedi, K., et al., *Different Tumor Microenvironments Contain Functionally Distinct Subsets of Macrophages Derived from Ly6C(high) Monocytes.* Cancer Research, 2010. **70**(14): p. 5728-5739.

74. Laoui, D., et al., *Tumor Hypoxia Does Not Drive Differentiation of Tumor-Associated Macrophages but Rather Fine-Tunes the M2-like Macrophage Population.* Cancer Research, 2014. **74**(1): p. 24-30.

75. Mantovani, A., et al., *Macrophage polarization: tumor-associated macrophages as a paradigm for polarized M2 mononuclear phagocytes.* Trends in Immunology. **23**(11): p. 549-555.

76. Bergers, G. and L. E. Benjamin, *Tumorigenesis and the angiogenic switch.* Nat Rev Cancer, 2003. **3**(6): p. 401-410.

77. Baeriswyl, V. and G. Christofori, *The angiogenic switch in carcinogenesis.* Seminars in Cancer Biology, 2009. **19**(5): p. 329-337.

78. Lin, E. Y., et al., *Macrophages Regulate the Angiogenic Switch in a Mouse Model of Breast Cancer.* Cancer Research, 2006. **66**(23): p. 11238-11246.

79. Zeisberger, S. M., et al., *Clodronate-liposome-mediated depletion of tumour-associated macrophages: a new and highly effective antiangiogenic therapy approach.* British Journal of Cancer, 2006. **95**(3): p. 272-281.

80. Halin, S., et al., *Extratumoral Macrophages Promote Tumor and Vascular Growth in an Orthotopic Rat Prostate Tumor Model.* Neoplasia (New York, N.Y.), 2009. **11**(2): p. 177-186.

81. Venneri, M.A., et al., *Identification of proangiogenic TIE2-expressing monocytes (TEMs) in human peripheral blood and cancer.* Blood, 2007. **109**(12): p. 5276-5285.

82. De Palma, M., et al., *Tie2-expressing monocytes: regulation of tumor angiogenesis and therapeutic implications.* Trends in Immunology, 2007. **28**(12): p. 519-524.

83. De Palma, M., et al., *Tie2 identifies a hematopoietic lineage of proangiogenic monocytes required for tumor vessel formation and a mesenchymal population of pericyte progenitors.* Cancer Cell, 2005. **8**(3): p. 211-226.

84. Mazzieri, R., et al., *Targeting the ANG2/TIE2 Axis Inhibits Tumor Growth and Metastasis by Impairing Angiogenesis and Disabling Rebounds of Proangiogenic Myeloid Cells.* Cancer Cell, 2011. **19**(4): p. 512-526.

85. Sica, A., et al., *Macrophage polarization in tumour progression.* Seminars in Cancer Biology, 2008. **18**(5): p. 349-355.

86. Kuang, D.-M., et al., *Activated monocytes in peritumoral stroma of hepatocellular carcinoma foster immune privilege and disease progression through PD-L1.* The Journal of Experimental Medicine, 2009. **206**(6): p. 1327-1337.

87. Fu, S., et al., *TGF-β Induces Foxp3 + T-Regulatory Cells from CD4 + CD25 − Precursors.* American Journal of Transplantation, 2004. **4**(10): p. 1614-1627.

88. Gu, L., et al., *Control of TH2 polarization by the chemokine monocyte chemoattractant protein-1.* Nature, 2000. **404**(6776): p. 407-411.

89. Pollard, J.W., *Trophic macrophages in development and disease.* Nat Rev Immunol, 2009. **9**(4): p. 259-270.

90. Ahn, G.O. and J.M. Brown, *Matrix Metalloproteinase-9 Is Required for Tumor Vasculogenesis but Not for Angiogenesis: Role of Bone Marrow-Derived Myelomonocytic Cells.* Cancer Cell, 2008. **13**(3): p. 193-205.

91. Rodriguez, P.C., et al., *Arginase I Production in the Tumor Microenvironment by Mature Myeloid Cells Inhibits T-Cell Receptor Expression and Antigen-Specific T-Cell Responses.* Cancer Research, 2004. **64**(16): p. 5839-5849.

92. Gocheva, V., et al., *IL-4 induces cathepsin protease activity in tumor-associated macrophages to promote cancer growth and invasion.* Genes & Development, 2010. **24**(3): p. 241-255.

93. Mohamed, M.M. and B.F. Sloane, *Cysteine cathepsins: multifunctional enzymes in cancer.* Nat Rev Cancer, 2006. **6**(10): p. 764-775.

94. Li, C. Y., et al., *Matrix metalloproteinase 9 expression and prognosis in colorectal cancer: a meta-analysis*. Tumour Biol, 2013. **34**(2): p. 735-41.

95. Wyckoff, J., et al., *A Paracrine Loop between Tumor Cells and Macrophages Is Required for Tumor Cell Migration in Mammary Tumors*. Cancer Research, 2004. **64**(19): p. 7022-7029.

96. Rohan, T. E., et al., *Tumor Microenvironment of Metastasis and Risk of Distant Metastasis of Breast Cancer*. Journal of the National Cancer Institute, 2014. **106**(8).

97. Wyckoff, J. B., et al., *Direct Visualization of Macrophage-Assisted Tumor Cell Intravasation in Mammary Tumors*. Cancer Research, 2007. **67**(6): p. 2649-2656.

98. Psaila, B. and D. Lyden, *The Metastatic Niche: Adapting the Foreign Soil*. Nature reviews. Cancer, 2009. **9**(4): p. 285-293.

99. Nagai, T., et al., *Targeting tumor-associated macrophages in an experimental glioma model with a recombinant immunotoxin to folate receptor β*. Cancer Immunology, Immunotherapy, 2009. **58**(10): p. 1577-1586.

100. Rogers, T. L. and I. Holen, *Tumour macrophages as potential targets of bisphosphonates*. Journal of Translational Medicine, 2011. **9**: p. 177-177.

101. Ries, Carola H., et al., *Targeting Tumor-Associated Macrophages with Anti-CSF-1R Antibody Reveals a Strategy for Cancer Therapy*. Cancer Cell. **25**(6): p. 846-859.

102. Panni, R. Z., D. C. Linehan, and D. G. DeNardo, *Targeting tumor-infiltrating macrophages to combat cancer*. Immunotherapy, 2013. **5**(10): p. 10.2217/imt.13.102.

103. Velasco-Velázquez, M., W. Xolalpa, and R. G. Pestell, *The potential to target CCL5/CCR5 in breast cancer*. Expert Opinion on Therapeutic Targets, 2014. **18**(11): p. 1265-1275.

104. Robinson, S. C., et al., *A Chemokine Receptor Antagonist Inhibits Experimental Breast Tumor Growth*. Cancer Research, 2003. **63**(23): p. 8360-8365.

105. Beatty, G. L., et al., *CD40 Agonists Alter Tumor Stroma and Show Efficacy Against Pancreatic Carcinoma in Mice and Humans*. Science (New York, N. Y.), 2011. **331**(6024): p. 1612-1616.

106. Hanna, E., R. Abadi, and O. Abbas, *Imiquimod in dermatology: an overview*. International Journal of Dermatology, 2016. **55**(8): p. 831-844.

107. Guiducci, C., et al., *Redirecting In vivo Elicited Tumor Infiltrating Macrophages and Dendritic Cells towards Tumor Rejection*. Cancer Research, 2005. **65**(8): p. 3437-3446.

108. Singh, M., et al., *Effective innate and adaptive anti-melanoma immunity through localized TLR-7/8 activation*. Journal of immunology (Baltimore, Md. : 1950), 2014. **193**(9): p. 4722-4731.

109. Edwards, J.P. and L.A. Emens, *The multikinase inhibitor sorafenib reverses the suppression of* IL-12 *and enhancement of* IL-10 *by* PGE(2) *in murine macrophages.* Int Immunopharmacol, 2010. **10**(10): p. 1220-8.

110. Huang, Z., et al., *Targeted delivery of oligonucleotides into tumor-associated macrophages for cancer immunotherapy.* Journal of Controlled Release, 2012. **158**(2): p. 286-292.

111. Mantovani, A. and P. Allavena, *The interaction of anticancer therapies with tumor-associated macrophages.* The Journal of Experimental Medicine, 2015. **212**(4): p. 435-445.

112. Banerji, S., et al., LYVE-1, *a New Homologue of the* CD44 *Glycoprotein, Is a Lymph-specific Receptor for Hyaluronan.* The Journal of Cell Biology, 1999. **144**(4): p. 789-801.

113. Jackson, D.G., *The Lymphatics Revisited.* Trends in Cardiovascular Medicine. **13**(1): p. 1-7.

114. Jackson, D.G., *Biology of the lymphatic marker* LYVE-1 *and applications in research into lymphatic trafficking and lymphangiogenesis.* APMIS, 2004. **112**(7-8): p. 526-538.

115. Carreira, C.M., et al., LYVE-1 *Is Not Restricted to the Lymph Vessels.* Expression in Normal Liver Blood Sinusoids and Down-Regulation in Human Liver Cancer and Cirrhosis. 2001. **61**(22): p. 8079-8084.

116. Schledzewski, K., et al., *Lymphatic endothelium-specific hyaluronan receptor* LYVE-1 *is expressed by stabilin-1$^+$, F4/80$^+$,* CD11b$^+$ *macrophages in malignant tumours and wound healing tissue in vivo and in bone marrow cultures in vitro: implications for the assessment of lymphangiogenesis.* The Journal of Pathology, 2006. **209**(1): p. 67-77.

117. Jackson, D.G., et al., LYVE-1, *the lymphatic system and tumor lymphangiogenesis.* Trends in Immunology. **22**(6): p. 317-321.

118. Prevo, R., et al., *Mouse* LYVE-1 *Is an Endocytic Receptor for Hyaluronan in Lymphatic Endothelium.* Journal of Biological Chemistry, 2001. **276**(22): p. 19420-19430.

119. Banerji, S., et al., *Distinctive Properties of the Hyaluronan-binding Domain in the Lymphatic Endothelial Receptor Lyve-1 and Their Implications for Receptor Function.* The Journal of Biological Chemistry, 2010. **285**(14): p. 10724-10735.

120. Nightingale, T.D., et al., *A Mechanism of Sialylation Functionally Silences the Hyaluronan Receptor* LYVE-1 *in Lymphatic Endothelium.* Journal of Biological Chemistry, 2009. **284**(6): p. 3935-3945.

121. Lawrance, W., et al., *Binding of Hyaluronan to the Native Lymphatic Vessel Endothelial Receptor* LYVE-1 *Is Critically Dependent on Receptor Clustering and Hyaluronan Organization.* The Journal of Biological Chemistry, 2016. **291**(15): p. 8014-8030.

122. Boensch, C., et al., *Identification, Purification, and Characterization of Cell-surface Retention Sequence-binding Proteins from Human SK-Hep Cells and Bovine Liver Plasma Membranes*. Journal of Biological Chemistry, 1995. **270**(4): p. 1807-1816.

123. Boensch, C., et al., *Cell Surface Retention Sequence Binding Protein-1 Interacts with the v-sis Gene Product and Platelet-derived Growth Factor β-Type Receptor in Simian Sarcoma Virus-transformed Cells*. Journal of Biological Chemistry, 1999. **274**(15): p. 10582-10589.

124. Huang, S. S., et al., *Cloning, Expression, Characterization, and Role in Autocrine Cell Growth of Cell Surface Retention Sequence Binding Protein-1*. Journal of Biological Chemistry, 2003. **278**(44): p. 43855-43869.

125. Platonova, N., et al., *Evidence for the interaction of fibroblast growth factor-2 with the lymphatic endothelial cell marker LYVE-1*. Blood, 2013. **121**(7): p. 1229-1237.

126. Johnson, L. A., et al., *Inflammation-induced Uptake and Degradation of the Lymphatic Endothelial Hyaluronan Receptor LYVE-1*. Journal of Biological Chemistry, 2007. **282**(46): p. 33671-33680.

127. Wong, H. L. X., et al., *MT1-MMP sheds LYVE-1 on lymphatic endothelial cells and suppresses VEGF-C production to inhibit lymphangiogenesis*. Nature Communications, 2016. **7**: p. 10824.

128. Nishida-Fukuda, H., et al., *Ectodomain Shedding of Lymphatic Vessel Endothelial Hyaluronan Receptor 1 (LYVE-1) Is Induced by Vascular Endothelial Growth Factor A (VEGF-A)*. Journal of Biological Chemistry, 2016. **291**(20): p. 10490-10500.

129. Gale, N. W., et al., *Normal Lymphatic Development and Function in Mice Deficient for the Lymphatic Hyaluronan Receptor LYVE-1*. Molecular and Cellular Biology, 2007. **27**(2): p. 595-604.

130. Huang, S. S., et al., *CRSBP-1/LYVE-1-null Mice Exhibit Identifiable Morphological and Functional Alterations of Lymphatic Capillary Vessels*. FEBS letters, 2006. **580**(26): p. 6259-6268.

131. Hou, W.-H., et al., *CRSBP-1/LYVE-1 ligands disrupt lymphatic intercellular adhesion by inducing tyrosine phosphorylation and internalization of VE-cadherin*. Journal of Cell Science, 2011. **124**(8): p. 1231-1244.

132. Wu, M., et al., *Low Molecular Weight Hyaluronan Induces Lymphangiogenesis through LYVE-1-Mediated Signalling Pathways*. PLoS ONE, 2014. **9**(3): p. e92857.

133. Yu, M., et al., *The cooperative role of S1P3 with LYVE-1 in LMW-HA-induced lymphangiogenesis*. Experimental Cell Research, 2015. **336**(1): p. 150-157.

134. Schmieder, A., et al., *The CD20 homolog Ms4a8a integrates pro- and anti-inflammatory signals in novel M2-like macrophages and is expressed in parasite infection*. European Journal of Immunology, 2012. **42**(11): p. 2971-2982.

135. Kzhyshkowska, J., et al., *Novel stabilin-1 interacting chitinase-like protein (SI-CLP) is up-regulated in alternatively activated macrophages and secreted via lysosomal pathway.* Blood, 2006. **107**(8): p. 3221-3228.

136. Schönhaar, K., *Expressionsanalyse muriner und humaner Tumor-assoziierter Makrophagen* in *Fakultät für Biowissenschaften*. 2015, Ruprecht-Karls-Universität Heidelberg. p. 96.

137. Mülhardt, C., *Der Experimentator: Molekularbiologie / Genomics*. 2009, Spektrum Akademischer Verlag: Heidelberg. p. Online-Ressource.

138. Ginzinger, D. G., *Gene quantification using real-time quantitative PCR: an emerging technology hits the mainstream.* Exp Hematol, 2002. **30**(6): p. 503-12.

139. Livak, K. J. and T. D. Schmittgen, *Analysis of relative gene expression data using real-time quantitative PCR and the 2(-Delta Delta C(T)) Method.* Methods, 2001. **25**(4): p. 402-8.

140. Schägger, H. and G. von Jagow, *Tricine-sodium dodecyl sulfate-polyacrylamide gel electrophoresis for the separation of proteins in the range from 1 to 100 kDa.* Analytical Biochemistry, 1987. **166**(2): p. 368-379.

141. Dumont, A., et al., *Hydrogen peroxide-induced apoptosis is CD95-independent, requires the release of mitochondria-derived reactive oxygen species and the activation of NF-kappaB*. Oncogene, 1999. **18**(3): p. 747-57.

142. Munder, M., *Arginase: an emerging key player in the mammalian immune system.* British Journal of Pharmacology, 2009. **158**(3): p. 638-651.

143. Coutinho, A. E. and K. E. Chapman, *The anti-inflammatory and immunosuppressive effects of glucocorticoids, recent developments and mechanistic insights.* Molecular and Cellular Endocrinology, 2011. **335**(1): p. 2-13.

144. Kadmiel, M. and J. A. Cidlowski, *Glucocorticoid receptor signalling in health and disease.* Trends in pharmacological sciences, 2013. **34**(9): p. 518-530.

145. Tuckermann, J. P., et al., *Molecular mechanisms of glucocorticoids in the control of inflammation and lymphocyte apoptosis.* Critical Reviews in Clinical Laboratory Sciences, 2005. **42**(1): p. 71-104.

146. Ehrchen, J., et al., *Glucocorticoids induce differentiation of a specifically activated, anti-inflammatory subtype of human monocytes.* Blood, 2007. **109**(3): p. 1265-1274.

147. Cuadrado, A. and Angel R. Nebreda, *Mechanisms and functions of p38 MAPK signalling.* Biochemical Journal, 2010. **429**(3): p. 403-417.

148. Zhang, Y. E., *Non-Smad pathways in TGF-β signalling.* Cell research, 2009. **19**(1): p. 128-139.

149. Jiménez-Garcia, L., et al., *Critical role of p38 MAPK in IL-4-induced alternative activation of peritoneal macrophages.* European Journal of Immunology, 2015. **45**(1): p. 273-286.

150. Jang, Y.-S., et al., IL-4 *stimulates mouse macrophages to express* APRIL *through p38* MAPK *and two different downstream molecules,* CREB *and Stat6.* Cytokine, 2009. **47**(1): p. 43-47.

151. Jackson, D. G., *Immunological functions of hyaluronan and its receptors in the lymphatics.* Immunological Reviews, 2009. **230**(1): p. 216-231.

152. Toole, B. P., T. N. Wight, and M. I. Tammi, *Hyaluronan-Cell Interactions in Cancer and Vascular Disease.* Journal of Biological Chemistry, 2002. **277**(7): p. 4593-4596.

153. Toole, B. P. and V. C. Hascall, *Hyaluronan and Tumor Growth.* The American Journal of Pathology, 2002. **161**(3): p. 745-747.

154. Simpson, M. A., C. M. Wilson, and J. B. McCarthy, *Inhibition of Prostate Tumor Cell Hyaluronan Synthesis Impairs Subcutaneous Growth and Vascularization in Immunocompromised Mice.* The American Journal of Pathology, 2002. **161**(3): p. 849-857.

155. Kobayashi, N., et al., *Hyaluronan Deficiency in Tumor Stroma Impairs Macrophage Trafficking and Tumor Neovascularization.* Cancer Research, 2010. **70**(18): p. 7073-7083.

156. Franklin, R. A. and M. O. Li, *Ontogeny of Tumor-Associated Macrophages and Its Implication in Cancer Regulation.* Trends in Cancer, 2016. **2**(1): p. 20-34.

157. Tymoszuk, P., et al., *In situ proliferation contributes to accumulation of tumor-associated macrophages in spontaneous mammary tumors.* European Journal of Immunology, 2014. **44**(8): p. 2247-2262.

158. Jalkanen, S., and M. Jalkanan, *Lymphocyte* CD44 *binds the* COOH*-terminal heparin-binding domain of fibronectin.* The Journal of Cell Biology, 1992. **116**(3): p. 817-825.

159. Schlossmacher, G., A. Stevens, and A. White, *Glucocorticoid receptor-mediated apoptosis: mechanisms of resistance in cancer cells.* Journal of Endocrinology, 2011. **211**(1): p. 17-25.

160. Zarubin, T. and J. Han, *Activation and signalling of the p38* MAP *kinase pathway.* Cell Res, 2005. **15**(1): p. 11-18.

161. Ponta, H., L. Sherman, and P. A. Herrlich, CD44*: From adhesion molecules to signalling regulators.* Nat Rev Mol Cell Biol, 2003. **4**(1): p. 33-45.

162. Cichy, J. and E. Puré, *The liberation of* CD44. The Journal of Cell Biology, 2003. **161**(5): p. 839-843.

163. Thorne, R. F., J. W. Legg, and C. M. Isacke, *The role of the* CD44 *transmembrane and cytoplasmic domains in co-ordinating adhesive and signalling events.* Journal of Cell Science, 2004. **117**(3): p. 373-380.

164. Nagano, O. and H. Saya, *Mechanism and biological significance of* CD44 *cleavage.* Cancer Science, 2004. **95**(12): p. 930-935.

165. Kessenbrock, K., V. Plaks, and Z. Werb, *Matrix Metalloproteinases: Regulators of the Tumor Microenvironment*. Cell, 2010. **141**(1): p. 52-67.

166. Egeblad, M. and Z. Werb, *New functions for the matrix metalloproteinases in cancer progression*. Nat Rev Cancer, 2002. **2**(3): p. 161-174.

167. Ha, H.Y., et al., *Overexpression of membrane-type matrix metalloproteinase-1 gene induces mammary gland abnormalities and adenocarcinoma in transgenic mice*. Cancer Res, 2001. **61**(3): p. 984-90.

168. Sounni, N.E., et al., *MT1-MMP expression promotes tumor growth and angiogenesis through an up-regulation of vascular endothelial growth factor expression*. The FASEB Journal, 2002. **16**(6): p. 555-564.

169. Yao, G., et al., *MT1-MMP in breast cancer: induction of VEGF-C correlates with metastasis and poor prognosis*. Cancer Cell International, 2013. **13**: p. 98-98.

170. Murphy, G., *The ADAMs: signalling scissors in the tumour microenvironment*. Nat Rev Cancer, 2008. **8**(12): p. 932-941.

171. Gooz, M., *ADAM-17: The Enzyme That Does It All*. Critical reviews in biochemistry and molecular biology, 2010. **45**(2): p. 146-169.

172. Kajita, M., et al., *Membrane-type 1 matrix metalloproteinase cleaves CD44 and promotes cell migration*. J Cell Biol, 2001. **153**(5): p. 893-904.

173. Ahrens, T., et al., *Soluble CD44 inhibits melanoma tumor growth by blocking cell surface CD44 binding to hyaluronic acid*. Oncogene, 2001. **20**(26): p. 3399-408.

174. Katoh, S., J.B. McCarthy, and P.W. Kincade, *Characterization of soluble CD44 in the circulation of mice. Levels are affected by immune activity and tumor growth*. The Journal of Immunology, 1994. **153**(8): p. 3440-9.

175. Katoh, S., et al., *Overexpression of CD44 on alveolar eosinophils with high concentrations of soluble CD44 in bronchoalveolar lavage fluid in patients with eosinophilic pneumonia*. Allergy, 1999. **54**(12): p. 1286-1292.

176. Goebeler, M., et al., *Migration of highly aggressive melanoma cells on hyaluronic acid is associated with functional changes, increased turnover and shedding of CD44 receptors*. Journal of Cell Science, 1996. **109**(7): p. 1957-1964.

177. Okamoto, I., et al., *Proteolytic Cleavage of the CD44 Adhesion Molecule in Multiple Human Tumors*. The American Journal of Pathology, 2002. **160**(2): p. 441-447.

178. Lowes, M.A., M. Suárez-Fariñas, and J.G. Krueger, *Immunology of Psoriasis*. Annual Review of Immunology, 2014. **32**(1): p. 227-255.

179. Shaverdashvili, K., et al., *MT1-MMP modulates melanoma cell dissemination and metastasis through activation of MMP2 and RAC1*. Pigment Cell & Melanoma Research, 2014. **27**(2): p. 287-296.

180. Wiig, H., K. Aukland, and O. Tenstad, *Isolation of interstitial fluid from rat mammary tumors by a centrifugation method.* American Journal of Physiology – Heart and Circulatory Physiology, 2003. **284**(1): p. H416-H424.

181. Haslene-Hox, H., et al., *A New Method for Isolation of Interstitial Fluid from Human Solid Tumors Applied to Proteomic Analysis of Ovarian Carcinoma Tissue.* PLoS ONE, 2011. **6**(4): p. e19217.

182. Berrios-Colon, E. W. S., *Melanoma Review: Background and treatment.* US Pharmacist, 2012. **37**(4): p. 3.

183. Karimkhani, C., R. Gonzalez, and R. P. Dellavalle, *A Review of Novel Therapies for Melanoma.* American Journal of Clinical Dermatology, 2014. **15**(4): p. 323-337.

184. Pardoll, D. M., *The blockade of immune checkpoints in cancer immunotherapy.* Nat Rev Cancer, 2012. **12**(4): p. 252-264.

185. Iyer, V., et al., *Estrogen Promotes ER-Negative Tumor Growth and Angiogenesis through Mobilization of Bone Marrow–Derived Monocytes.* Cancer Research, 2012. **72**(11): p. 2705-2713.

186. Cho, C.-H., et al., *Angiogenic Role of LYVE-1-Positive Macrophages in Adipose Tissue.* Circulation Research, 2007. **100**(4): p. e47-e57.

187. Munson, J. M. and A. C. Shieh, *Interstitial fluid flow in cancer: implications for disease progression and treatment.* Cancer Management and Research, 2014. **6**: p. 317-328.

188. Swartz, M. A. and A. W. Lund, *Lymphatic and interstitial flow in the tumour microenvironment: linking mechanobiology with immunity.* Nat Rev Cancer, 2012. **12**(3): p. 210-219.

189. Pathak, A. P., et al., *Lymph Node Metastasis in Breast Cancer Xenografts Is Associated with Increased Regions of Extravascular Drain, Lymphatic Vessel Area, and Invasive Phenotype.* Cancer Research, 2006. **66**(10): p. 5151-5158.

190. Shields, J. D., et al., *Autologous Chemotaxis as a Mechanism of Tumor Cell Homing to Lymphatics via Interstitial Flow and Autocrine CCR7 Signalling.* Cancer Cell, 2007. **11**(6): p. 526-538.

191. Ng, C. P., B. Hinz, and M. A. Swartz, *Interstitial fluid flow induces myofibroblast differentiation and collagen alignment in vitro.* Journal of Cell Science, 2005. **118**(20): p. 4731-4739.

192. Ng, C. P., C.-L. E. Helm, and M. A. Swartz, *Interstitial flow differentially stimulates blood and lymphatic endothelial cell morphogenesis in vitro.* Microvascular Research, 2004. **68**(3): p. 258-264.

193. Boardman, K. C. and M. A. Swartz, *Interstitial Flow as a Guide for Lymphangiogenesis.* Circulation Research, 2003. **92**(7): p. 801-808.

194. Tronche, F., et al., *Disruption of the glucocorticoid receptor gene in the nervous system results in reduced anxiety.* Nat Genet, 1999. **23**(1): p. 99-103.

195. Clausen, B. E., et al., *Conditional gene targeting in macrophages and granulocytes using LysMcre mice.* Transgenic Res, 1999. **8**(4): p. 265-77.

196. Bhattacharyya, S., et al., *Macrophage glucocorticoid receptors regulate Toll-like receptor 4–mediated inflammatory responses by selective inhibition of p38 MAP kinase.* Blood, 2007. **109**(10): p. 4313-4319.

197. Tuckermann, J. P., et al., *Macrophages and neutrophils are the targets for immune suppression by glucocorticoids in contact allergy.* Journal of Clinical Investigation, 2007. **117**(5): p. 1381-1390.

198. Greenstein, S., et al., *Mechanisms of Glucocorticoid-mediated Apoptosis in Hematological Malignancies.* Clinical Cancer Research, 2002. **8**(6): p. 1681-1694.

199. Tronche, F., et al., *Disruption of the glucocorticoid receptor gene in the nervous system results in reduced anxiety.* Nat Genet, 1999. **23**(1): p. 99-103

7. ABBREVIATIONS

ADAM	a disintegrin and metalloproteinase
ANG-2	angiopoietin
APC	antigen-presenting cell
APS	ammonium persulphate
APS	ammonium persulfate
BCG	bovis bacillus Calmette-Guerin
BMDM	bone-marrow derived macrophages
BrdU	5-bromo-2′-deoxy-uridine
BSA	bovine serum albumin
BSA	bovine serum albumin
CD	cluster of differentiation
CEBP	CCAAT/enhancer-binding protein
COX	cyclooxygenase
CRSBP-1	cell surface retention sequence binding protein-1
CRS	cell surface retention sequence
CTF	C-terminal fragment
DAF2-DA	4,5-Diaminofluorescein
DC	dendritic cell
dexa	dexamethasone
ECM	extracellular matrix
EGF	epidermal growth factor
ELISA	enzyme-linked immunosorbent assay
EMP	erythromyeloid progenitor
ERK	extracellular signal regulated kinase
EtOH	ethanol
EV	empty vector
FACS	fluorescence associated cell sorting
F_cR	F_c receptor
FCS	fetal calf serum
FGF	fibroblast growth factor
Fig.	Figure
FITC	fluorescein isothiocyanate
GC	glucocorticoid
GM-CSF	granulocyte-macrophage colony stimulating factor
GRE	GR responsive elements

GR	glucocorticoid receptor
GTP	guanosine triphosphate
HA	hyaluronic acid
HGF	hepatocyte growth factor
HLA-DR	Human leucocyte antigen-antigen D related
HMW	high molecular weight
HRP	horse raddish peroxidase
HSC	hematopoietic stem cell
ICAM	intercellular adhesion molecule
IFN	interferon
IGFBP	insulin-like growth factor binding protein
Ig	immunoglobulin
IKKb	inhibitor of nuclear factor kappa-B kinase subunit beta
IL	interleukin
iNOS	inducible nitric oxide synthase
IP	immunoprecipitation
IRES	internal ribosomal entry site
LEC	lymphatic endothelial cells
LLC	Lewis lung carcinoma
LMW	low molecular weight
LPS	lipopolysaccharide
Ly6C	lymphocyte Antigen 6 C
Lyve-1	lymphatic vessel endothelial hyaluronan receptor
M-CSF	macrophage-colony stimulating factor
MACS	magnet associated cell sorting
MAPK	mitogen activated protein kinase
MCP-1	monocyte chemoattracting protein-1
MCS	multiple cloning site
MDI	M-CSF/dexamethasone/IL-4
MDSC	myeloid derived supressor cell
MHC	major histocompability complex
MMP	metalloproteinase
MPS	mononuclear phagocyte system
MR	mannose receptor
MT-MMP	membrane-type metalloproteinase
NADPH oxidase	nicotinamide adenine dinucleotide phosphate oxidase
NFκB	nuclear factor κ-light-chain-enhancer of activated B cells
NK cell	natural killer cell
NOD	nucleotide binding oligomerization domain
NOS	reactive nitrogen species
NRL	leucine-riche repeat-containing receptors

NSAID	non-steroidal anti-inflammatory drugs
PAGE	polyacrylamide gelelectrophoresis
PAMP	pathogen associated molecular patterns
PBMC	peripheral blood monocytes
PBS	phosphate buffered saline
PCR	polymerase chain reaction
PD-L1	programmed cell death-ligand 1
PDGF	platelet derived growth factor
PKC	protein kinase C
PPAR γ	peroxisome proliferator-activated receptor γ
PRR	pattern recognition receptor
qRT-PCR	quantitative real-time PCR
ROS	reactive oxygen species
RT	reverse transcription
S.C.	subcutan
S1P3	sphingosine 1 phosphate 3 receptor
SCD44	soluble CD44
SCS	subcapsular sinus
SDS	sodium dodecyl sulphate
SDS	sodium dodecyl sulphate
sLyve-1	soluble Lyve-1
SN	supernatant
STAT	signal transducer and activator of transcription
STREPTA	streptavidin
TACE	TNF-α converting enzyme
TAM	tumour associated macrophage
TCM	tumour conditioned medium
TCR	T cell receptor
TEMED	tetramethylethylenediamine
TEM	TIE2 expressing macrophages
TGF	transforming growth factor
Th1/2	T helper 1/2
TIF	tumour interstitial fluid
TLR	toll-like receptor
TMEM	tumour microenvironment for metastasis
TNF	tumour necrosis factor
Treg	regulatory T cell
VEGF	vascular endothelial growth factor
YS	yolk sac
ZA	zoledronic acid

8. ACKNOWLEDGEMENTS

I would like to express my highest appreciation to Prof. Dr. rer. nat. Viktor Umansky for his support and guidance. Thank you for giving me the opportunity to carry out my doctoral thesis.

Furthermore, I would like to thank Prof. Dr. Sergij Goerdt for his expertise, his support and valuable advices. Thank you for providing all necessary facilities to accomplish my thesis and my experiments. Experiencing education in the course of the RTG 2099 'Hallmarks of Skin Cancer' was a personal enrichment.

My sincerest gratitude goes to PD Dr. A. Schmieder for her constant support and her guidance throughout my PhD thesis. Dr. Schmieder always sustained me with helpful suggestions regarding the experiments and provided excellent help to interpret experimental outcomes. Astrid, thank you so much for your positive attitude, for always motivating me and for believing in me.

I would like also to thank Dr. Kai Schledzewski for his expertise and his valuable scientific input which helped a lot to promote my research. My warmest thanks go to my current and former colleagues Dr. Jules Michel, Dr. Kathrin Becker, Loreen Kloss, Andreas Krewer and Susanne Melchers. Thank you guys so much for your support, your open ears and the amicable atmosphere. I could always count on you and I really enjoyed working with you!

Many heartfelt thanks go to Hilli Schönhaber for technical assistance, helping with good advices and especially for providing solutions to any kind of problem.

Special thanks are due to my special colleague Jochen Weber. He did not only support me with experimental recommendations, but he was also open for every fun. Jochen, working with you was a pleasure! Without you I would have already failed in the AK1!

Thanks to all colleagues in the Dermatology Department. I always enjoyed working here. I am grateful for the time I spent here and I will keep it in good memory.

Furthermore, thanks to Viktor Costina (Mass Spectrometry) and Stefanie Uhlig (FACS Sorting) for the fruitful cooperation.

Last but not least, I want to express my greatest gratitude to my family for their incredible support, for believing in me and for their affirmations.

Finally, I want to express my deepest appreciation for Nicolai. Nici, without you I would not have made it. Thank you so much for your support. Thank you for your patience. Thank you for your encouraging words. Thank you for always being there for me. Thank you for everything.